JAERI-Tech
2001-011

DEPRESSURIZATION ANALYSES OF PWR STATION BLACKOUT WITH MELCOR 1.8.4

March 2001

Anhar R. ANTARIKSAWAN*, Akihide HIDAKA,
Kiyofumi MORIYAMA and Kazuichiro HASHIMOTO*

日本原子力研究所
Japan Atomic Energy Research Institute

本レポートは，日本原子力研究所が不定期に公刊している研究報告書です。
入手の問合わせは，日本原子力研究所研究情報部研究情報課（〒319－1195 茨城県那珂郡東海村）あて，お申し越しください。なお，このほかに財団法人原子力弘済会資料センター（〒319－1195 茨城県那珂郡東海村日本原子力研究所内）で複写による実費頒布をおこなっております。

This report is issued irregularly.
Inquiries about availability of the reports should be addressed to Research Information Division, Department of Intellectual Resources, Japan Atomic Energy Research Institute, Tokai-mura, Naka-gun, Ibaraki-ken 〒319－1195, Japan.

編集兼発行　日本原子力研究所

JAERI-Tech 2001-011

Depressurization Analyses of PWR Station Blackout with MELCOR 1.8.4

Anhar R. ANTARIKSAWAN*, Akihide HIDAKA, Kiyofumi MORIYAMA and Kazuichiro HASHIMOTO**

Department of Reactor Safety Research
Nuclear Safety Research Center
Japan Atomic Energy Research Institute
Tokai-mura, Naka-gun, Ibaraki-ken

(Received January 31, 2001)

A total station blackout (SBO) accident sequence, namely TMLB′, of PWR was found as a dominant accident leading to core severe damage. It was also found that the sequence could lead to High Pressure Melt Ejection (HPME) followed by Direct Containment Heating (DCH), and, in turn, challenge the containment integrity. An intentional RCS depressurization had been proposed to prevent or mitigate the effects of DCH during a station blackout. Moreover, during such sequence, a primary coolant pump seal might be deteriorated due to loss of cooling. This particular LOCA is designated as S3-TMLB′. This report describes the analytical studies for variations of a TMLB′ sequence of PWR four loops plant of Indian Point 3. The analyses also include S3-TMLB′ with or without RCS depressurization and a series of sensitivity analyses. Analytical tool used in this calculation is the MELCOR 1.8.4 code. Seven runs of different scenario have been performed.

* Science & Technology Agency (STA) Fellowship
National Nuclear Energy Agency of Indonesia (BATAN)
** Japan Nuclear Cycle Development Institute

For the TMLB′ accident, the calculation results predicted a vessel breach as a result of debris relocation in lower plenum, while the RCS pressure was kept at PORV set point. Such condition could allow a HPME. On the other hand, the RCP seal leak during TMLB′, might give the different effects on accident sequence depending on the timing of the seals failure. Early failure after initiation of SBO, i.e. 10 minutes, resulted in an early core damage. Contrarily, if the seal failure occur later, the core damage could delay from about 2000 s to more than 1 hr compared to the TMLB′ sequence. An intentional RCS depressurization by PORVs latched open during TMLB′ did not show an important effect; the predicted sequence was similar to TMLB′. But, if the discharging valves flow area is increased, which is assumed by SRVs latched open together with PORVs in this study, the core damage progression could be delayed by about 6000 s. This last strategy was also applied to S3-TMLB′ accident. However, the calculation result showed that, compared to the S3-TMLB′ without intentional RCS depressurization, the accident progression could be delayed only by 3000 s.

Keywords: Severe Accident, Station Blackout, RCP Seal LOCAs, Intentional RCS Depressurization, Accident Mitigation, MELCOR 1.8.4 Code.

MELCOR1.8.4 コードによる PWR 電源喪失事故時の減圧解析

日本原子力研究所東海研究所安全性試験研究センター原子炉安全工学部
Anhar R. ANTARIKSAWAN*・日高　昭秀・森山　清史・橋本　和一郎**

(2001 年 1 月 31 日受理)

PWR の全電源喪失事故（TMLB'）は、炉心損傷に至る主要な事故シーケンスの一つに挙げられている。TMLB'は一次冷却系が高圧に保たれるため、原子炉圧力容器破損時の高圧溶融物放出とそれに続く格納容器直接加熱により格納容器の健全性が脅かされる可能性がある。このため、一次冷却系の強制減圧操作は、TMLB'時の格納容器直接加熱を防止あるいはその影響を緩和する方策として推奨されている。また、TMLB'の途中では、一次冷却系ポンプのシール部が冷却不十分のために破損する可能性がある。ポンプシール部が破損する冷却材喪失事故（LOCA）シーケンスを S3-TMLB'と呼ぶ。本報告書では、4 ループ PWR である Indian Point 3 号炉の TMLB'シーケンスとその一次系強制減圧に関する解析結果について記述する。また、一次冷却系の減圧がある場合と無い場合の S3-TMLB'シーケンスの解析結果を記述する。解析で使用した計算コードは MELCOR1.8.4 であり、合計 7 ケースに対して計算を行った。

TMLB' シーケンスでは、一次冷却系圧力が PORV 開閉圧力に保たれたまま、デブリが下部ヘッドに落下して原子炉圧力容器が破損し、高圧溶融物放出が起きる可能性がある。一方、TMLB'中にポンプシール破損が起きると、その破損タイミングによって事故進展への影響が異なる。たとえば、TMLB'開始後 10 分でポンプシールが破損すると、ポンプシールが破損しない場合と比べて炉心損傷が早まるのに対し、ポンプシール破損のタイミングが遅れると、炉心損傷開始は 2000 秒から 1 時間程度遅れる結果となった。TMLB'中に加圧器逃がし弁（PORV）を強制的に開放して減圧を行った場合の炉心損傷の進展は、減圧を行わない時のそれとほぼ同じであった。しかしながら、減圧に使用する弁として安全弁（SRV）も加えた場合には、事故進展が約 6000 秒遅れた。同様の影響を S3-TMLB'シーケンスに対して調べた結果、減圧操作を行うことにより、事故進展が約 3000 秒遅れることが明らかになった。

東海研究所：〒319-1195　茨城県那珂郡東海村白方白根 2-4
*　科学技術庁フェローシップ研究員（インドネシア原子力庁）
**　核燃料サイクル開発機構

This is a blank page.

CONTENTS

目　次

This is a blank page.

LIST OF TABLES

LIST OF FIGURES

ACRONYMS

DCH	:	Direct Containment Heating
ECCS	:	Emergency Core Cooling System
HPI	:	High Pressure Injection
HPME	:	High Pressure Melt Ejection
LOCA	:	Loss-of-Coolant Accident
LPI	:	Low Pressure Injection
MSIV	:	Main Steam Isolation Valve
MSRV	:	Main Steam Relief Valve
MSSV	:	Main Steam Safety Valve
PORV	:	Power Operated Relief Valve
RCS	:	Reactor Coolant System
RN	:	Radionuclide
RPV	:	Reactor Pressure Vessel
SBO	:	Station Blackout
SG	:	Steam Generator
SRV	:	Safety Relief Valve

1. INTRODUCTION

Accidents leading to severe core damage have been one of the major reactor safety issues after the TMI-2 and the Chernobyl accidents. Since, severe accident research programs are performed with the objectives are, among others, to understand physical phenomena and to develop analytical methods to predict such phenomena. One of the analytical tools for severe accident analysis is the MELCOR code[1]. MELCOR is being developed at Sandia National Laboratories (SNL) for the U.S. Nuclear Regulatory Commission (USNRC) as a second-generation plant risk assessment tool and the successor to the Source Term Code Package (STCP)[2]. Initially, the MELCOR code was envisioned as being predominantly parametric with respect to modeling complicated physical processes. However, over the years as phenomenological uncertainties have been reduced and user expectations and demands from MELCOR have increased, the models in the MELCOR code is gradually being mechanistic, but the code is still parametric. The MELCOR version 1.8.4[3] is released to users in July 1997.

Meanwhile, recent PSA level I for PWRs has shown that an accident initiated from a total station blackout, so-called TMLB′, is one of the dominant accidents leading to severe core damage[4]. Moreover, TMLB′ sequence would result in a high pressure melt ejection (HPME) of which consequence may lead to direct containment heating (DCH) and early failure of the containment building.

In the past, several analytical studies of TMLB′ accident had been performed. As a part of MELCOR 1.8.2 assessment program, Kmetyk et al.[5] performed a calculation of Surry station blackout. In their study, TMLB′ was analyzed in conjunction with DCH study. Then, Heames and Smith[6] conducted Surry station blackout accident study using integrated MELPROG/TRAC code. The study included the analysis of the coolant pump seals failure. A similar study had been performed by Hidaka et al.[7] for Surry plant using SCDAP/RELAP5 code. The analysis was compared with the experimental studies conducted in ROSA-IV program. Recently, Hidaka et al.[8] performed another analytical study with SCDAP/RELAP5 and ART codes to evaluate the integrity of Steam Generator U-tubes during Surry station blackout accident.

On the other hand, as a part of severe accident mitigation strategies, an intentional reactor coolant system (RCS) depressurization during TMLB′ was proposed. The analytical studies are performed by, among others, Chambers et al.[9] and Brownson et al.[10]

The current study was performed to assess the PWR system responses during Station Blackout accident and to investigate the fission products (FP) decay heat on the accident progression. The MELCOR 1.8.4 code is used because it represents an integral RCS and containment analyses code, and can treat both thermal-hydraulics and FP behavior during accident progression. Concerning the system design, the Indian Point 3, a Westinghouse PWR 4 loops with thermal power of 3025 MWth was chosen as studied plant. The analyses include variations on TMLB′ sequence, such as primary pump seal leakage (namely RCP seal LOCA or S3-TMLB′), an intentional RCS depressurization, and variation between both events. The calculation results might be considered for developing the severe accident management strategies. This report describes and discusses the calculation results obtained.

2. PLANT DESCRIPTION

The MELCOR analyses described in this report were based on the Indian Point Power Station 3. Operated by Consolidated Edison Company of New York (Con Ed), it is located adjacent to and south of Indian Point 1 on the east bank of the Hudson River, at Indian Point, Village of Buchanan in upper Westchester County, New York. The Indian Point 2 plant is adjacent to and north of Indian Point 1[11].

The Indian Point 3 is a 3025 MWt pressurized water reactor (PWR) designed and built by Westinghouse Electric Corporation. The Reactor Coolant System (RCS) is a four loop design, with a reactor coolant pump (RCP) and steam generator (SG) U-tube in each loop. In addition, one loop contains the primary system pressurizer. Figure 1 shows a schematic of Indian Point 3 RCS. Under normal operating conditions, the RCS operates at ~ 15,2 MPa (2235 psig), with a core inlet coolant temperature of 556.67 K (542.6 °F)and core exit coolant temperature of 588.78 K (600.4 °F). The RCS coolant flow rate during normal operation is 4,100 kg/s(32.55 10^6 lb/hr).

The reactor pressure vessel (RPV) contains the core, core barrel, core support structures, and control rod and instrumentation component structures (see Figure 2). Water from the SGs is pumped through the cold legs by the RCPs to the RPV inlet nozzles, transiting the downcomer and RPV lower plenum prior to passing through the lower core, the coolant flows out the top and exits the RPV via the outlet nozzles, flowing through the hot legs into the SGs again. The reactor core consists of 39,372 Zircaloy-4 clad fuel rods containing sintered UO_2 distributed in 193 fuel assemblies. The total fuel weight (as UO_2) is ~ 100,498 kg (221,600 lbs). The core active height is 3.6576 m (144 inches).

RCS over pressure control is assured by three safety valves set to open at a nominal pressure of ~16.9 MPa (2485 psig). Capacity of each safety valve is 52.91 kg/s (420,000 lb/hr). Two Power Operated Relief Valves (PORVs) are available, set to relieve RCS pressure when it reaches ~15.9 MPa (2335 psig). PORV nominal relief capacity is 22.55 kg/s (179,000 lb/hr).

Each loop contains a vertical shell and U-tube SG. Reactor coolant enters the inlet side of the channel head at the bottom of the SG through the inlet nozzle, flows through the U-tubes to an outlet channel and leaves SG through another bottom nozzle. The number of Inconel U-tubes in each SG is 3260 representing the total heat

transfer surface area of ~ 4127 m^2 (44,430 ft^2). Feedwater to the SG enters just above the top of U-tubes through a feed water ring. The water flows downward through an annulus between the tube wrapper and the shell and then upward through the tube bundle where it is converted to a steam-water mixture. The steam-water mixture passes the separator assembly. Each SG has a capacity to produce 417,6 kg/s(3,315,000 lb/hr) saturated steam at 51.36 MPa(755 psig).

Safety grade emergency systems are designed to protect the RCS in the event of an accident. The principal components of the Safety Injection System, which provide emergency core cooling system (ECCS) immediately following a loss of coolant accident (LOCA), are the accumulators (one for each loop), the three safety injection pumps (High Pressure Injection, HPI) and the two residual heat removal pumps (Low Pressure Injection, LPI). The accumulators, which are passive Engineered Safety Features because the gas forces injection, discharge into the cold legs of the reactor coolant piping when pressure decrease to 4.42 MPa (650 psig). Following small break which does not immediately depressurize the RCS to the accumulator discharge pressure, ECCS provide safety injection pumps. The safety injection pumps (high head) deliver borated water to two separate discharge headers. The flow from each header is injected into each of the four cold legs of the RCS. For large break LOCA, the RCS would be depressurized and voided coolant rapidly and a high flow rate is required to quickly recover the exposed fuel rods and limit possible core damage. To achieve this objective, one residual heat removal pump (high flow, low head) is required to deliver borated water to the cold legs of the reactor coolant loops. Two pumps are available in order to provide for an active component failure. Should normal feedwater flow be lost, the auxiliary feed water system (AFWS) is available to provide coolant to the steam generator secondaries. The AFWS has three pumps: two are driven by electric motors; the third is driven by a steam turbine. The AFWS takes suction from the condensate storage tank (CST).

The Reactor Containment completely encloses the entire reactor and RCS and ensures that essentially no leakage of radionuclide materials to the environment would result even if gross failure of the RCS were to occur. The Reactor Containment structure is a reinforced concrete vertical right cylinder with a flat base and hemispherical dome. A welded steel liner with a minimum thickness of 0.00625 m (1/4 inch) is attached to the inside face of the concrete to insure a high degree of leak-tightness. The

side walls of the cylinder and the dome are about 1.4 m (4 ft-6 inch) and 1.1 m (3 ft-6 inch) thick, respectively. The flat concrete base mat is 2.74 m (9 ft) thick with the bottom liner plate located on top of this mat. The bottom liner plate is covered with 0.9 m (3 ft) of concrete, the top of which forms the floor of the Containment. Containment volume is 73,906.97 m^3 (2,610,000 ft^3), and the design pressure is 0.32 MPa (47 psig, 61.7 psia). For the MELCOR analysis, a containment failure pressure of 1.0 MPa (147 psig, 161.7 psia) was used. Emergency containment heat removal is accomplished by the spray system. Figure 3 shows a cross section of the containment.

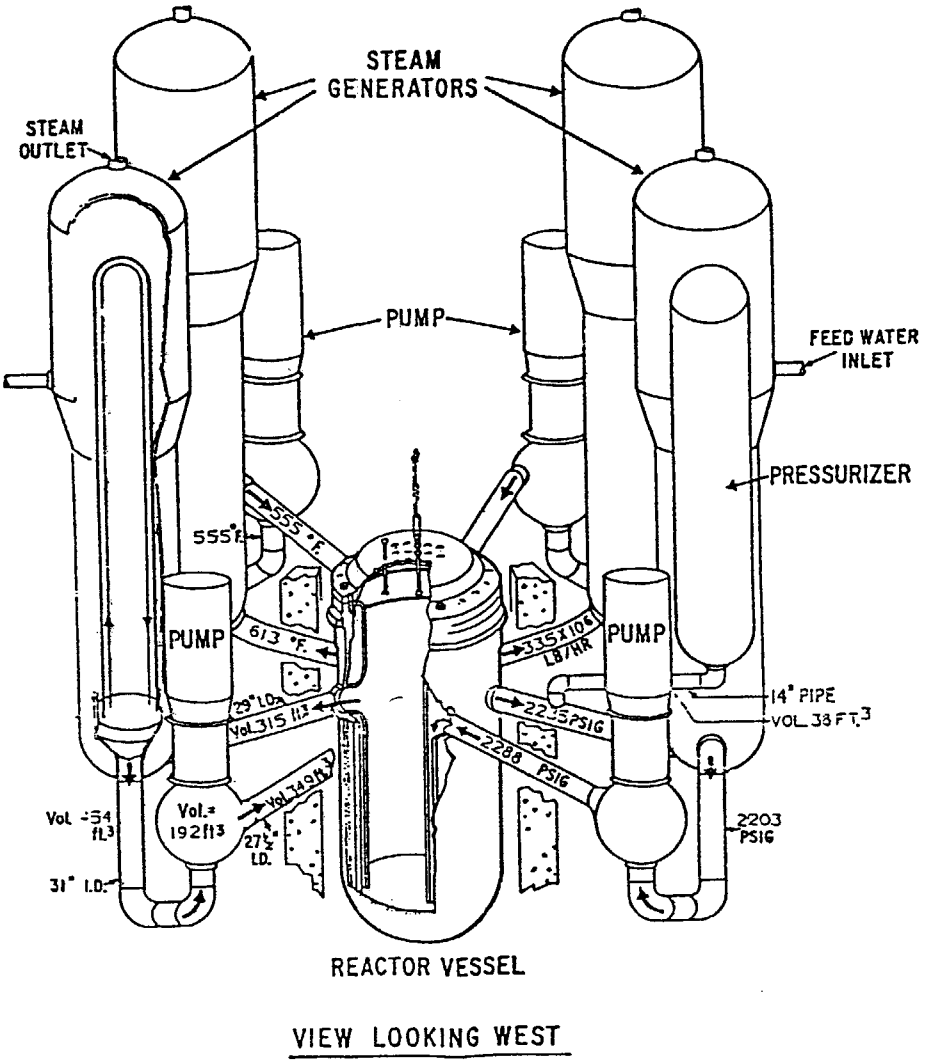

Figure 1. RCS of Indian Point 3[11)]

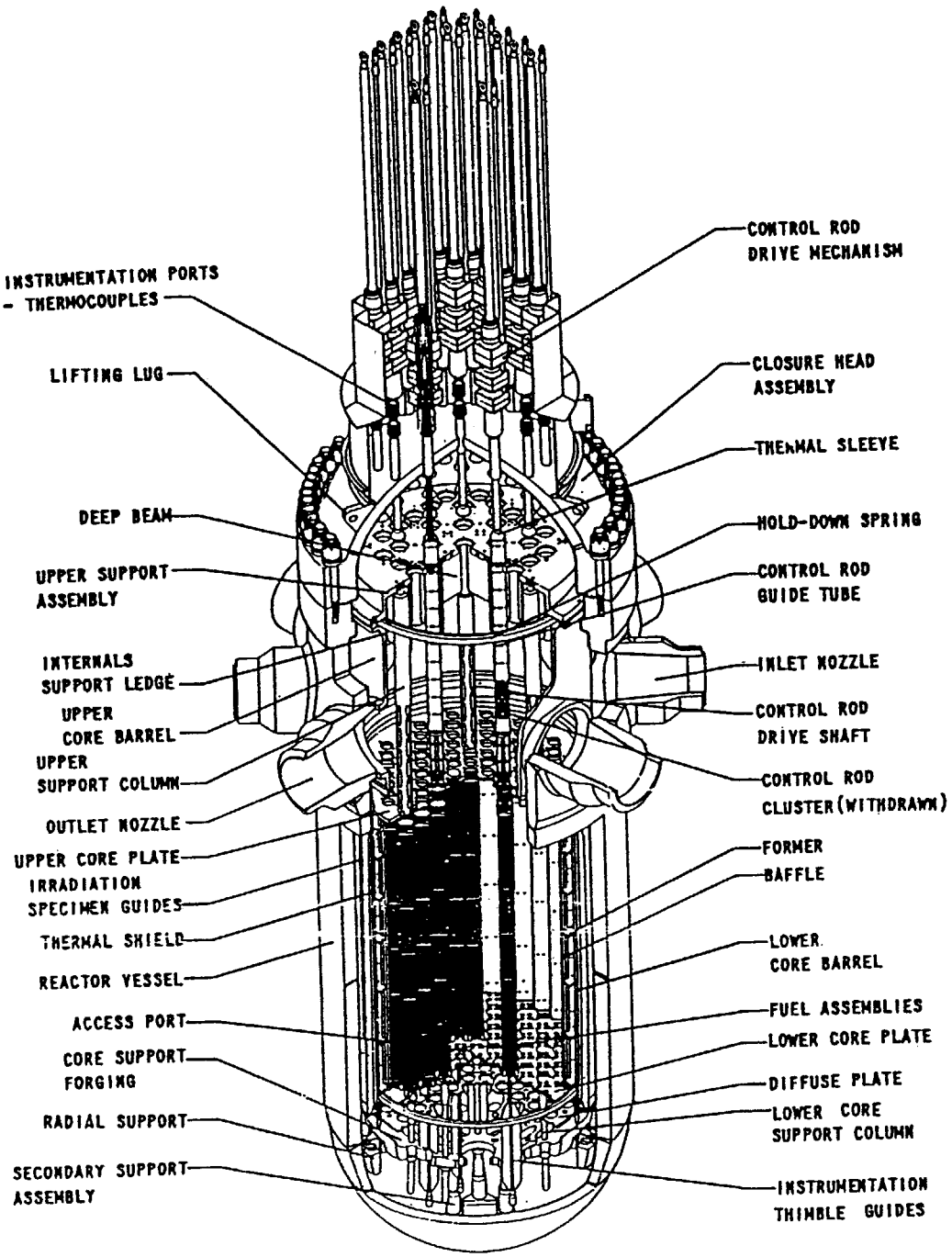

Figure 2. Reactor Vessel of Indian Point 3[11)]

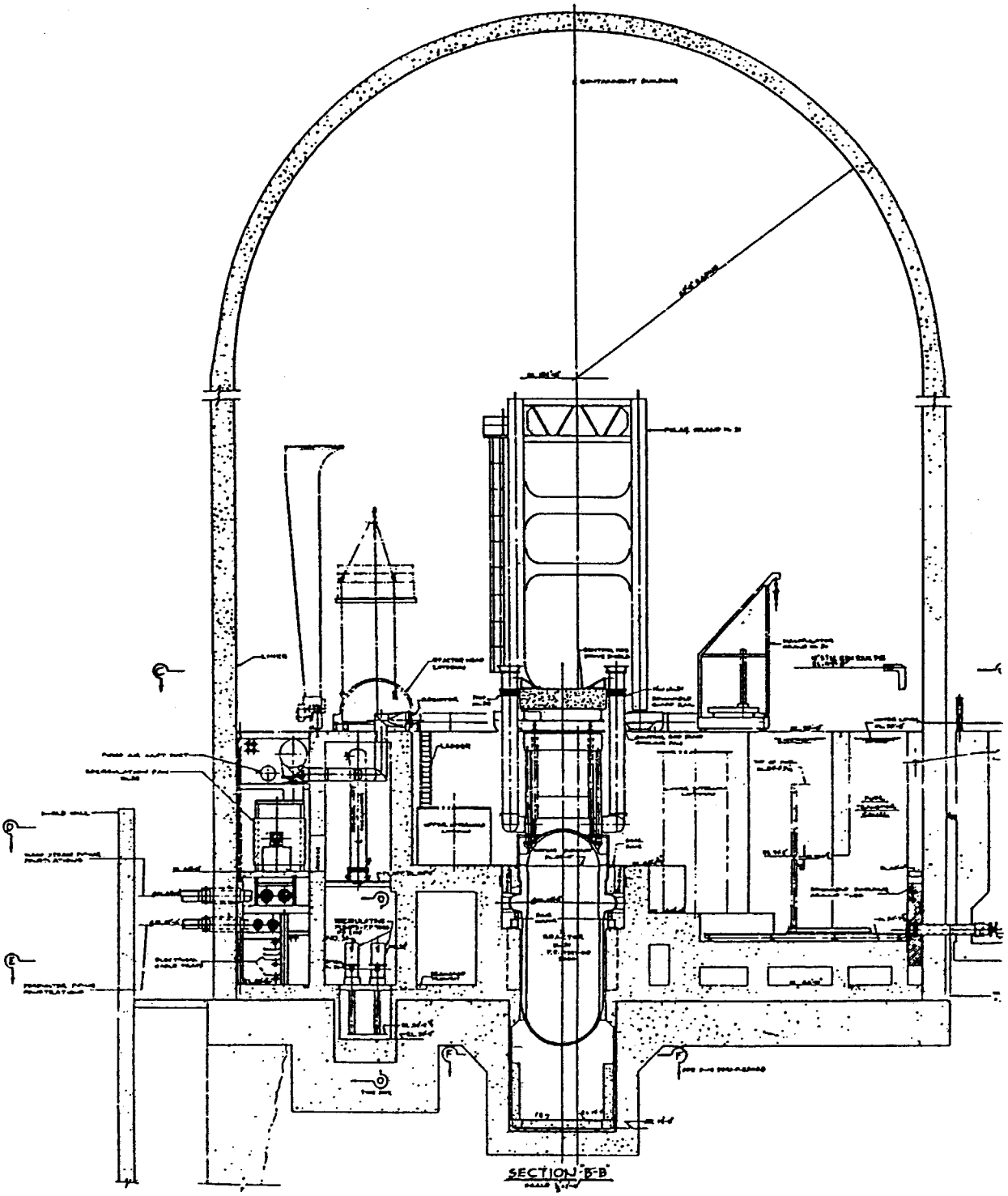

Figure 3. View of Containment of Indian Point 3[11)]

3. MODEL DESCRIPTION

The MELCOR 1.8.4 Indian Point 3 calculation model was originally prepared at JAERI. In the model, the four loops of RCS was modeled by two loops; one represents pressurizer attached loop (loop-A) and the other represents lumped of three other loops (loop-B). This calculation model has 39 control volumes (4 for the reactor vessel and internals, 21 for the primary system loops, 12 for the steam generator secondaries, 1 for the containment, and 1 for the environment); 44 flow paths (27 internal to the RCS, 14 associated with the steam generator secondary side, and 3 connecting the RCS to containment); and 65 heat structures (61 for the RCS and 4 for the containment). Figure 4 gives a schematic representation of the basic nodalization used for the primary, secondary system, the containment building, and environment. The bypass flow in reactor vessel and hot leg counter current natural circulation are not modeled. Two flow paths (226 and 276) were added to model the leakage for all pump seals.

All control volumes were specified to use nonequilibrium thermodynamics[3)] and were specified to be vertical or horizontal volumes; all heat structures used the steady-state temperature-gradient self-initialization option. Detailed volume-altitude tables and junction flow segments were used to correctly represent sub-components in and between the major components modeled.

The vessel was represented by four control volumes: the downcomer, lower plenum, core, and upper plenum and upper head. The pressurizer and the surge line were represented separately by the control volumes. The PORVs and SRVs were represented by valved flow paths from the top of the pressurizer to the containment, with hysteresis control functions used to govern opening and closing at the desired pressure set points. The emergency core cooling system (ECCS) was modeled with three control volumes with related flow paths for each loop representing the high pressure injection system (HPI), the low pressure injection system (LPI), and the accumulator.

The steam generator secondary side was modeled using three control volumes: for the downcomer, the riser (boiler) and the steam dome. The feed water flows into the downcomer from a defined condenser control volume. Two outlet flow paths were used to represent the main steam isolation valve (MSIV) which outlet to the condenser and the relief valves communicating with an ambient-environment control volume. The auxiliary feed water (AFW) was supplied

from condenser storage tank (CS) control volume into the riser.

The heat structures were generally specified to use the "internal" set of heat transfer coefficient correlations on the inside of most heat structures, while on the outside surface boundary, most the heat structures were specified to use "external" set of heat transfer coefficient correlation. The critical pool and atmosphere fractions were set to be 0.5 and 0.5, respectively, for most of the heat structure surfaces.

The reactor core nodalization (see also Figure 5), as a separate model from model listed above, consisted of 45 core cells divided in 15 axial levels and 3 rings. The axial level 1 through 3 modeled lower plenum, including the core support structure in level 4, while level 5 to 15 correspond to the active core region.

The radiation heat transfer in the core used the default values. The core material eutectic interaction model is disabled by default. Debris relocation model enabled by default, while the core plate and bottom head penetration failure temperatures, and the falling debris and lower head penetration heat transfer coefficients were all set to their default values in the MELCOR 1.8.4 calculation.

The cavity was specified to have an internal depth and radius of 7.925 m and 3.13 m, respectively with no initial layer content. The concrete thickness was 2.134 m both on the side and below the cavity. The standard concrete from CORCON was used with no change in the property.

One radionuclide (RN) class for CsI was added to the default class in the MELCOR 1.8.4 RN and DCH packages. The calculation was done using the CORSOR-M release model.

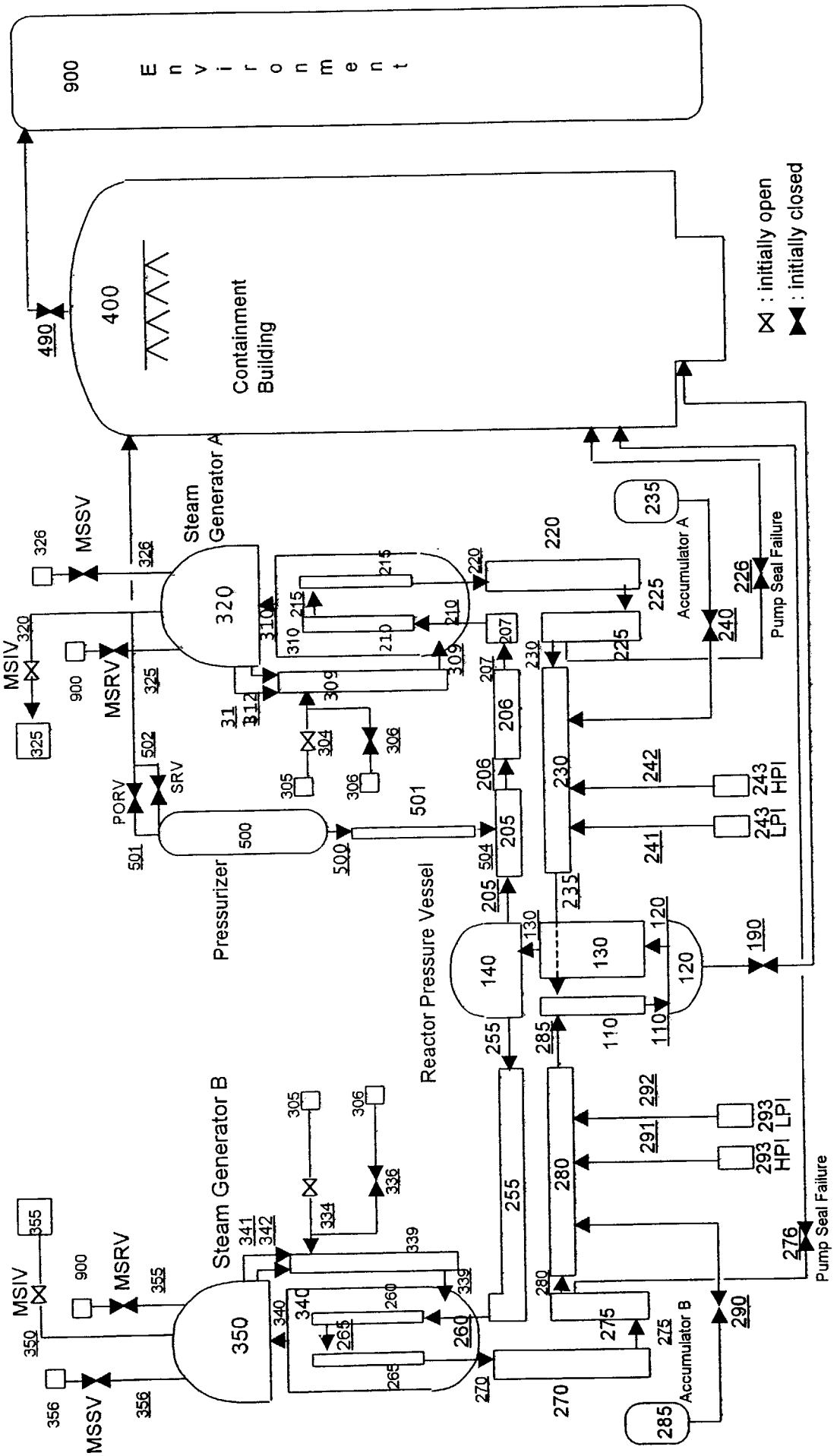

Figure 4. Nodalization Scheme for MELCOR 1.8.4. Analysis of Indian Point 3 Station Blackout

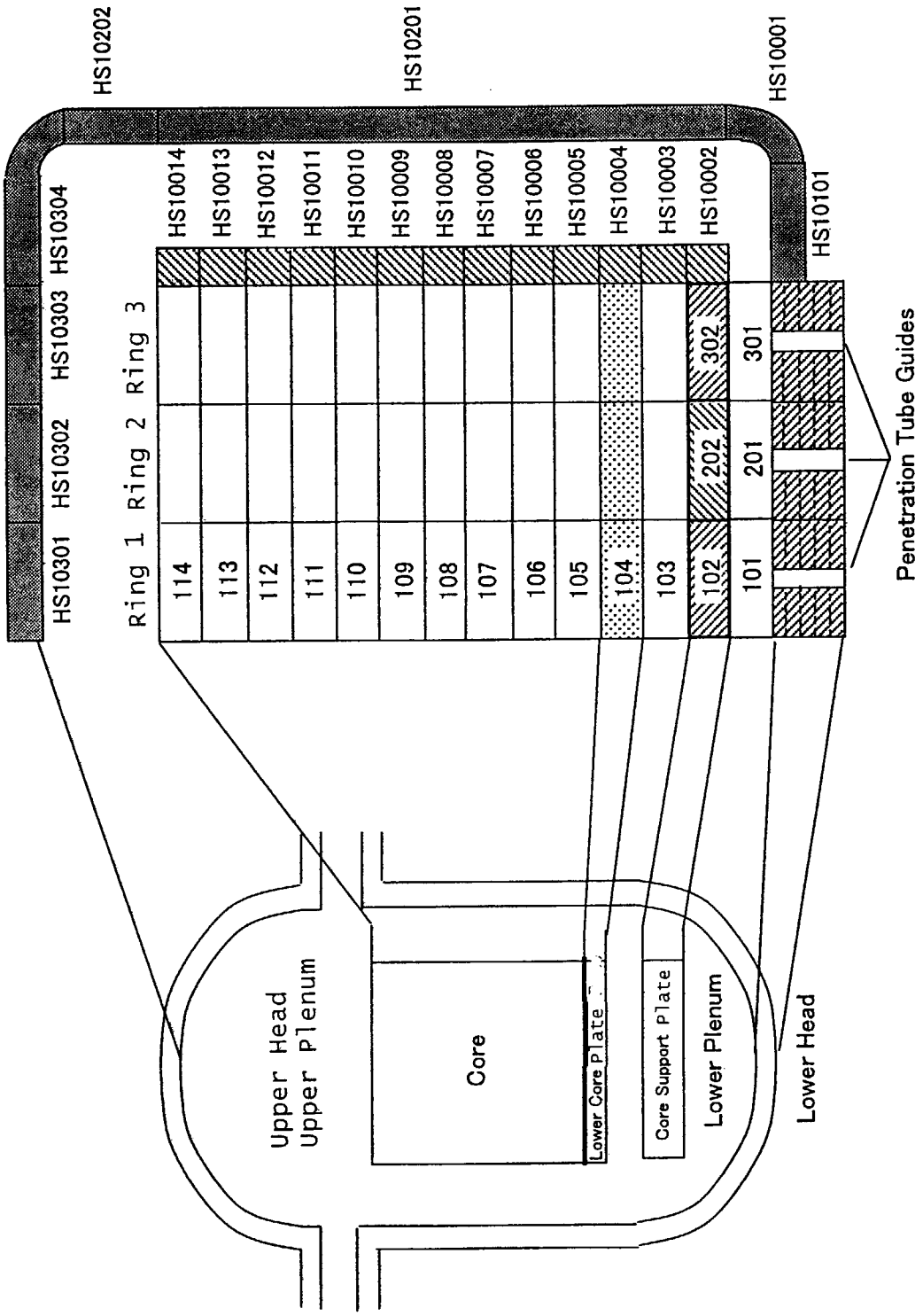

Figure 5. RPV Nodalization for Indian Point 3

4. ASSUMPTIONS

The major assumptions for present TMLB′ calculation are as follows:

1) The total thermal power (fission and decay heat power) during normal operation is 3025 MWth. As a default in MELCOR, it is assumed that the reactor was operated for 2 years full power operation before the accident.
2) Steady sate is calculated for 50 s before initiation of station blackout.
3) At 0 s, total station blackout occurs.
4) Reactor scram occurs with the delay of 1 s.
5) The scram signal trips the primary coolant pump, close feed water valve and main steam isolation valve.
6) The auxiliary feed water pumps are unavailable.
7) The high and low pressure injection systems are unavailable. The accumulator injection is set up when primary system pressure decrease less than 4.42 MPa.
8) The oxidation of zirconium starts at 1000 K.
9) The cladding failure occurs when the cladding temperature reaches 1173 K.
10) The lower head penetration failure is assumed when the temperature of the penetration reaches 1273.15 K (TPFAIL).
11) The lower head failure allowing a debris ejection occurs when the temperature of bottom lower head node exceeds TPFAIL. And, a total molten mass of 5000 kg or a melt fraction of 0.1 is necessary before debris ejection initiation (default of MELCOR 1.8.4).

Those assumptions were used for all calculation in this study. The other assumptions related to specific case (specific run) studied will be given later.

5. CALCULATION MATRIX

Several analytical calculations are performed in this study. All calculations are related to the total station blackout initiating accident (TMLB'). The TMLB' sequence is analyzed as a reference case. The variation of TMLB' sequence analyzed includes primary pump seal leaks during station blackout (S3-TMLB'), and an intentional RCS depressurization by pressurizer PORVs latched open as a part of an accident mitigation. Table 1 shows the calculation matrix done in this current study. Seven runs have been performed as shown in Table 1. All calculations concern on accident sequence during 20,000 s, including 50 s of steady state calculation.

The run 1 is related to TMLB' sequence and used as reference calculation. The runs 2, 2A and 2B concern on TMLB' with RCP seal LOCAs (S3-TMLB') sequence. The difference of these three calculations is the timing of the pump seal leakage initiation. In the transient phenomena, it is believed that the timing is an important parameter, because it determines the boundary conditions of the system studied. The run 2 is performed using similar assumptions used in the previous studies, i.e. the seals fail when the coolant in core reached the saturation temperature. The run 2A assumed early failure of pump seals, at about 10 minutes after Station Blackout (SBO) initiation. At that time the coolant in the core is in subcooled condition, and all steam generators are still "wet". On the other hand, the run 2B represents late failure. The pump seals of all loops are assumed to fail at about 2.5 hr. after SBO initiation. At that time, the steam generators are "dry", the core upper region is already uncovered, and began to heat up.

From the view point of the severe accident management strategies, the occurrence of early containment failure due to DCH must be avoided. Therefore, one proposed strategy for mitigating DCH is to reduce the pressure in the RCS so that the ejected core material would not be finely fragmented and widely dispersed. Because the RCS pressure must be significantly reduced for the strategy of intentional depressurization to be effective, investigation of the capability to rapidly depressurize RCS has to be performed. The run 3 calculates the TMLB' sequence with intentional RCS depressurization through PORVs latched open. In this study, the timing of PORVs latched open is similar to time proposed at ref.10, i.e. when the exit core temperature fluid reaches 922 K. The reason of late depressurization is that it permits to more rapid RCS depressurization because the quality of the PORV discharge

was higher[10]. While, the run 3A is a variation of run 3, where it is assumed that beside PORVs, the safety relief valves (SRVs) are also latched open. The timing of valves opening is the same as in run 3. This calculation was performed to investigate the depressurization rate on the accident progression by increasing of flow area of discharging valves.

The run 4 is conducted to study the accident mitigation in the case of S3-TMLB′ accident by intentional RCS depressurization. The assumptions in the runs 2 and 3A are used.

Table 1. Calculation matrix.

Run No.	Sequence Description	Remarks
1	TMLB′	Reference calculation
2	S3-TMLB′	Pump seals fail when coolant in the core reaches saturation temperature
2A	S3-TMLB′	Pump seals fail 10 minutes after station blackout initiation (early failure)
2B	S3-TMLB′	Pump seals fail at 2.5 hr. after initiation of station blackout (late failure)
3	TMLB′ with an Intentional RCS de-pressurization	Pressurizer power-operated-relief valves (PORVs) are intentionally latched open when core exit temperature reaches 922 K.
3A	TMLB′ with an Intentional RCS de-pressurization	Pressurizer power-operated-relief valves (PORVs) and safety relief valves (SRVs) are intentionally latched open when core exit temperature reaches 922 K.
4	S3-TMLB′ with an intentional RCS Depressurization	Pump seals fail when coolant in the core reaches saturation temperature, and PORVs and SRVs are latched open when core exit temperature is 922 K.

6. RESULTS AND DISCUSSIONS

6.1 TMLB′ (Run 1)

6.1.1. Accident Sequence

The total loss of power during station blackout caused the primary coolant pumps coasted down, reactor scrammed and, the auxiliary feed water system was unavailable. The last led to secondary coolant inventory boiled off and dried out while the decay heat being transferred from the core. After that, the temperature and the pressure of the primary system increased. The water vented out through PORVs when it reached the top of pressurizer. Then, the water level in reactor vessel decreased progressively. The reactor core started to heat up when it uncovered. The cladding temperature increase was accelerated by Zr-water reaction. When the melting temperature was exceeded, the debris formed, and relocated downward. Once reaching the core support plates, the support plates temperature increased and failed. The debris fell into the lower plenum and relocated at lower head vessel. The heat transferred from debris to vessel wall by conduction caused the lower head penetration to fail while the primary system pressure was still at PORV set point.

The Table 2 gives the timing of key events predicted by run 1.

6.1.2. System Response

(1) Primary Coolant Flow Rate

Figure 6 shows the primary coolant flow rate during TMLB′ sequence. After the loss of power in the station blackout, the primary coolant pumps coasted down from full power to zero in approximately 300 s. Then, primary system coolant flow was driven by natural circulation. During that time, the heat being generated by the core continued to be transferred to the steam generators even after loss of pumped flow. The natural circulation ceased practically at about 8,800 s (2.4 hr) due to increase of voiding of the primary system. It is noted that the hot leg countercurrent vapor flow was not taken into account in the present calculation.

(2) Primary Pressure

At the beginning of the accident initiation, due to the loss of pumped power flow, primary coolant circulation decreased causing the heat removal decreasing and, accordingly, the primary coolant temperature increased, and

then the pressure went up (see Figure 7). The pressure reached quickly at PORVs set point. But, the pressure decreased when the heat is effectively transferred to the SG secondary side due to loop natural circulation during the boil off of secondary coolant inventory. After the secondary side coolant inventory dried out, the pressure rose again, and reached the PORVs set point at 5961 s. The PORVs cycled, open and close according to the pressure value. The pressure increased momentarily above the PORVs set point at about 8000s because the PORVs began venting liquid and the PORVs does not have the capacity to remove decay heat by venting liquid. At the timing of the vessel failure, the pressure fell very rapidly, causing the accumulator to deliver the borated water to the core almost instantaneously.

(3) Water Level in Pressurizer

Figure 8 gives the calculation result of the water level in the pressurizer. After the SG secondary side boiled off at about 5000 s, the water level in the pressurizer increased continuously up to the top of pressurizer (at 6360 s). Beyond that time, water was vented through pressurizer PORVs. At 8220 s, the water level started to decrease slowly. Just before RPV failure, about 60% of pressurizer volume was still filled with water.

(4) Water level in Reactor Vessel

Figure 9 shows the swollen water level in upper plenum and upper head, core and lower plenum. The water level in upper plenum began to decrease at about 7400 s. At about 7439 s, the coolant in the center part of core was effectively at saturation temperature. The leak of coolant liquid through pressurizer PORVs accelerated the water level decreased. At about 7980 s, water reached the top of the core. The water level continued to drop, and the core was no longer covered by the water coolant. The core was completely uncovered at about 13,023 s. At about 13,600s, all the coolant inventory blew down due to the lower head penetration failure.

(5) SG secondaries coolant inventory

With continued heat transfer from the primary system and with no feed water nor auxiliary feed water supply available to replenish the secondary system, the secondary coolant started to boil off at about 500s. Because the MSIV was closed, the secondary side pressure quickly rose to the MSRVs set point, and the heat from the primary was removed with the steam vented out the relief valve. Dry out of the

secondary side occurred at about 5000 s (1.4 hr), as illustrated by the SGs secondary side liquid levels in Figure 10.

(6) Core damage

As stated above, the loss of primary coolant through the PORVs led to a progressive uncovery of the core. The core heat up started at uppermost part at about 8900 s, but the temperature rose significantly only when the coolant level reached approximately the middle of the core (at 10,620 s). At that time, the fuel cladding temperature in all rings began to rise as shown in Figures 11, 12 and 13. The upper most temperature rose earlier because it was uncovered first and the innermost ring rose faster because highest-powered. The oxidation of zircaloy cladding started to occur just before the cladding failed, at 11,400 s, as could be seen from Hydrogen generation shown in Figure 14. The gap release occurred at 11,492 s, 11,612 s and 11,889 s for Ring 1, Ring 2, and Ring 3, respectively.

The fuel and cladding temperatures continued to increase without interruption until the failure limit was exceeded. The debris was formed when the temperature reached the melting point or when the core material was no longer supported by other intact metal material (particulate debris). The debris from upper part relocated downward to the lower cell. The core support plate failed when the limit temperature was exceeded. At 13,600 s, the core support plate at ring 2 was failed (see Figure 15) allowing particulate debris to fall through into the lower plenum. At the time of lower head penetration failure, about 33 tons of UO_2 debris was relocated in three rings of lower head vessel. Figures 16, 17 and 18 show the debris mass in the lower plenum.

The temperature of the lower head penetration in ring 2 rose quickly above the failure temperature of penetration guide tube (1273.15 K). The vessel breach occurred at 13,603 s with an initial diameter of hole of 0.19 m. It caused all of coolant inventory remained in lower plenum was discharged out of the vessel, and the pressure decreased almost instantaneously. Even though, as modeling in MELCOR, the ejection of debris would occur when the melt fraction of debris reached 0.1; in this calculation it occurred at about 17,000 s.

(7) Radionuclide release

The loss of integrity of the fuel cladding caused the radionuclide resided in the gap between fuel and cladding

to be released in the core and primary coolant system. The Radionuclide package in MELCOR calculates the release and transport behavior of fission product vapors and aerosols. By default the release models are used to calculate the release of radionuclide from core fuel material only, which exists in the intact fuel component, a refrozen fuel material on other components and in particulate debris.

Rather than tracking all fission product isotopes, the masses of all the isotopes of an element are modeled as a sum, which then, according to the similar chemical behavior, are combined into material classes. As the default, MELCOR 1.8.4 considers 15 material classes. However in this study, one class of CsI was added. The combination of Cs and I to form CsI molecules occurs instantaneously upon release and modeled by moving stoichiometric amounts of Cs and I masses.

Figure 19 shows the radionuclide mass released from fuel in the core control volume prior to vessel rupture. The noble gases class (Xe class) and alkali metals class (Cs class) were among the most important release; 147.5 kg of Xenon and approximately 100 kg of Cesium (if Cesium in CsI included). About 12 kg of CsI, and so Halogens class (I class), were also released in core. As for Chalcogens class (Te class), about 10 kg of radionuclide mass was released. The other radionuclide classes had minor contribution to the release.

Concerning the deposition of radionuclide mass, the calculation result showed that the deposited radionuclide mass was mostly found at the inside wall of pressurizer surge line. Some radionuclide masses were deposited at the inner wall of loop-A hotleg pipe closest to the RPV (control volume CV205, symbols HL1-AU is for upper part and HL1-AL for lower part of the wall). Figure 20 shows the deposited mass in the loop-A.

(8) Wall Temperature

With regard to RCS pressure boundary structural integrity, the pressurizer surge line and SGs U-tubes could be challenged by excesses in either pressure or temperature. So, the wall temperature observation will be focused on these two components.

Figures 21 shows the wall temperature of pressurizer surge line and steam generator U-tube. The wall temperature of pressurizer surge line started to increase after the onset of SG dry out. When the core was heated up, the temperature increase occurred quickly. A sharp peak of temperature occurred during the hydrogen generation in the

core. The surge line temperature began to decrease after 13,000s because coolant discharge through PORV became small due to decrease in steam generation in the core. On the other hand, the wall temperature of U-tubes increased after the secondary coolant inventory boiled off, and remained constant until vessel failure. In all cases the wall temperature was generally far below 1000 K.

Figure 22 shows the penetration guide temperature and the bottom lower head temperature. After relocation of the debris in the lower plenum, the penetration guide temperature increased rapidly exceeding the failure temperature.

6.1.3 Discussion

From the above results without hot leg counter current flow, it was predicted that during TMLB′, a vessel failure could occur at about 3.25 hr. after the TMLB′ initiation. At the time of vessel failure, the coolant pressure was at PORV set point. So, HPME was likely happen. The overall sequence trends predicted in the current calculation are similar with the previous TMLB′ studies, for example ref. 4. However, in the case that the hotleg countercurrent flow was taken into account, pressurizer surge line or hot leg could fail earlier than the RPV meltthrough (see ref. 16).

Concerning the vessel breach, as shown by the calculation result, it occurred approximately 50 s from the core support failure. This relatively fast failure relies to high heat transfer coefficient between debris and the lower head and the penetration guides, i.e. 1000 W/m^2K. This value is a default in MELCOR 1.8.4. The high value of heat transfer coefficient might be achieved if there is a perfect contact between debris and lower head wall. However, it is already well known that a gap between debris and lower head wall might grow as the structure deformed, increasing the thermal resistance between them. So, the values as low as 200 W/m^2K during a certain period after contact, or 500 W/m^2K in average, might be more reasonable[12].

Table 2. Sequence of Key Events for TMLB′(Run 1)

Events	Time ,s	/(hr)
Station blackout initiation	0	(0)
SG dried out	4981	(1.38)
RCS pressure at PORV set point	5340	(1.48)
Liquid at top of pressurizer	6360	(1.77)
Core coolant at saturation	7408	(2.06)
Start of core uncovery	7980	(2.22)
Start of oxidation*	11,400	(3.17)
Gap release		
Ring 1	11,492	(3.19)
Ring 2	11,612	(3.23)
Ring 3	11,889	(3.30)
Core completely uncovered	13,023	(3.62)
Core support plate failure		
Ring 1	15,823	(4.39)
Ring 2	13,550	(3.49)
Ring 3	15,398	(4.28)
Lower head penetration failure		
Ring 1	15,449	(4.29)
Ring 2	13,603	(3.78)
Ring 3	13,634	(3.79)
Debris ejection	17,000	(4.72)

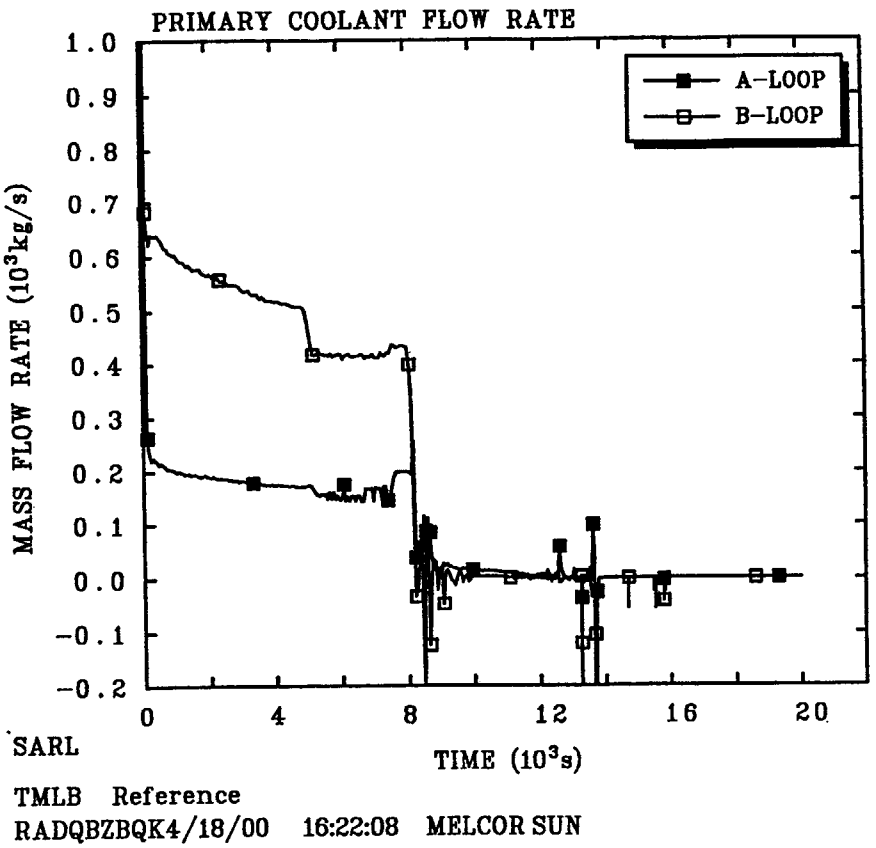

Figure 6. Run 1: Primary coolant flow rate

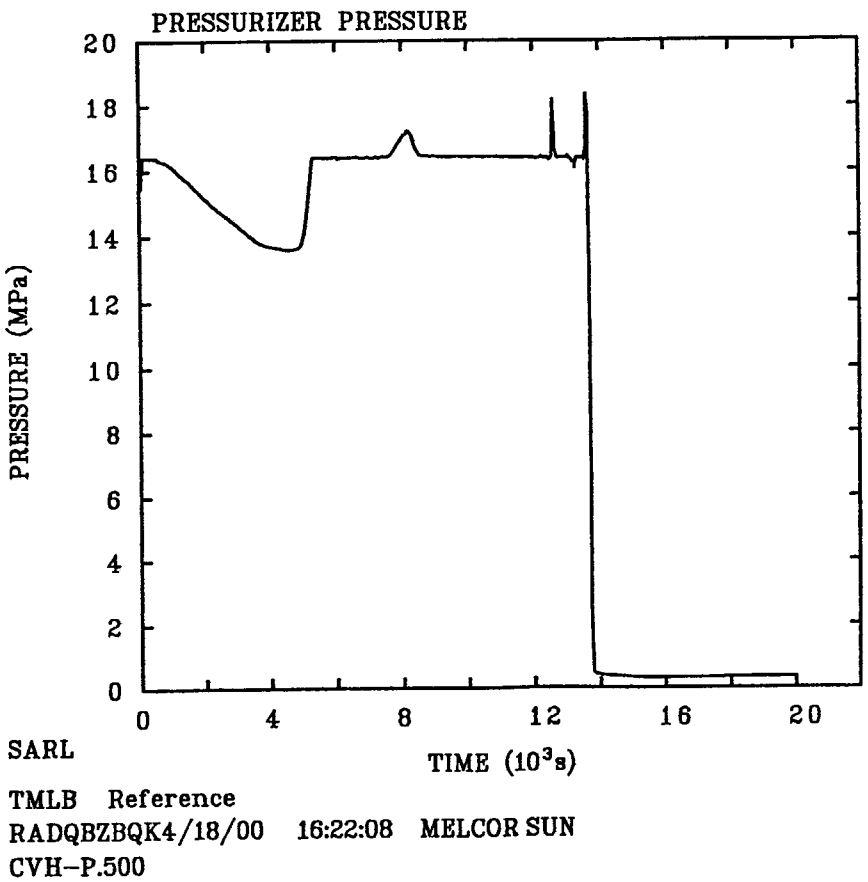

Figure 7. Run 1: Pressurizer pressure

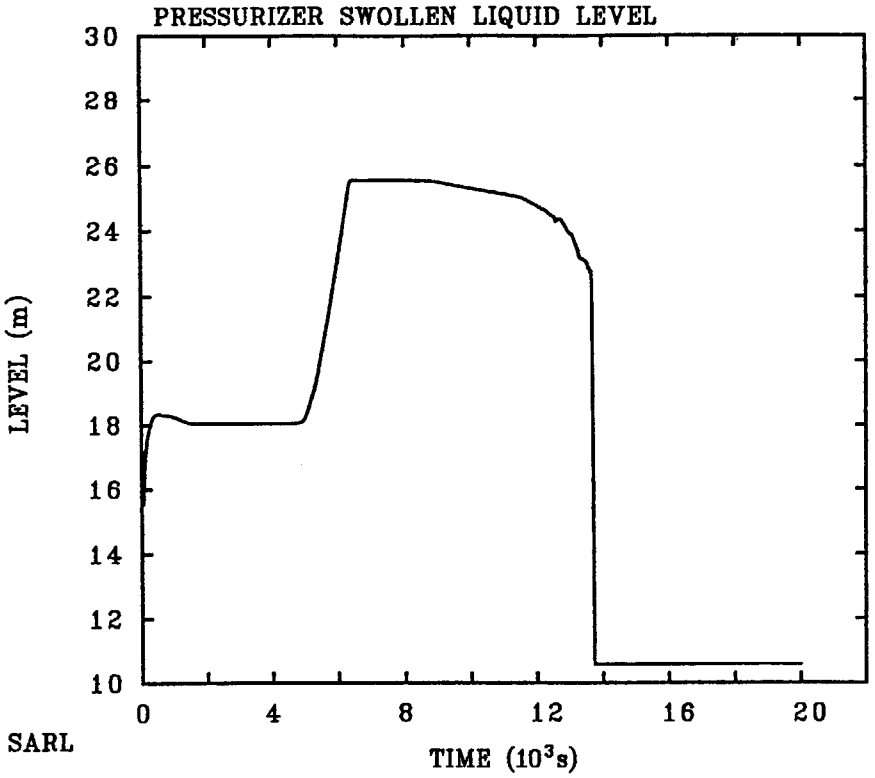

Figure 8. Run 1: Swollen liquid level in pressurizer

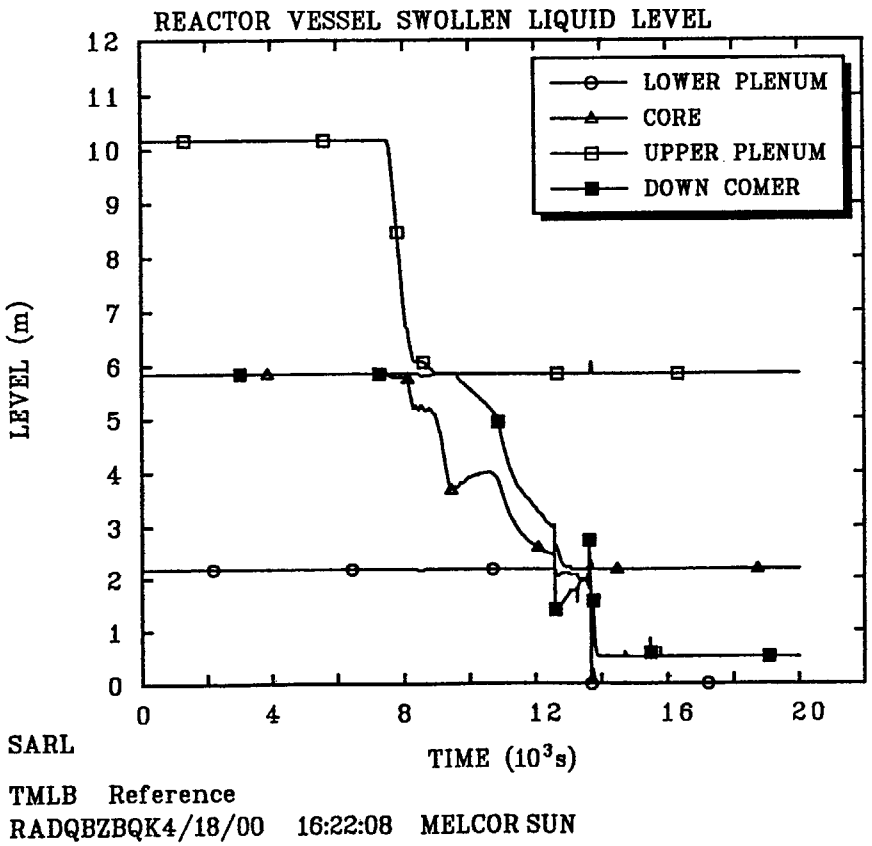

Figure 9. Run 1: Swollen liquid level in reactor vessel

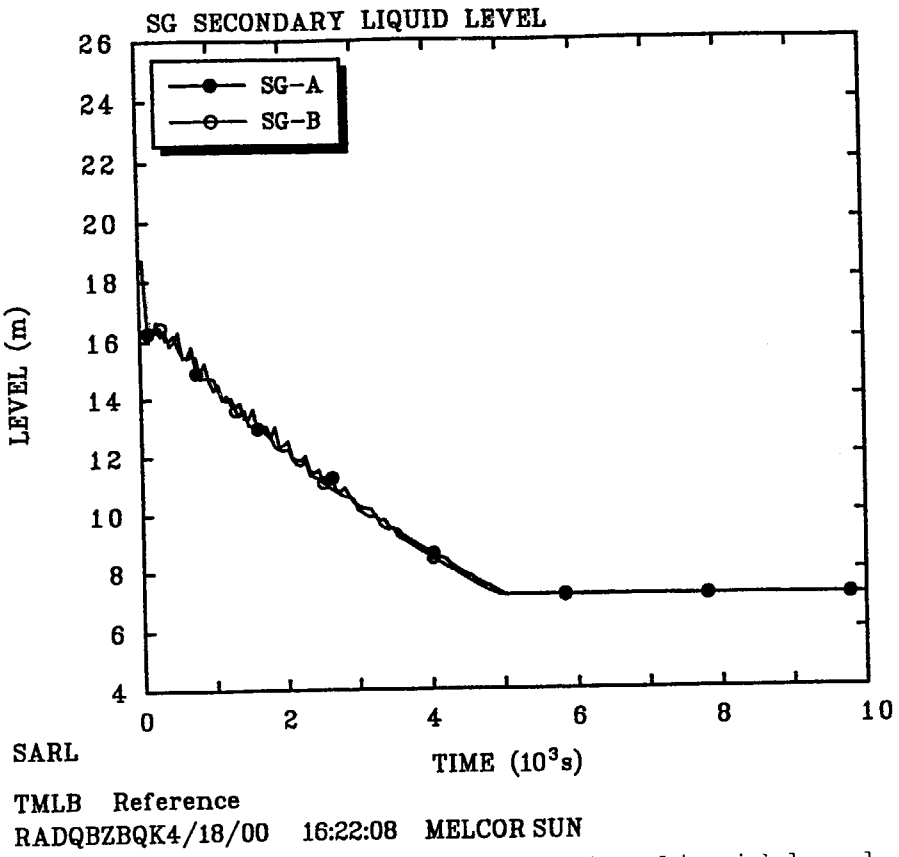

Figure 10. Run 1: SGs secondaries liquid level.

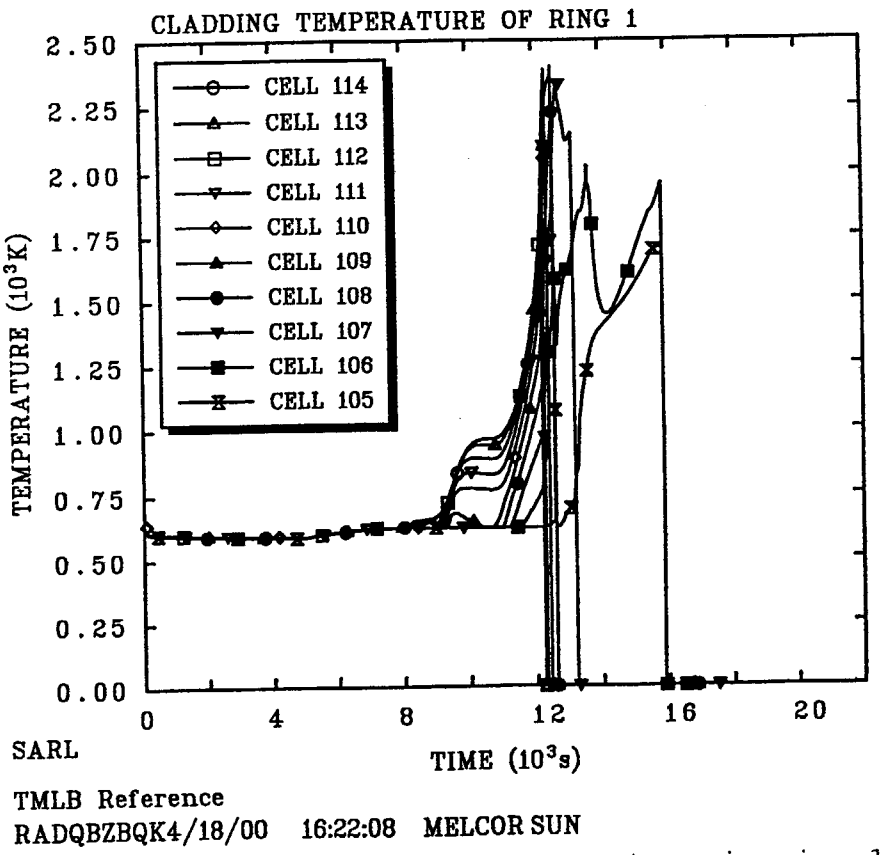

Figure 11. Run 1: Cladding temperature in ring 1.

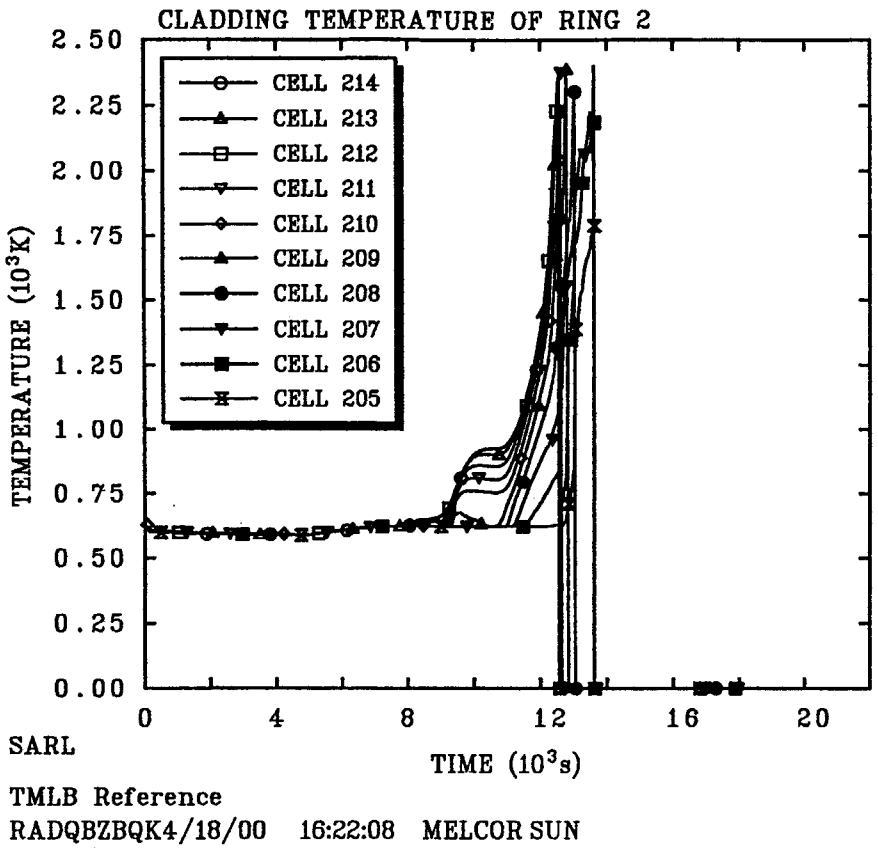

Figure 12. Run 1: Cladding temperature in ring 2.

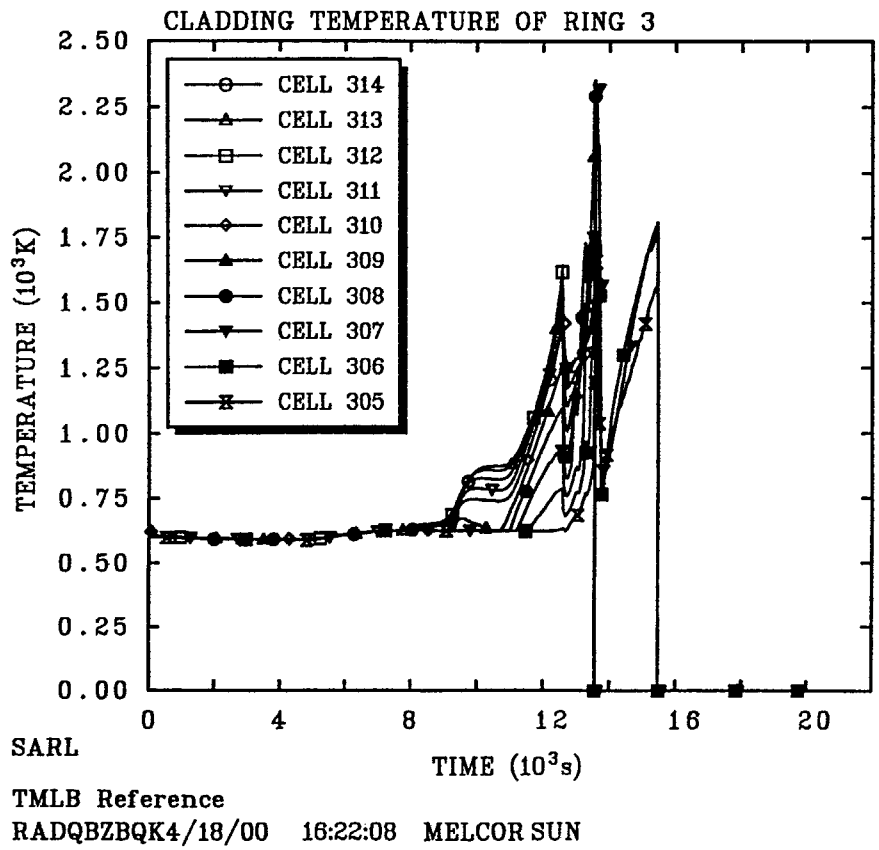

Figure 13. Run 1: Cladding temperature in ring 3.

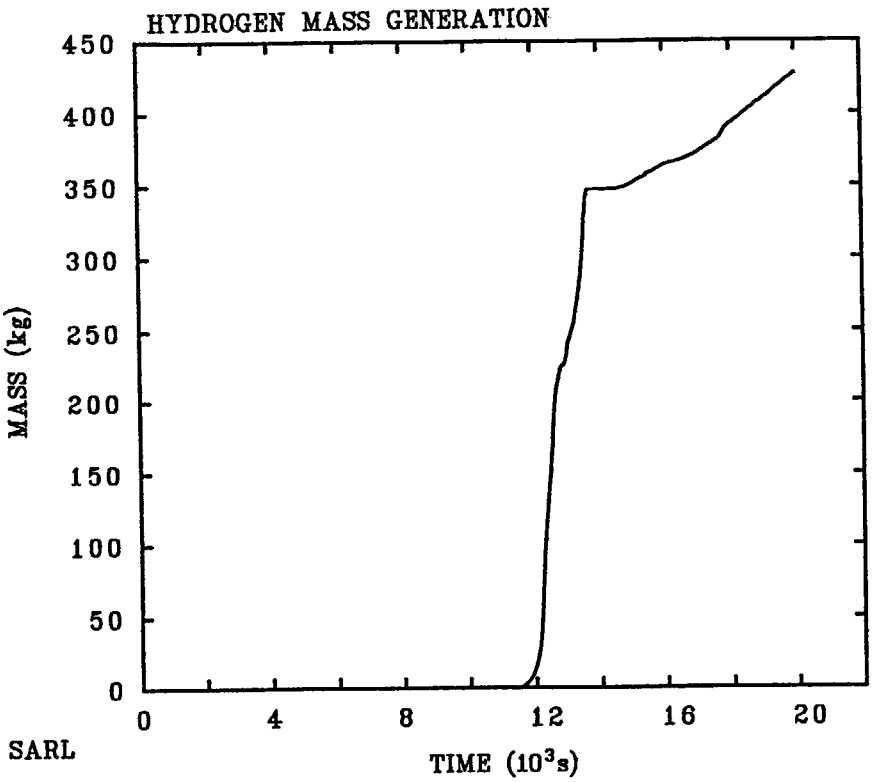

Figure 14. Run 1: Hydrogen mass generated.

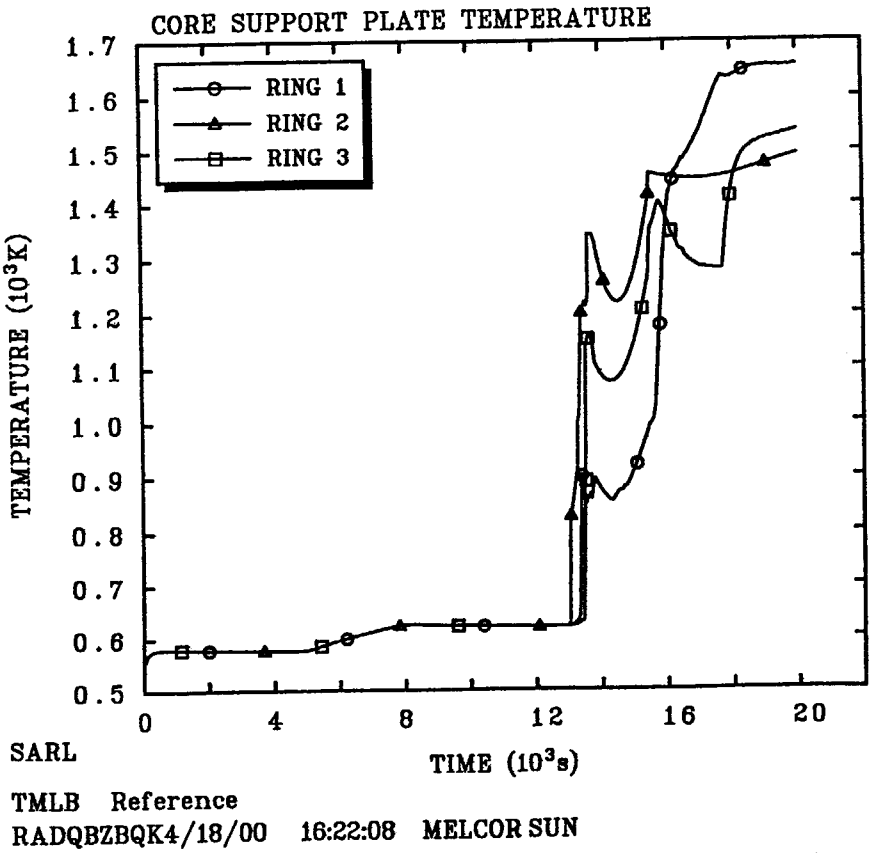

Figure 15. Run 1: Core support plate temperature.

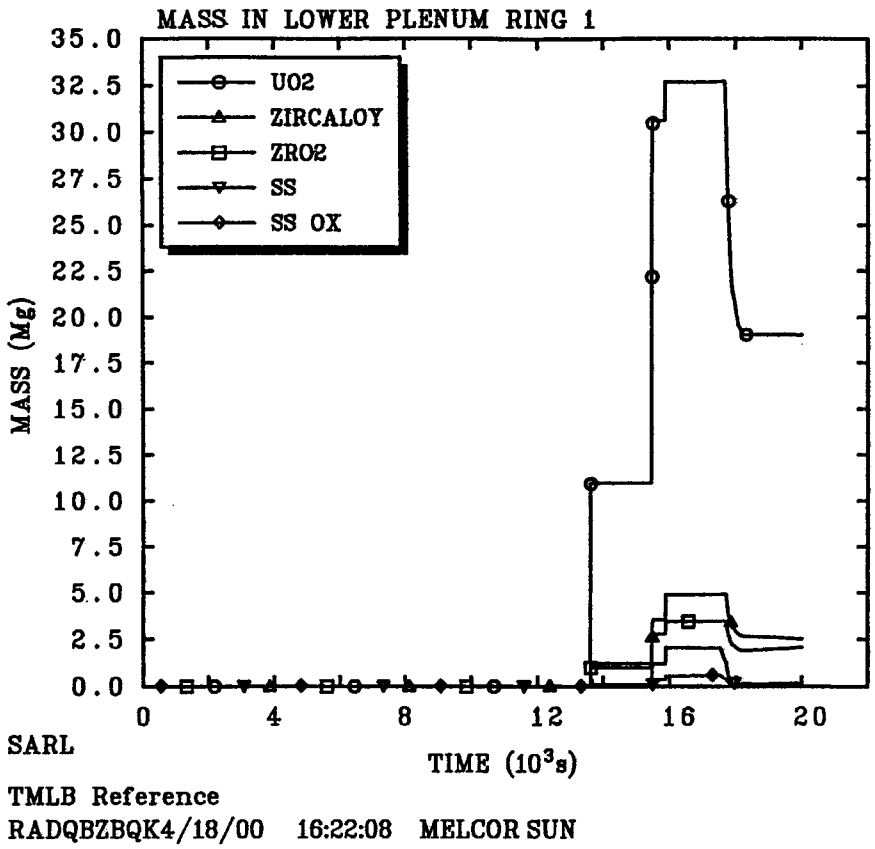

Figure 16. Run 1: Debris mass in lower plenum ring 1.

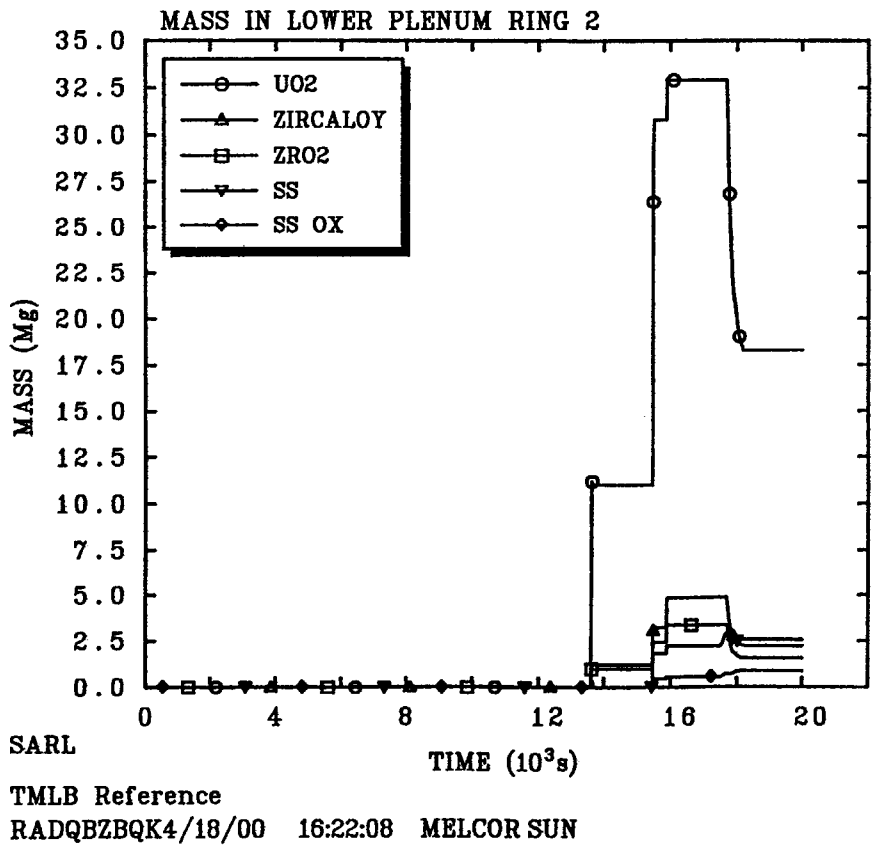

Figure 17. Run 1: Debris mass in lower plenum ring 2.

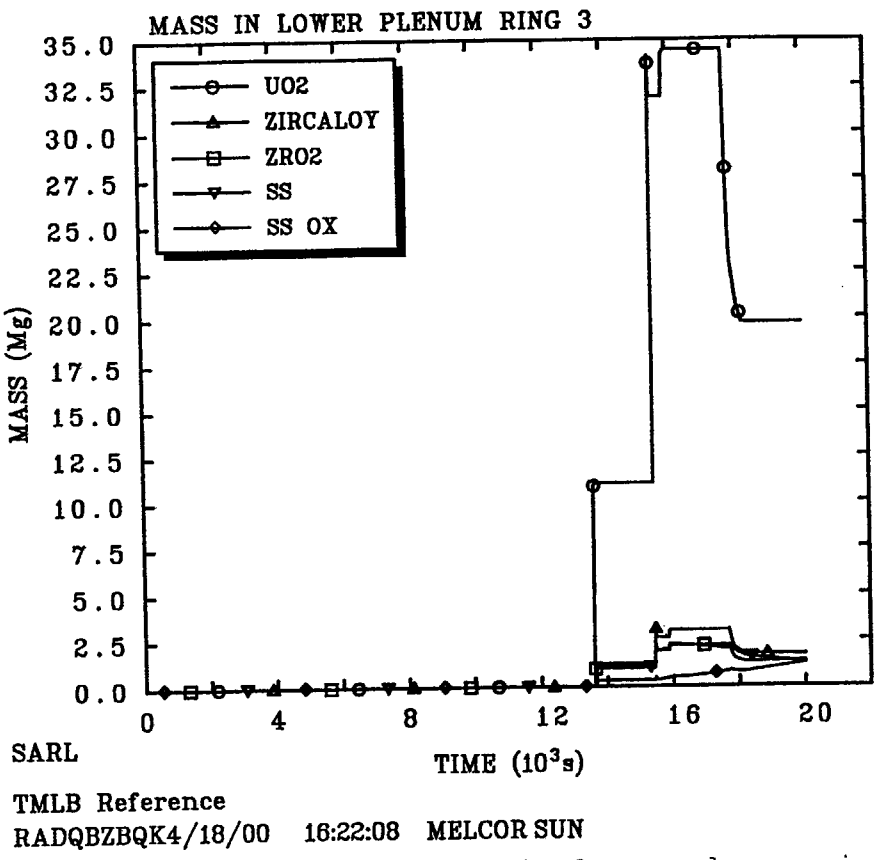

Figure 18. Run 1: Debris mass in lower plenum ring 3.

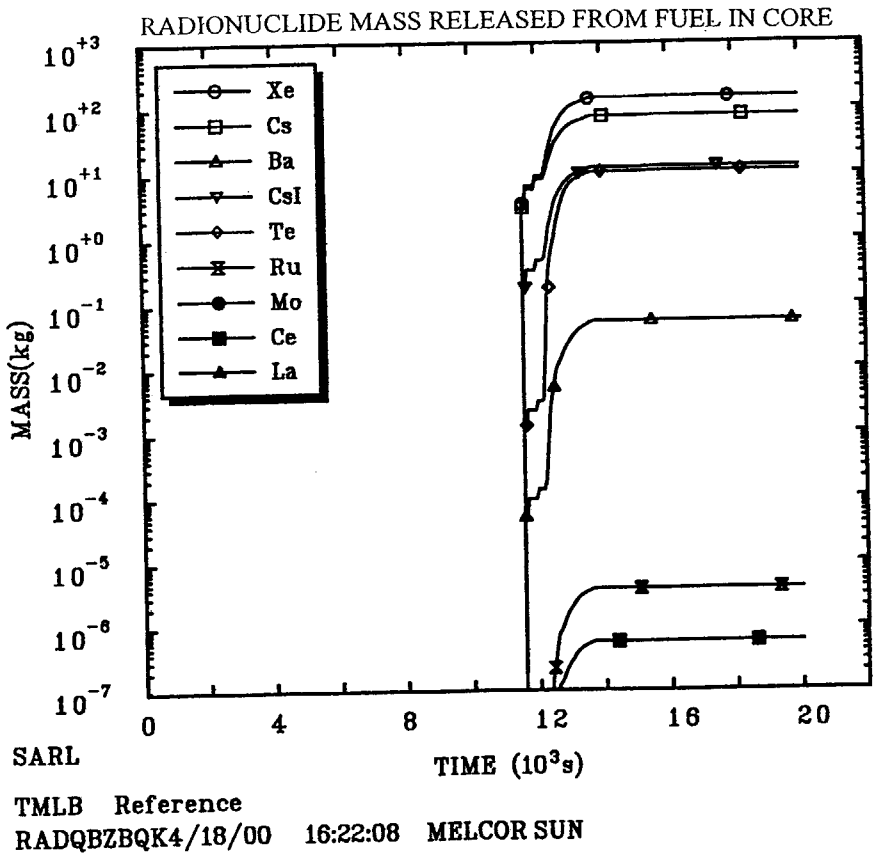

Figure 19. Run 1: Radionuclide mass release from fuel in core.

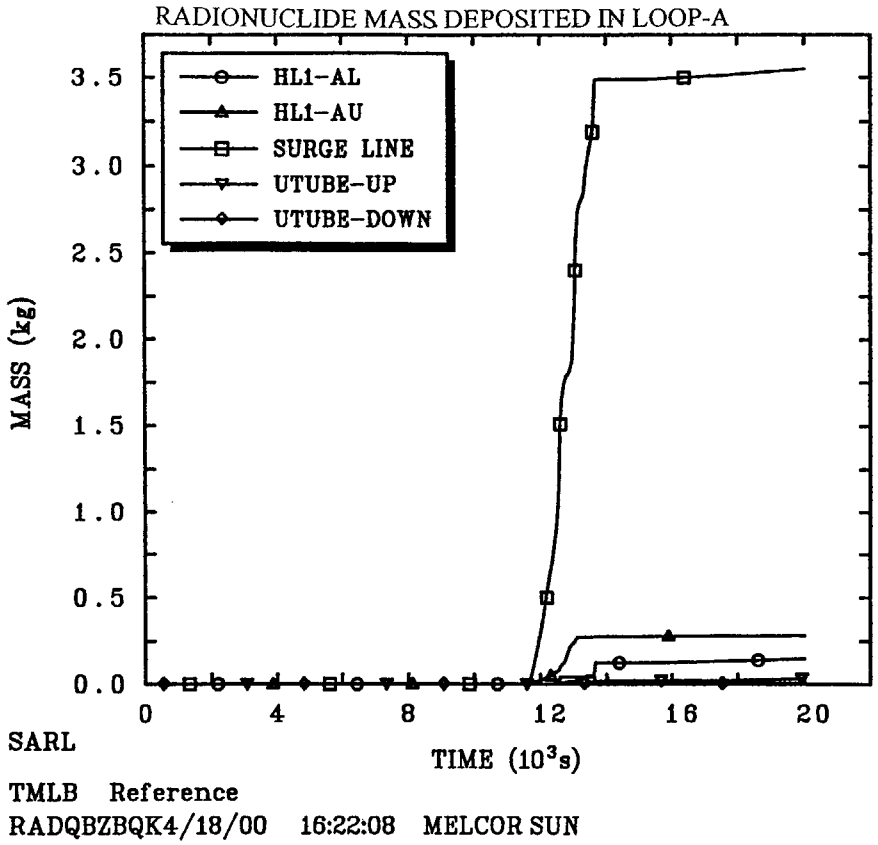

Figure 20. Run 1: Deposited radionuclide mass.

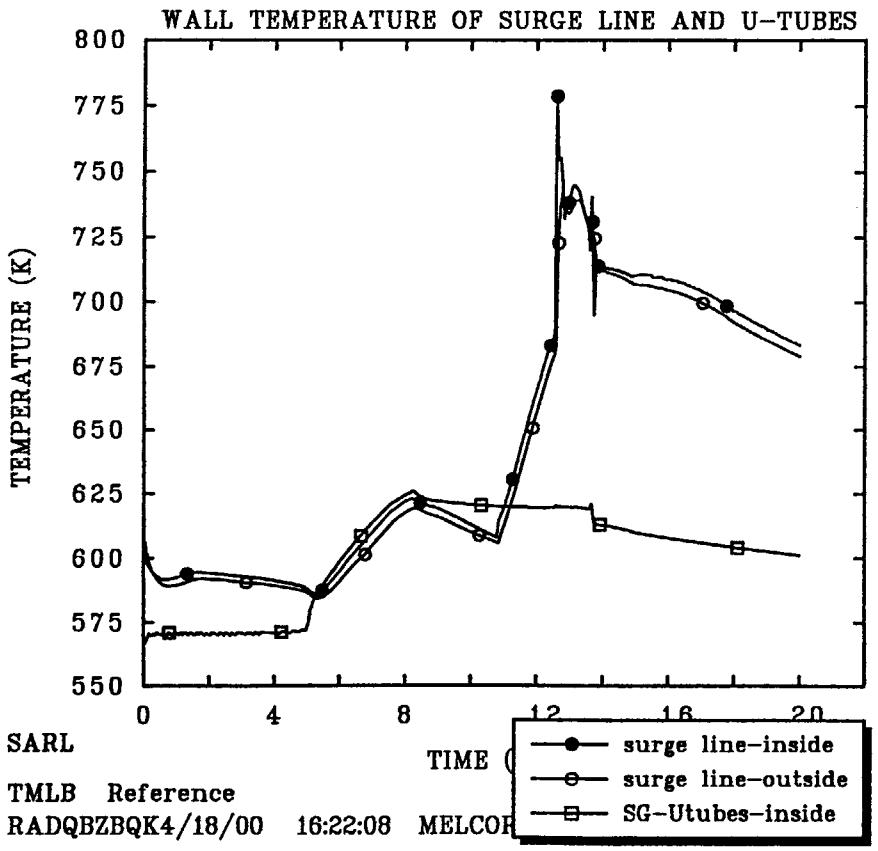

Figure 21. Run 1: Wall temperatures of surge line and SG U-tubes.

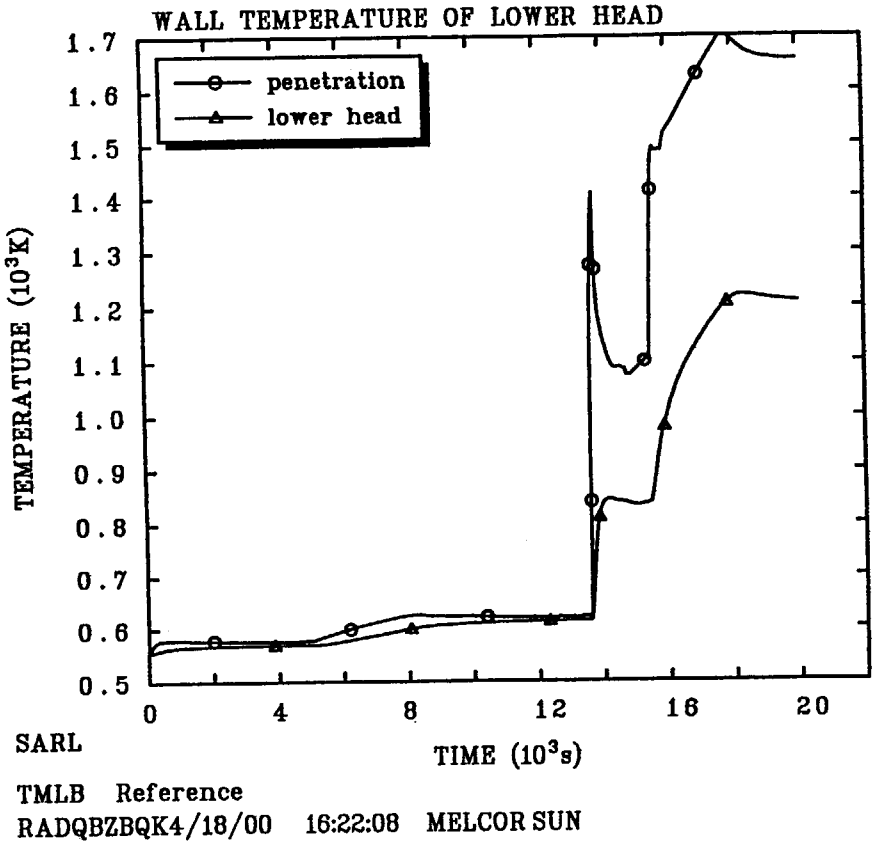

Figure 22. Run 1: Wall temperature of penetration guide and lower head.

6.2. S3-TMLB′ (Run 2, 2A, and 2B)

During TMLB′ sequence, a leakage at coolant pump seal, generally called RCP seal LOCAs, and denoted as S3-TMLB′, could occur due to loss of seal cooling. The probabilistic study for Surry indicated that the frequency of short term station blackout core damage event that would involve an RCP seal LOCA of 946 Lpm/pump or greater was approximately 3.0×10^{-6}/RY[11]. The same study indicated the low probability of small leakage (less than 79 Lpm/pump) early following a loss of seal cooling, and the probability that RCP seal LOCAs of 946 Lpm/pump or greater are introduced at 90 minutes after TMLB′ initiation is about 53 percent. Then, the analysis of RCP seal LOCAs should be performed to know the influence of such events on system response during TMLB′.

The study by Heames and Smith[6] showed that if RCP seal LOCAs occur during TMLB′, the depressurization of RCS would result in early initiation of accumulator injection, and subsequent enhancement of core cooling would delay vessel meltthrough and prevent HPME. But, this result was not confirmed by the analytical study of Hidaka et al [7]. The occurrence of seal leakage had only delayed the core damage for about 1000s at most. This analytical study also showed that two parameters play an important role, i.e. upper plenum by pass flow and break size. It indicated that with smaller upper plenum bypass and larger break size, bigger chance that accumulator injection would be early initiated delaying the core failure.

In both previous studies, the timing of RCP seal LOCAs was assumed when the coolant temperature in the core region reaches saturation temperature. But, during transient process, the timing is an important parameter, because it determines the boundary conditions. So, in the current study, the timing will be varied, even though ref. 11 had indicated the low probability of large seal LOCAs occurred within the first minutes.

All assumptions for TMLB′ calculation are still used. An additional assumption is that pump seal leak occurs at the same time for all the primary coolant pumps due to loss of the seal cooling. The dimension of seal leak is equivalent to the hole with a diameter of 1.25×10^{-2} m for each pump. Three calculations were performed with different timing leakage. In the first calculation (run 2), it was assumed that RCP seal LOCA occurs when the coolant of the core central region reaches the saturation temperature. The calculation was performed for comparison with the previous study. In the second calculation (2A), the leakage is

assumed to occur early after station blackout initiation, i.e. at 600 s. This assumption is to model the occurrence of RCP seal LOCA when SG is still "wet". The third calculation (run 2B) assumed pump seals leak at 2.5 hr from the initiation of station blackout. This case represents late failure of pump seals. At that time, the SG secondaries were already "dry", the core was partially uncovered, and the uppermost part of the core had begun to heatup.

In all calculations, the upper plenum bypass and upper head bypass were not considered. So, it will allow loop seal clearing to occur easily[7]. This fact must be considered in the interpretation of the calculation results.

6.2.1. Run 2

(1) Accident Sequence

The sequence of event from the initiation of station blackout and just prior to RCP seal leaks was similar to the reference calculation. Table 3 shows the timing of key events of run 2. Following the station blackout initiation, all pumps were tripped and coasted down, the reactor was scrammed. Due to decay heat generation, the coolant temperature and pressure increased. In a short time, the pressure reached the PORV set point. After about 10 minutes, the pressure decreased because the steam generator had effectively played as decay heat sink by boiling off secondary coolant inventory. As SG secondary dried out, the RCS temperature and pressure increased again. The pressure reached quickly PORVs set point. Steam was first discharged when PORVs cycled to maintain the pressure. When the water level in the pressurizer attained the top, the liquid began to be discharged. During the time, the fluid temperature in core region rose and reached saturation temperature at 7439 s. At that time, the pump seals failed.

The water level in the pressurizer started to decrease at 8700s. Then, the pressurizer pressure decreased at 1500 s later. As the liquid was discharged from PORVs and the failed seals, the core began to uncover at 8460 s. The core uncovery caused the upper part of the core began to heatup. At 11,040 s, when the cladding temperature exceeded 1000 K, the oxidation of zircaloy cladding started. The temperature of the fuel and cladding continued to increase, while the core liquid level decreased progressively. When the temperature exceeded the failure temperature of cladding at 2098 K, the debris was formed at the upper part. The relocation of the debris to the lower

cells reached the core support plate in ring 1 and caused the temperature of the plates to increase quickly exceeding the failure temperature (at 15,899 s). The failure of support plate in ring 1 allowed the debris to fall and relocate in lower plenum. Due to high temperature of the debris, the weld failure of the penetration guides in the lower head failed quickly at 15,933 s. The water and the debris were discharged from the failed guides hole causing the pressure dropped.

(2). System Response

1) Pressurizer Pressure

Calculated pressurizer pressure is shown in Figure 23. The pressurizer pressure began to decrease at 10,680 s. At about 12,200 s, it appeared a fast pressure increase which reached PORVs set point. This pressure peak was caused by the generation of steam due to relocation of debris into water in the lower plenum. With the continuous venting of vapor from seal break holes, the pressure decreased again. At some times, it appeared another small pressure peaks which were due to increase of steam generation in the core each time the liquid coolant was transferred from loop seal to the core by manometric effect.

At about 14,100 s, when the pressurizer and surge line was empty, the pressure decreased faster. The pressure was at about 7.5 MPa. when the lower head vessel failed at 15,933 s.

2) Liquid Level in Reactor Vessel

Figure 24 shows the swollen liquid level in reactor vessel. The core coolant saturation temperature was reached at 7408 s. At 8460, the core began to uncover. The liquid at the downcomer started to collapse about 600 s later. It can be seen that some peaks were predicted in the downcomer after the decrease of the liquid level. It was caused by small amount of water supply from the crossover leg to downcomer due to manometric effect.

The liquid level decreased slower than in TMLB'. The core was completely uncovered at 14,700 s. The liquid coolant in lower plenum began to decrease while it was evaporated.

3) Distribution of coolant in RCS

The loop seal void fraction of loop-A and loop-B are shown in Figures 25 and 26, respectively. The hot leg

started to void at about 8000 s. The SG U-tubes were voided first, and almost completely voided at 10,000 s. The cold leg pipe of loop-B was voided at 10,000 s, and 11,000 for loop-A. At that time, the void fraction in the downflow of crossover legs of both loops attained 0.8, while the upflow pipes were progressively voided. There was a possibility of loop seal clearing occurrence in loop-B at about 9200 s.

4) Coolant mass discharged from failed seal

Figures 27 and 28 show the mass flow rate of coolant discharged from seal break holes of loop-A and loop-B, respectively. Liquid coolant was discharged through the seal break holes when the seal failure occurred. At about 9200 s, at loop-B, failed seal discharged only vapor. On the other side, at loop-A, two-phase flow liquid-vapor was vented out until about 10,000 s, after that the only vapor was discharged. The total coolant mass discharged out of RCS was shown in Figures 29 and 30.

5) Core damage

During the core uncovery, the core was heated up. The temperature of fuel and cladding started to increase as shown in Figures 31, 32 and 33 for ring 1, ring 2, and ring 3 respectively. The upper region in innermost ring (ring 1) was heated up first and fastest. It started at about 8500 s. But a significant increase began at 10,200 s for almost all cells. The cladding oxidation started at 11,040 s as could be seen from hydrogen generation in Figure 34. About 390 kg of Hydrogen was produced prior to vessel breach. Due to temperature increase of the cladding, at about 12,500 s, the core material in upper region of ring 1 became debris, and began to relocate to the lower cell. However, the core lower part was still intact for a while. The same sequence happened in two outer rings. Only at about 15,899 s, the lower part failed. The debris fell down to the core support plate. The temperature of the support plate in ring 1 increased very fast, and exceeded the failure temperature (see Figure 35). The debris went down to the upper plenum and relocated in the vessel lower head.

The debris which are relocated in the lower plenum are shown in Figures 36, 37, and 38. About 30 s after the support plate failure, the penetration guides in ring 1 failed, as consequence, the coolant was discharged through the breach, and the pressure dropped rapidly.

6) Radionuclide release

Calculated radionuclide mass release from fuel in the

core was shown in Figure 39. The radionuclide release began at 11,188 s when the cladding in ring 1 failed allowing the fission product gas resided in the gap was released to the core and sequentially RCS.

Prior to the vessel failure, about 225 kg of Xe class and about 120 kg of Cs class were released. For CsI and Te class, the released was about 20 kg. The other radionuclide classes were released less than 1 kg.

The deposited mass of radionuclide material in hot leg of loop-A is shown in Figure 40. The pressurizer surge line was the location where the most radionuclide was deposited. The other locations are the SG U-tubes and the hotleg pipe closest to the RPV (HL1-AU and HL1-AL).

7) RCS wall temperature

The wall temperature of pressurizer surge line is shown in Figure 41. The maximum temperature of inner wall was about 655 K achieved at about 12,500 s. The temperature remained at 650 K for about 1500 s from 12, 500 s to 14,000 s before decreasing.

The SGs U-tubes wall temperatures for loop-A and loop-B are given in Figures 42 and 43 respectively. The SGs U-tubes temperature of loop-B was higher than loop-A, because the loop natural circulation of vapor was established in loop-B. The maximum temperature was about 760 K achieved just before the vessel failure.

6.2.2. Run 2A

(1) Accident Sequence

Run 2A assumed the RCP leakage at 10 minutes (600 s) after initiation of station blackout. Table 4 shows the timing of key events predicted by the run 2A. Soon after the seals failed, the pressure decreased. A large quantity of subcooled coolant liquid was discharged from the seal break holes. As a consequence, the core coolant level decreased faster, and the core was uncovered. Accordingly, the temperature of core materials began to increase quickly due to the high flux of decay heat generated. The poor coolability of the core caused faster degradation of the core material, especially in the uppermost part. Only about 100 minutes from the SBO initiation, the lower head guide penetration failed when the debris relocated into the lower plenum.

(2) System Response

1) Pressurizer Pressure

Calculated pressurizer pressure for run 2A is shown in Figure 44. The pressure decreased until about 11 MPa soon after the seals leakage occurred at 600 s. As RCS temperature rose and steam was generated, the pressure increased as well. However, due to the effective heat transfer by SGs, the pressure decreased again. At 4000 s, the pressure reached the SGs secondary side pressure, about 8.2 MPa, and remained for a while. At about 5800 s, the pressure increased quickly due to the steam generation caused by relocation of molten debris into water in the lower plenum (the timing corresponds to Ring 1 support failure). At the time of vessel failure, at 5900 s, the pressure dropped instantaneously to ambient pressure.

2) Liquid level in the reactor vessel

Swollen liquid level in the reactor vessel is shown in Figure 45. The liquid in the core began to decrease at 2220 s, about 5660 s earlier than in TMLB′ case. The liquid level in the core decreased slightly faster than in TMLB′ due to discharged subcooled coolant from seal break holes. At 3500 s, the liquid level touched the bottom of the core. But it increased again up to about mid-height of the core, when, due to pressure difference, the liquid level in the downcomer began to decrease supplying liquid coolant to the core. After that, at about 4300 s the water level in the core decreased again, and at the time of lower head failure, the core was almost uncovered.

3) Distribution of coolant in RCS

When the seal leakage occurred, the RCS was full with liquid coolant. The leakage from seal break holes caused the mass liquid coolant reduced quickly. As the upper plenum liquid depleted, the hot leg, and SG U-tubes of both loops began to void. At about 3500 s, the void fraction of cold leg increased to 0.5. While the hot leg continued to be voided, the cold leg and loop seal void fractions were practically unchanged until the lower head vessel failed. Figures 46 and 47 show the void fraction of cross-over leg of loop-A and loop-B, respectively.

4) Coolant mass discharged from failed seal

Figures 48 and 49 show the mass flow rate leakage of loop-A and loop-B, respectively. And, Figure 50 and 51 give

the total mass discharged. It could be seen from those Figures that only liquid coolant was discharged from seal break holes from the beginning of seal failure until the vessel failure.

5) Core damage

The calculated cladding temperatures of ring 1, ring 2 and ring 3 are shown in Figures 52, 53 and 54, respectively. When the core was first time uncovered (at 3500 s), the fuel temperature increased. But, it decreased again due to cooling provided by the liquid coolant that moved into the core from downcomer. At about 4000 s, the fuel was heated up quickly as a result of core liquid level decrease. The temperature increased quickly such that the upper region of ring 1 failed and relocated to the lower region. The oxidation of zircaloy cladding generated hydrogen of about 200 kg at the time of lower head failure in ring 1(see Figure 55).

The temperature of core support plate increased quickly when the debris reached the plate in ring 1 as shown in Figure 56. Since the failure temperature was exceeded, the plate failed and the debris above the plate fell down into the lower plenum. Just before being ejected through vessel breach at 5924 s, UO_2 debris of about 53.95 tons was relocated in the lower head vessel. Figures 57, 58, 59 show the debris mass relocated in lower plenum ring 1, ring 2 and ring 3, respectively.

6) Radionuclide release

Radionuclide mass released from fuel in core is shown in Figure 60. The release began at 4750 s following the cladding failure. The most important releases were Xe class and Cs class. About 90 kg of Xe, and 60 kg of Cs classes were released from fuel in core. The deposited radionuclide mass was most found in surge line as shown in Figure 61. Beside, the deposited radionuclide was also found at the upper part of inner wall of hotleg pipe of CV205 (HL1-AU).

7) Wall temperature

Calculated wall temperature of pressurizer surge line is shown in Figure 62. The temperature tended to decrease from the beginning. The maximum peak temperature was about 605 K. The wall temperature of the top SG-A U-tubes and SG-B U-tubes are shown in Figures 63 and 64, respectively. The maximum temperature was rather low, 592.5 K for SG-A and 597 K for SG-B, respectively.

6.2.3. Run 2B

(1) Accident Sequence

The Table 5 shows the timing of key sequence predicted by run 2B. The sequence before pump seal failure was similar to the TMLB′ reference calculation. In the calculation of run 2B, the coolant was discharged from PORVs and the failed pump seals after 9000 s (2.5 hr). Following this, the liquid level in the pressurizer began to decrease. The pressure in the pressurizer started to decrease at about 10,000 s, while the steam generation in the core was reduced due to low liquid level. As a result of core uncovery, at about 9600 s the upper part of the core (cell 9 to 14) heated up quickly. Then, at about 11,500 s, those cells were failed. The debris began to relocate to the lower cells. But, a sufficient cooling was still assured by steam generation in core, such that the lower part was practically kept intact. An occasional supply of liquid from the loop seals to the core through the downcomer occurred due to manometric effect adding the cooling. At about 14,000 s, the RCS of loop-B was practically voided, the pressure decreased faster. The natural flow of hot steam from the core to the seal break hole accelerated the hot core cooling. At 18,241 s, the pressure fell below the accumulator set point allowing the borated water was injected to the RCS. The core was flooded, and the hot materials were cooled. Until the calculation failed at about 20,400 s the core support plate was still kept intact avoiding relocation of the debris into the lower plenum.

(2) System Response

1) Pressurizer Pressure

Figure 65 shows the pressurizer pressure predicted by the calculation run 2B. The pressure history before pump seals failure was similar with the TMLB′ reference calculation. After pump seals failed, due to the discharge of coolant mass, the pressure began to decrease at 10,000 s. At the beginning of discharge, the pressure decrease was rather slow. The short pressure peak at 11,500 s was due to steam generation caused by debris relocation process. From about 14,000 s, the pressure decreased faster.

At 18,241 s, the pressure reached the accumulator set point. About 40% of borated water volume in accumulator tanks was injected. The water flooded and cooled the hot reactor core materials, and accordingly, the temperature of the materials decreased. When the borated water was

injected from accumulator tanks, the pressure decreased quickly, but then it increased again due to a large quantity of steam generated in the core.

2) Liquid level in the reactor vessel

The swollen liquid level in the reactor vessel is shown in Figure 66. When the pump seals failed, the liquid level in the core was at about the middle of the core height. The liquid level continued to decrease. At about 11,100 s the liquid level in the down comer dropped suddenly. It might be due to loop-B seal clearing. When the injection of water from accumulators occurred at 18,241 s, the water level increased rapidly. However, due to a large steam generation as the water flooded the hot core, the water level decreased again.

3) Distribution of coolant in RCS

Since the core began to uncover, the RCS started to void. The steam generator U-tubes became void at first. When the seal leakage occurred, the cold leg of both loops became quickly void (see Figures 67 and 68). At 9,000 s, in loop-B, the hot leg was almost voided; a quantity of mass of liquid remained in loop seal, especially in the upward leg. At about 11,100 s, it was high possibility that loop-B seal clearing occurred. But, in loop-A, the loop seal was practically still full by liquid. At about 13,000 s, the void fraction in the downward leg of the loop seal increased quickly (Figure 67). That event occurred at the same time as the voiding of the pressurizer surge line.

4) Coolant mass discharged from failed seals

Figures 69 and 70 show the leakage mass flow rate from seal break holes in loop A and loop B, respectively. While, Figures 71 and 72 give the total mass flow for loop A and loop B, respectively. At the beginning of seal failure, the water liquid was discharged from the break holes. After 9500 s, in the loop A, the two phases steam-liquid was vented out. In the loop B, only steam was discharged. The liquid was discharged again in loop A when the accumulator injection occurred.

5) Core damage

The core heat up started at about 9600 s. The temperature of fuel and cladding rose quickly in the uppermost part. Figures 73, 74 and 75 show the cladding temperatures for ring 1,2, and 3, respectively. The uppermost part of fuel in the ring 1 was failed at about

10,500 s, while the lower part was not heated up yet. The hydrogen mass produced during the oxidation of the cladding increased quickly at the beginning as shown in Figure 76. The debris from upper cell relocated to the lower cell. Most of debris was held at the middle height of active core (cell 7,8 and 9 in the model). A small amount of debris reached lowest core region (cell 5 and 6). The cell 10, 11, 12, 13, and 14 (almost 30% of total core volume) were practically empty.

Figure 77 shows the core support plate temperature. Because the core support plate was kept intact until the end of calculation (i.e. 20,000 s), there was no fuel debris relocation in the lower plenum.

6) Radionuclide release

Calculated radionuclide mass released from fuel in the core is shown in Figure 78. About 200 kg of Xe class, 120 of Cs class, and 20 kg of CsI and Te class were released from the core. Most of them were released from gap released event occurred at the beginning of the fuel cladding failure.

After released in core, some radionuclide aerosols was deposited in RCS piping. Figure 79 shows the deposited radionuclide mass in several parts of RCS. Two location where significant radionuclide deposition were found are surge line and upper part of the inner wall hotleg pipe of loop-A closest to the RPV (HL1-AU).

7) Wall temperature

Figure 80 shows the wall temperature of pressurizer surge line. The temperature began to increase significantly at 12,200 s and reached about 705 K around 14,000 s. But, then it decreased as fast as it increased.

The wall temperature of SG-A U-tubes is shown in Figure 81. The temperature increased since the SG secondary side dried out, and reached the maximum temperature of 625 K at 8000 s. The liquid coolant flow to seal failed hole cooled the wall temperature. As the core dried out and superheated steam became important, the wall temperature increased again. The temperature decreased after injection of cold water from accumulator tanks.

The wall temperature of SG-B U-tubes is shown in Figure 82. The temperature started to increase when the secondary coolant inventory in SGs dried out. Since, the wall temperature increased continuously. At the end of calculation, the temperature reached about 840 K. The

temperature of SG-B U-tubes was higher than in SG-A. The reason might be related to the loop natural circulation of hot vapor in loop B after loop seal clearing.

6.2.4. Discussions

Three calculations concerning S3-TMLB′ had been performed with different timing of seal failure initiation. The early failure of seal pumps, i.e. 10 minutes from the initiation of total station blackout, caused early core damage compared with the TMLB′ sequence. Only in about 100 minutes from transient initiation, the reactor vessel melt-through was occurred. But, in the case of seal failure at the time of core coolant saturation, the reactor vessel breach was delayed about 2300 s (38.3 minutes) compared with the TMLB′ reference calculation. The delay of more than 6400 s (106 minutes) was predicted in late failure (i.e. 2.5 hr after initiation of station blackout) calculation.

The effect of the difference in timing of RCP failure on predicted sequence might depend on the RCS state at the time of seal failure. In case of early failure (run 2A), a large amount of subcooled coolant was discharged from the RCS through seal break holes, and core coolant was depleted rapidly. As consequence, the core coolability was very poor, and the core was heated up quickly.

In the case of late failure (run 2B), the seal pumps failed when the RCS was partly voided. The coolant liquid was discharged at the beginning, after that only the vapor was discharged. Such condition allowed hot steam natural flow from core to the seal break holes, which in turn accelerated the core cooling by steam generated in core. Such natural circulation could occur after loop seal clearing in loop B. That condition assured the sufficient cooling of the hot core materials and heating of other RCS structures. On the other hand, the RCS pressure could also decrease faster and could reach the accumulator set point allowing cold liquid coolant to be injected. The last enhanced cooling to the core.

However, as indicated in the run 2B, the temperature of SG U-tubes in loop-B tended to increase higher. The pressure difference at the end of calculation was about 4.0 MPa with secondary side was higher than the pressure inside the tubes. The problem of tube integrity must be considered.

Table 3. Timing of Key Events of S3-TMLB′: Run 2.

Events	Time ,s	/(hr)
Station blackout initiation	0	(0)
SG dried out	4981	(1.38)
Core coolant at saturation	7408	(2.06)
Pump seals leak	7408	(2.06)
Start of core uncovery	8460	(2.35)
Start of oxidation	11,040	(3.07)
Gap release		
Ring 1	11,188	(3.11)
Ring 2	11,332	(3.15)
Ring 3	11,664	(3.24)
Core completely uncovered	14,700	(4.08)
Core support plate failure		
Ring 1	15,899	(4.42)
Ring 2	17,687	(4.91)
Ring 3	18,348	(5.10)
Lower head penetration failure		
Ring 1	15,933	(4.43)
Ring 2	16,059	(4.46)
Ring 3	18,371	(5.10)
Debris ejection	15,933	(4.43)

Table 4. Timing of Key Events of S3-TMLB′: Run 2A.

Events	Time ,s	/(hr)
Station blackout initiation	0	(0)
Pump seals leak	600	(0.17)
Core coolant at saturation	~1800	(0.5)
Start of core uncovery	2220	(0.62)
Start of oxidation	4734	(1.315)
Gap release		
Ring 1	4750	(1.32)
Ring 2	4835	(1.34)
Ring 3	5008	(1.39)
Core completely uncovered	5900	(1.64)
SG dried out	5940	(1.65)
Core support plate failure		
Ring 1	5876	(1.63)
Ring 2	7544	(2.09)
Ring 3	8112	(2.26)
Lower head penetration failure		
Ring 1	5906	(1.64)
Ring 2	5935	(1.65)
Ring 3	8133	(2.26)
Debris ejection	5924	(1.645)

Table 5. Timing of Key Events of S3-TMLB′: Run 2B.

Events	Time ,s	/(hr)
Station blackout initiation	0	(0)
SG dried out	4981	(1.38)
Core coolant at saturation	7408	(2.06)
Start of core uncovery	7980	(2.22)
Pump seals leak	9000	(2.50)
Start of oxidation	10,448	(2.90)
Gap release		
Ring 1	10,557	(2.93)
Ring 2	10,637	(2.95)
Ring 3	10,906	(3.03)
Core completely uncovered	14,690	(4.08)
Accumulator opens	18,241	(5.07)
Core support plate failure		
Ring 1	> 20,000	(>5.55)
Ring 2	> 20,000	(>5.55)
Ring 3	> 20,000	(>5.55)
Lower head penetration failure		
Ring 1	> 20,000	(>5.55)
Ring 2	> 20,000	(>5.55)
Ring 3	> 20,000	(>5.55)
Debris ejection	> 20,000	(>5.55)

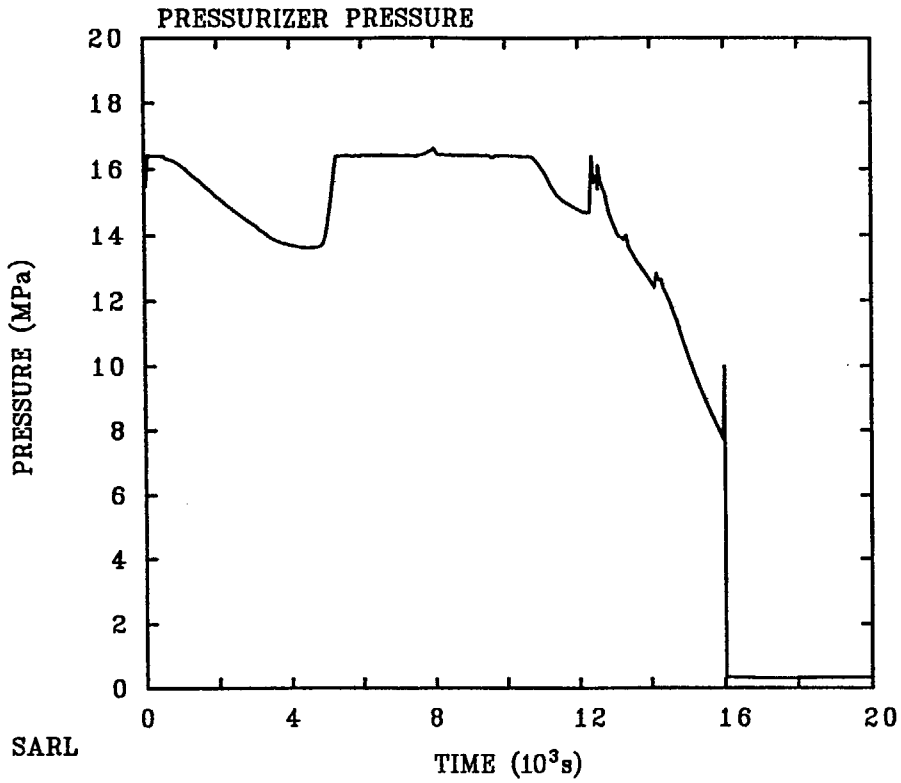

Figure 23. Run 2: Pressurizer pressure.

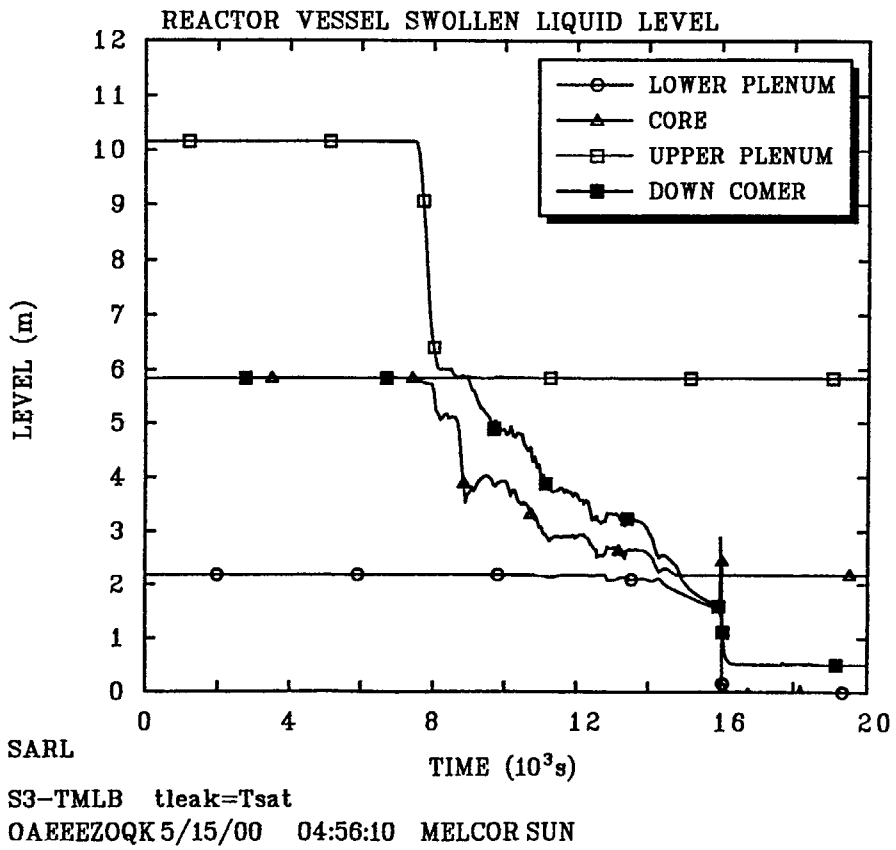

Figure 24. Run 2: Swollen liquid level in reactor vessel.

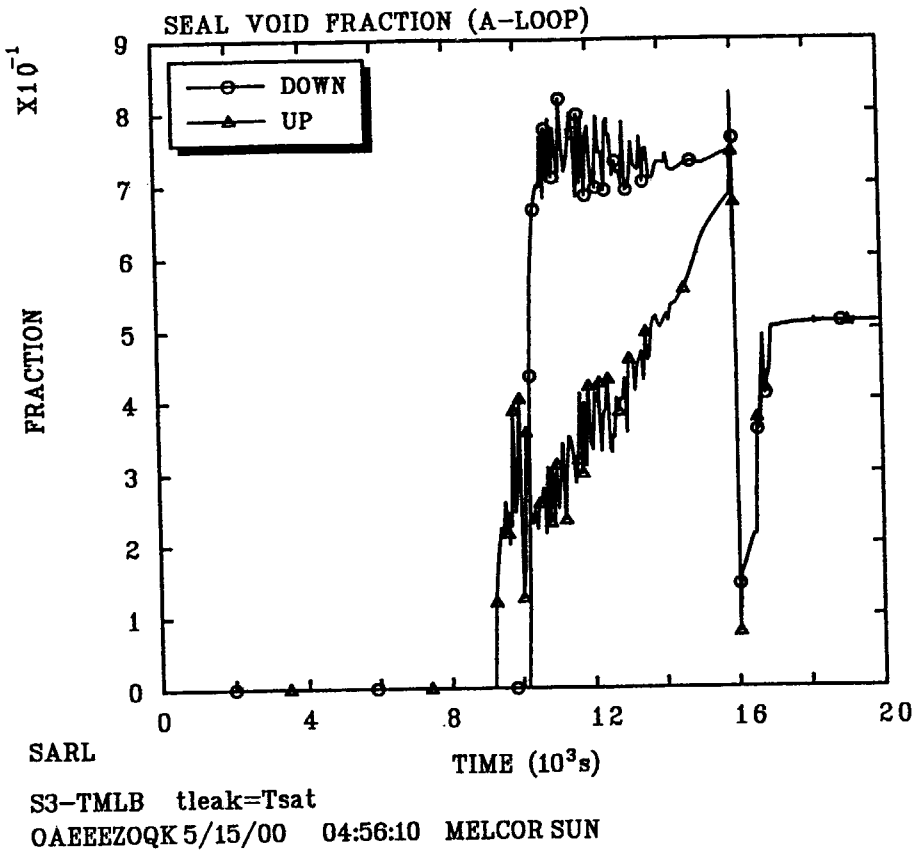

Figure 25. Run 2: Loop seal void fraction of loop-A.

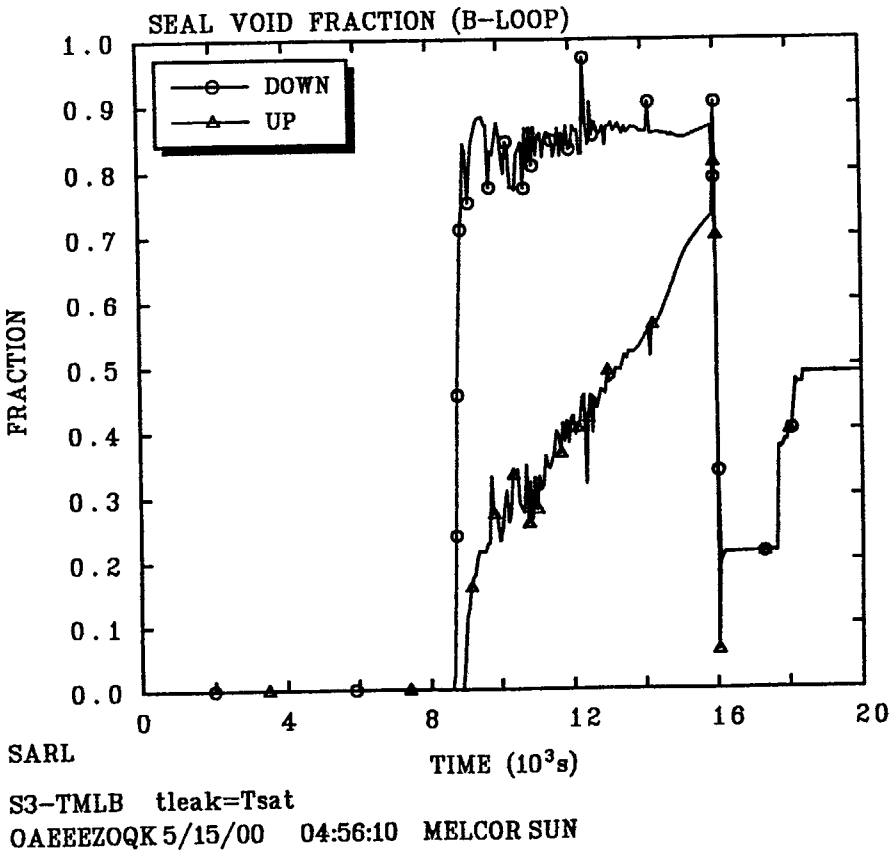

Figure 26. Run 2: Loop seal void fraction of loop-B.

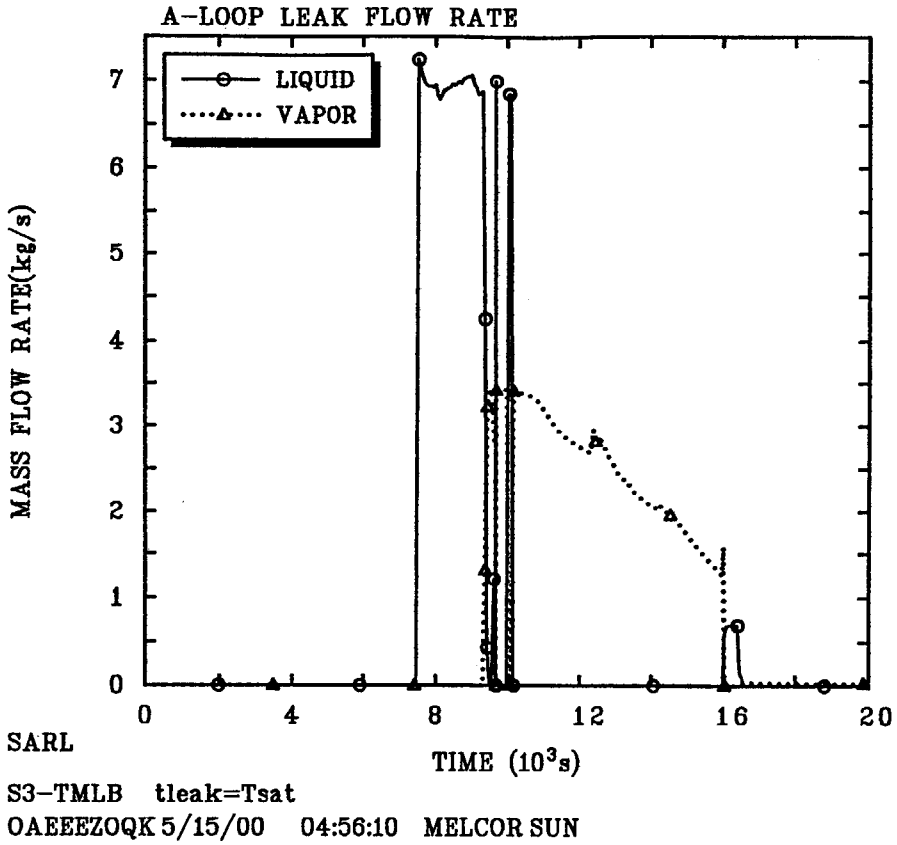

Figure 27. Run 2: Coolant mass flow rate discharged from failed seal of loop-A.

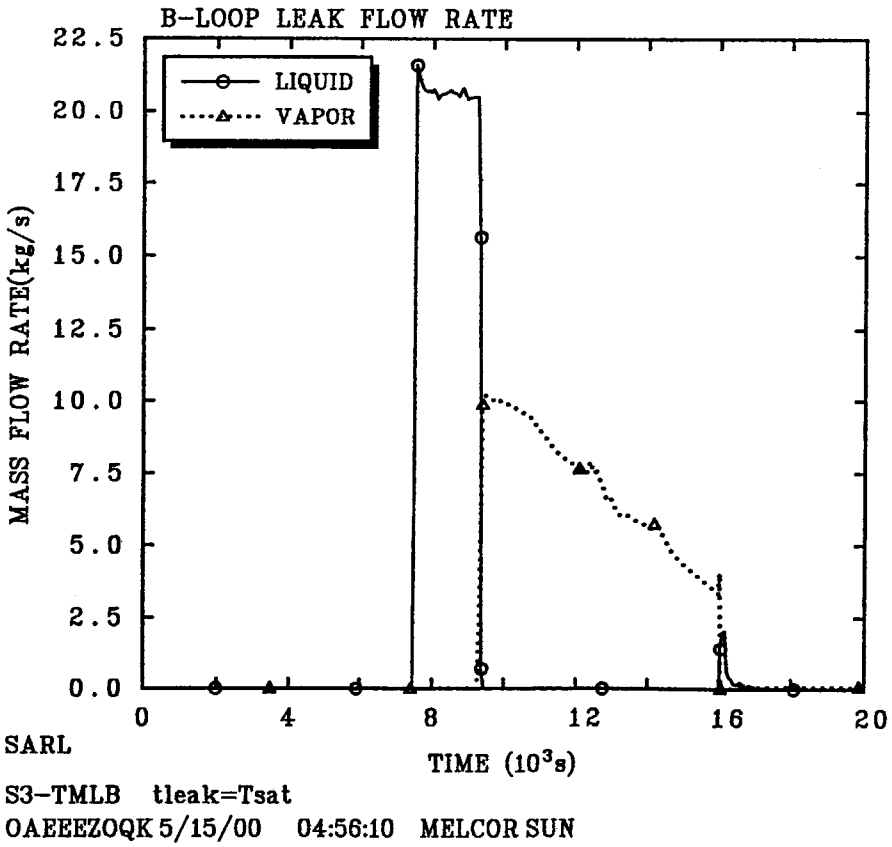

Figure 28. Run 2: Coolant mass flow rate discharged from failed seal of loop-B.

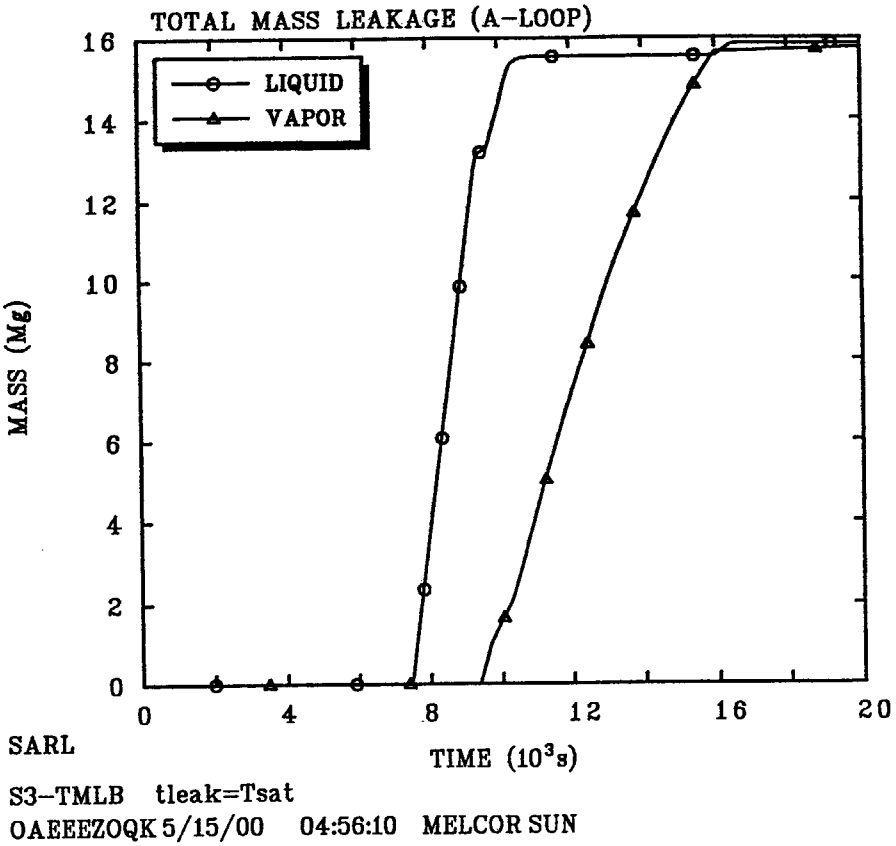

Figure 29. Run 2: Total coolant mass discharged from failed seal of loop-A.

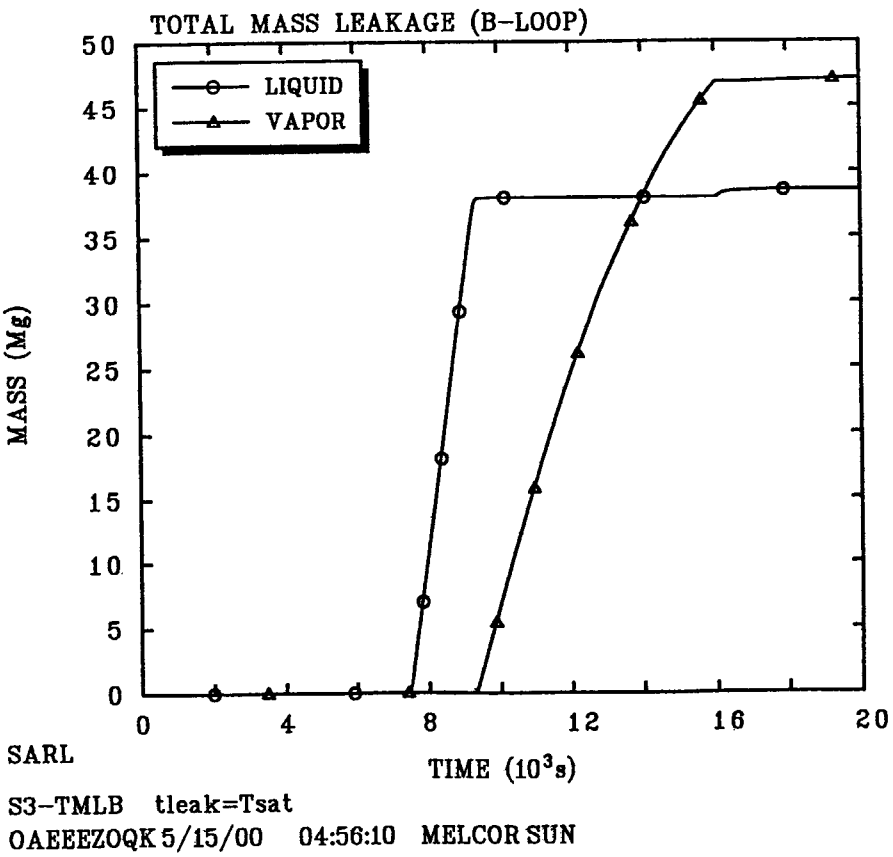

Figure 30. Run 2: Total coolant mass discharged from failed seal of loop-B.

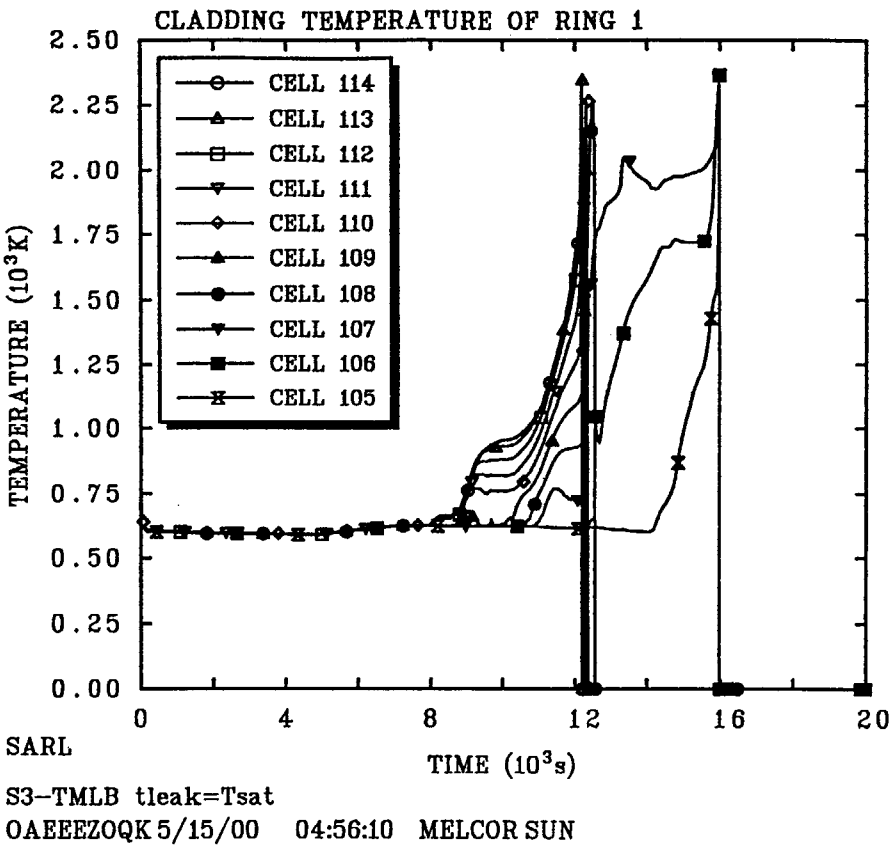

Figure 31. Run 2: Cladding temperature in ring 1.

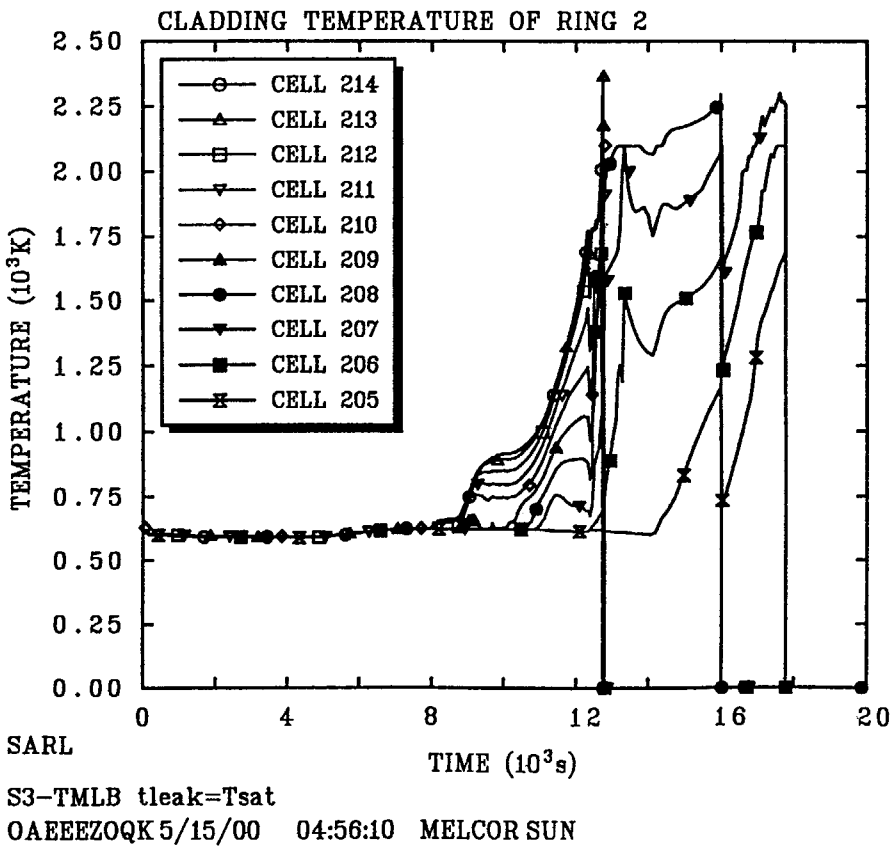

Figure 32. Run 2: Cladding temperature in ring 2.

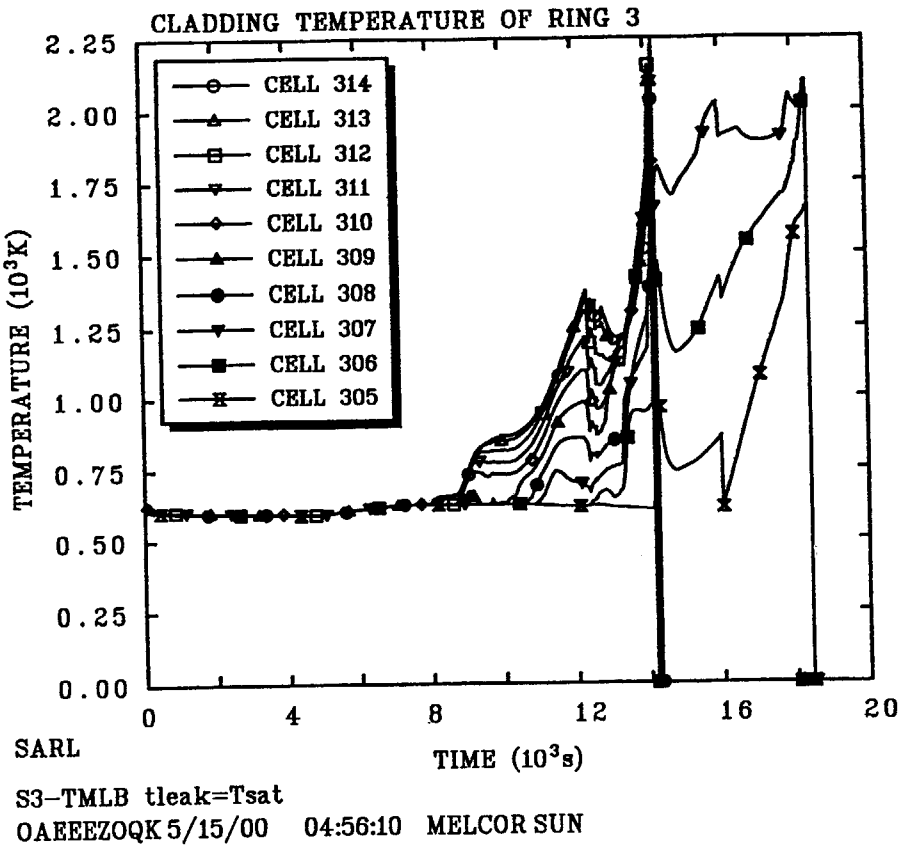

Figure 33. Run 2: Cladding temperature in ring 3.

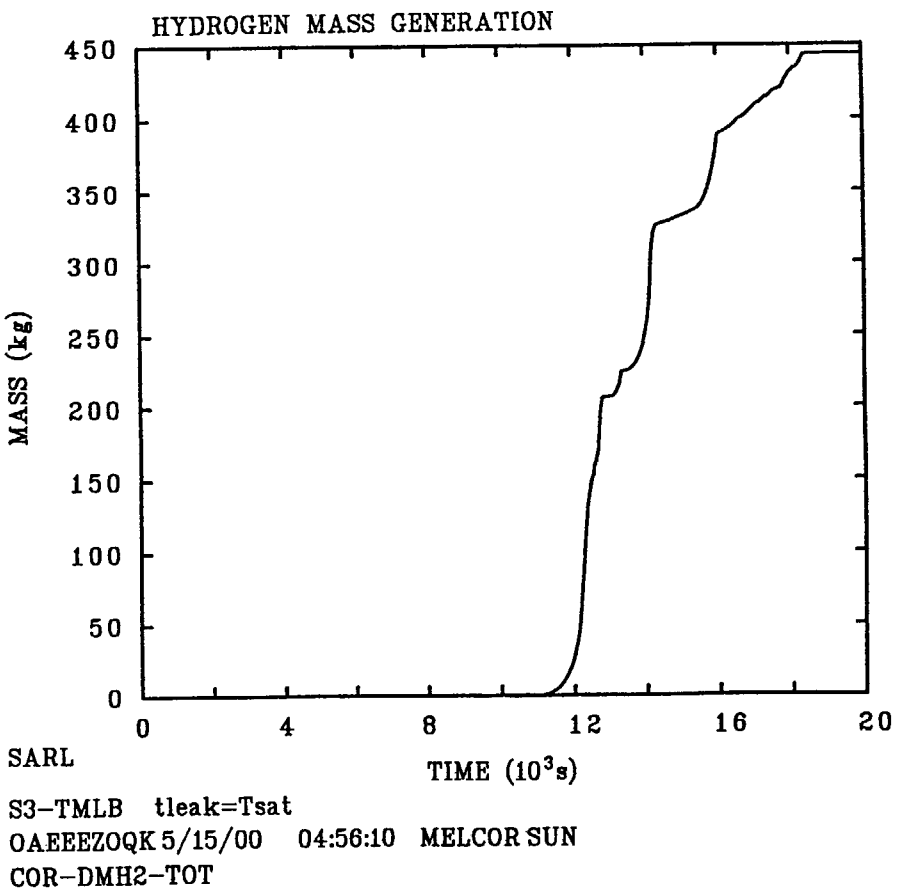

Figure 34. Run 2: Hydrogen mass generated.

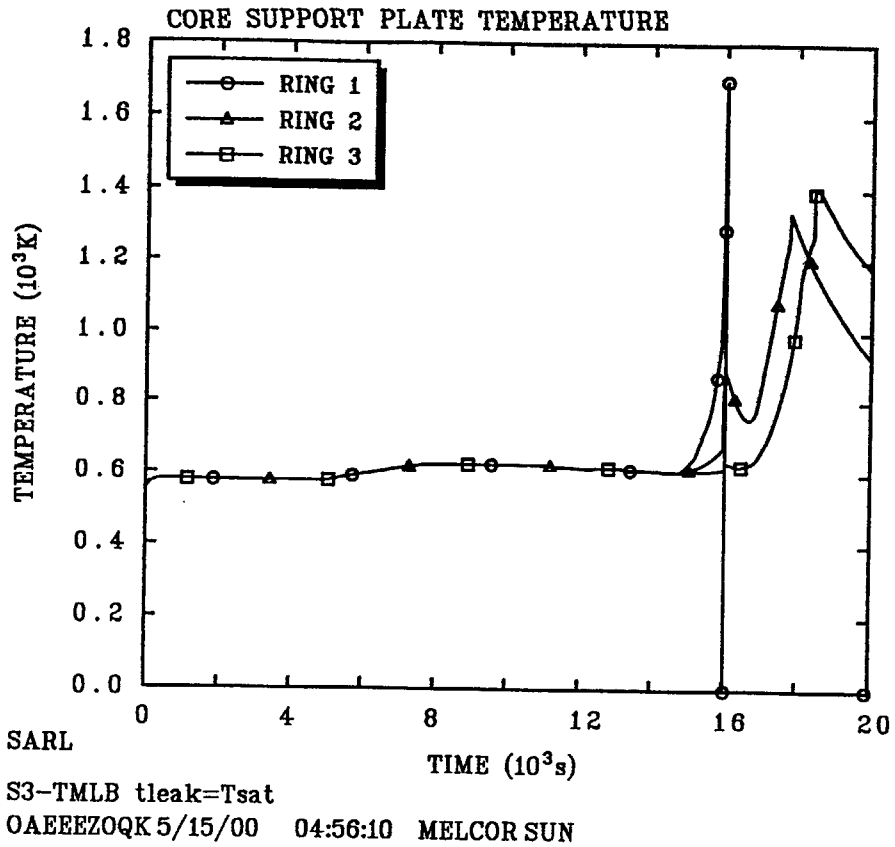

Figure 35. Run 2: Core support plate temperature.

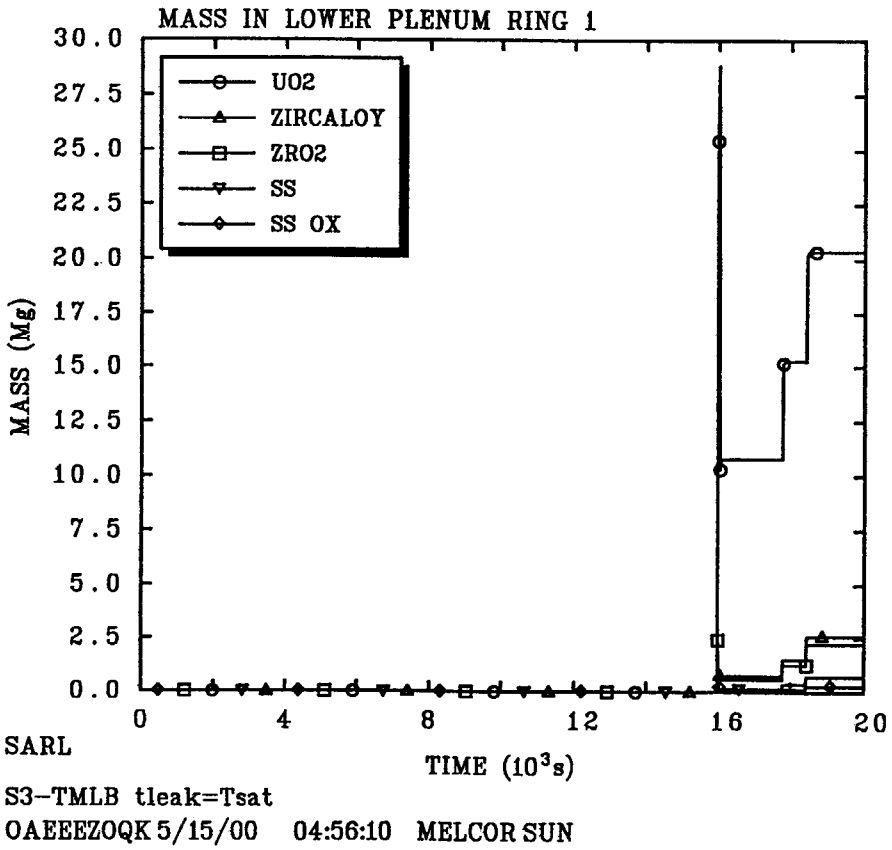

Figure 36. Run 2: Debris mass in lower plenum ring 1.

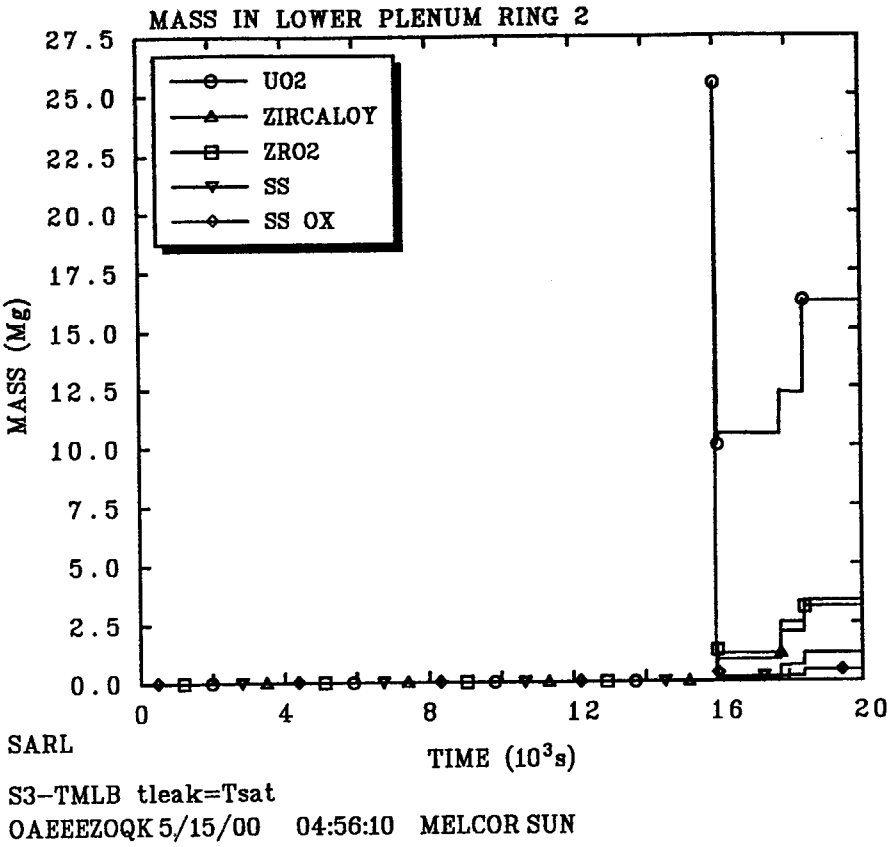

Figure 37. Run 2: Debris mass in lower plenum ring 2.

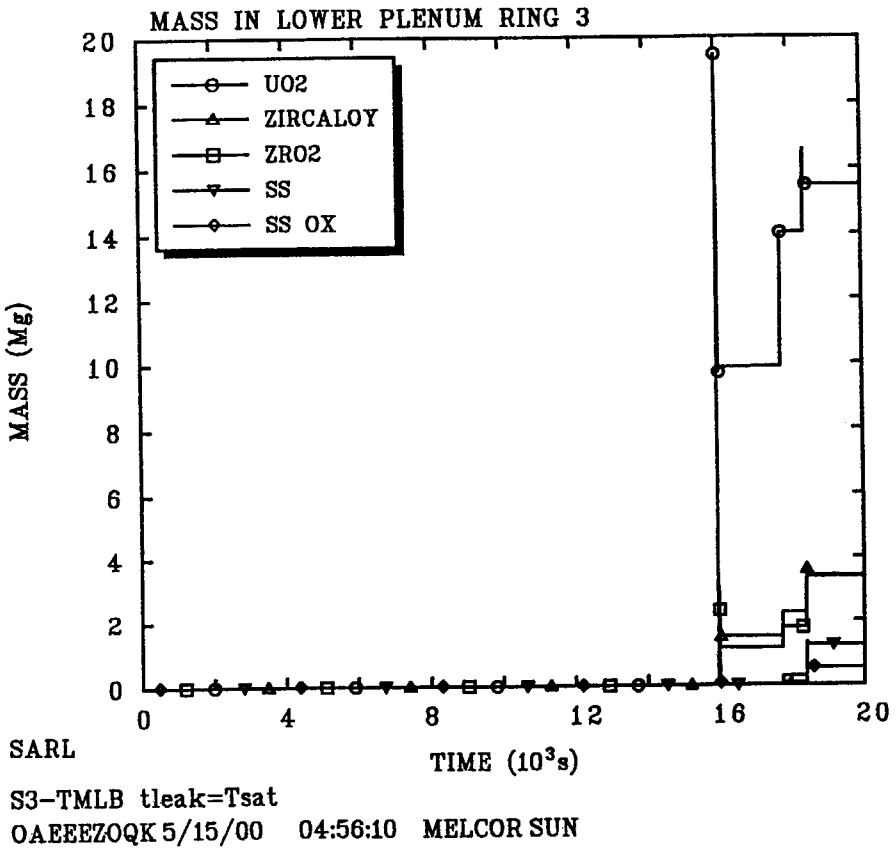

Figure 38. Run 2: Debris mass in lower plenum ring 3.

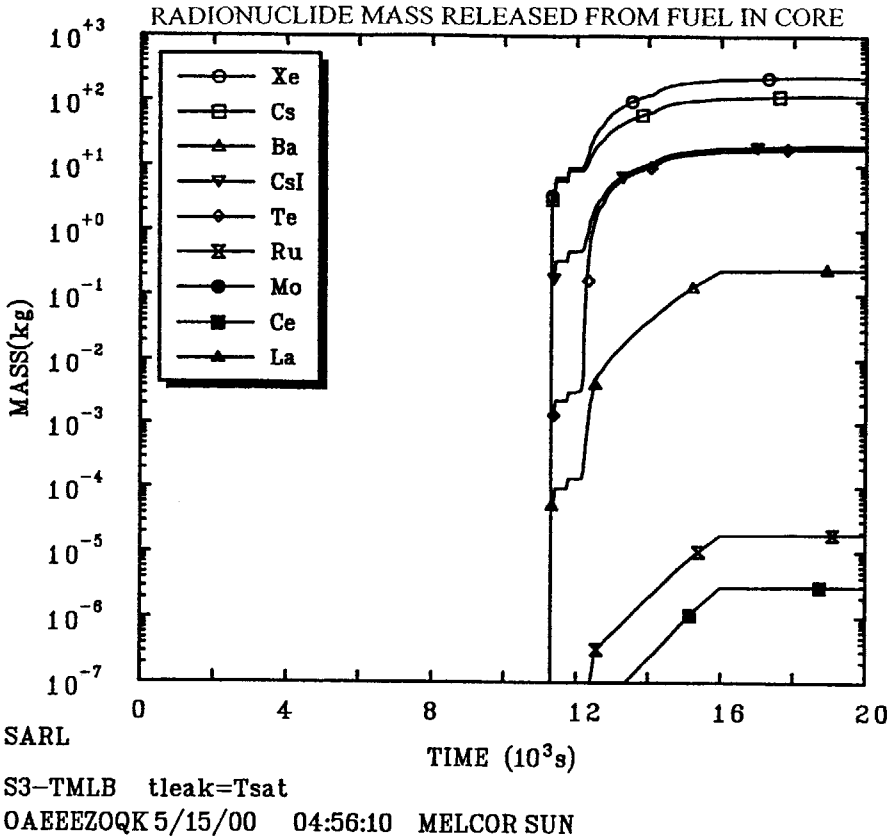

Figure 39. Run 2: Radionuclide mass released from fuel in core.

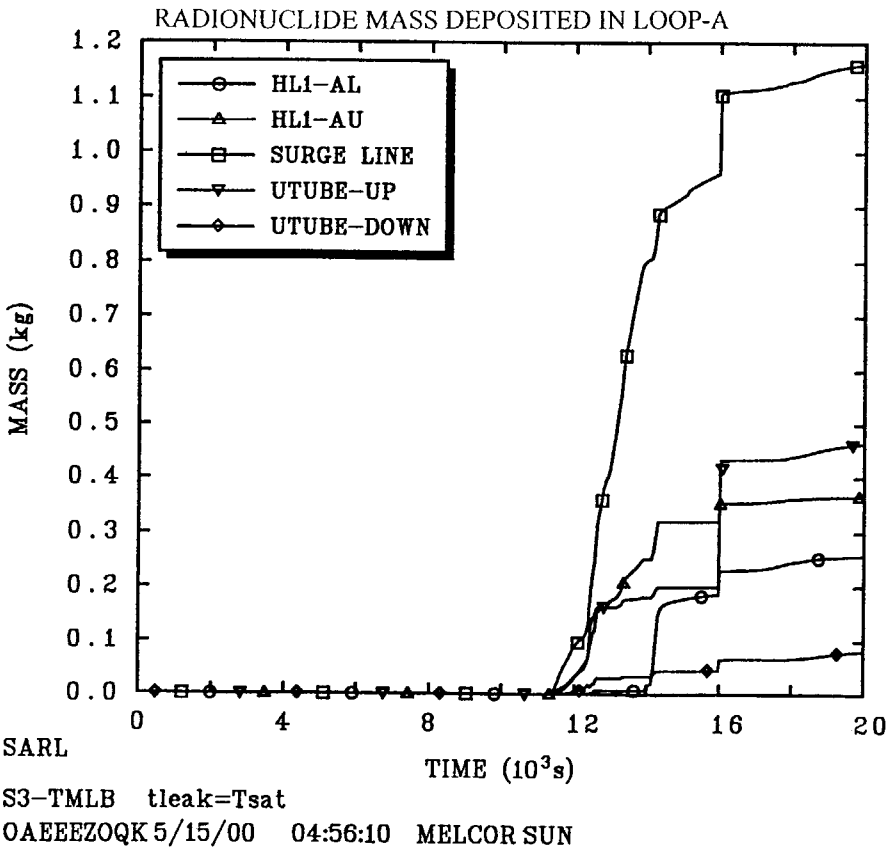

Figure 40. Run 2: Deposited radionuclide mass.

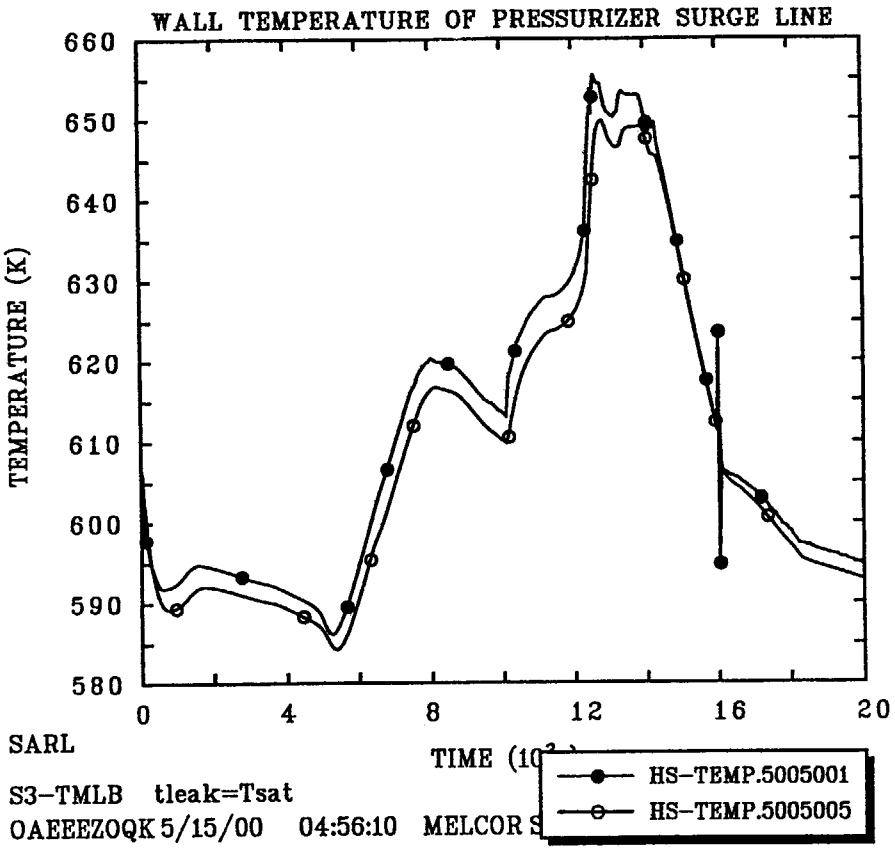

Figure 41. Run 2: Wall temperature of surge line.

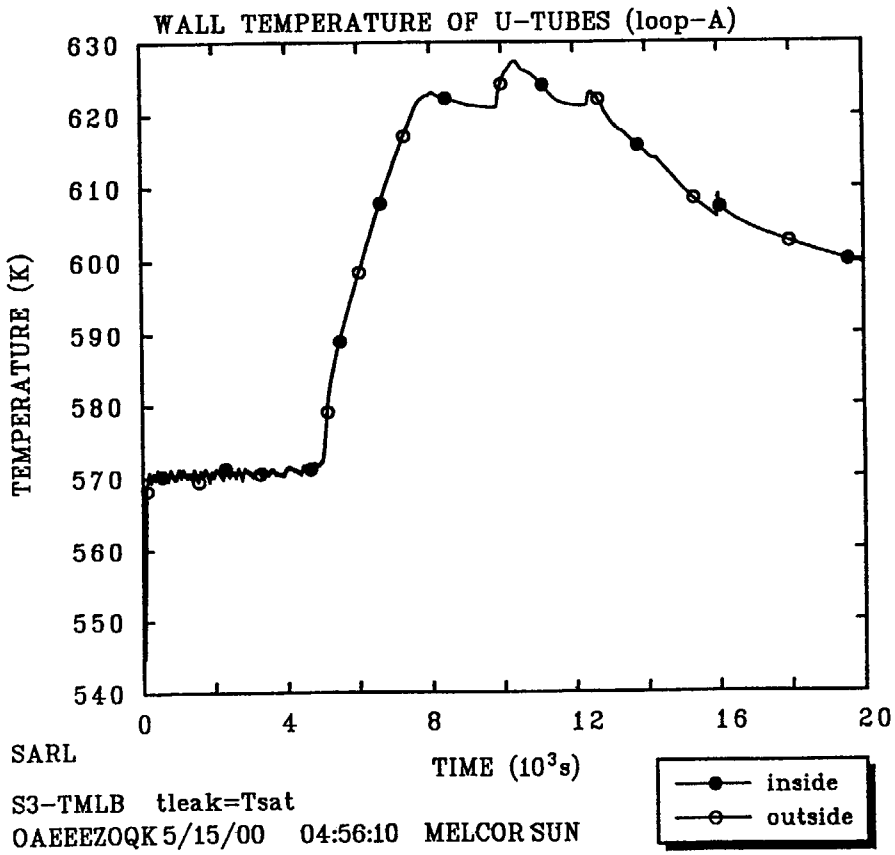

Figure 42. Run 2: Wall temperature of SG-A U-tubes.

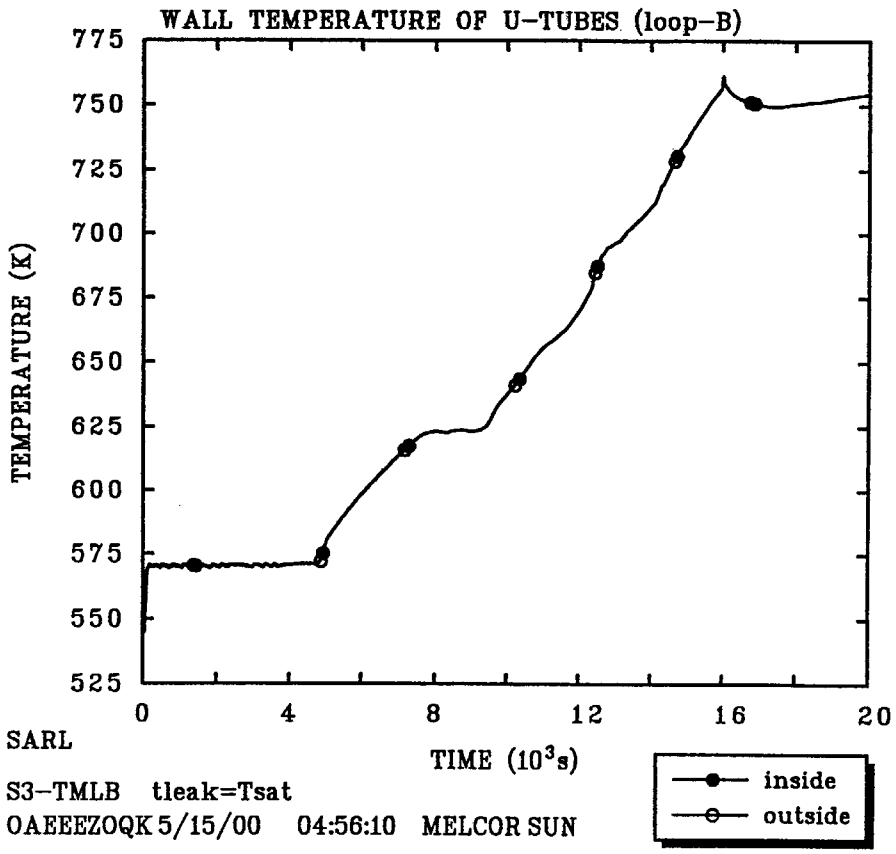

Figure 43. Run 2: Wall temperature of SG-B U-tubes.

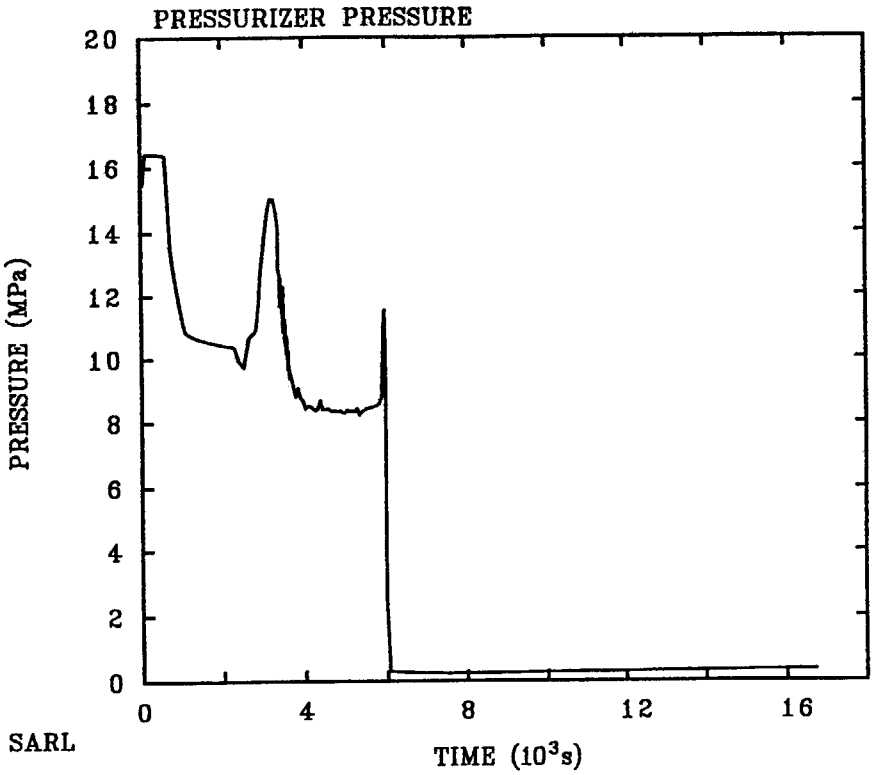

Figure 44. Run 2A: Pressurizer pressure.

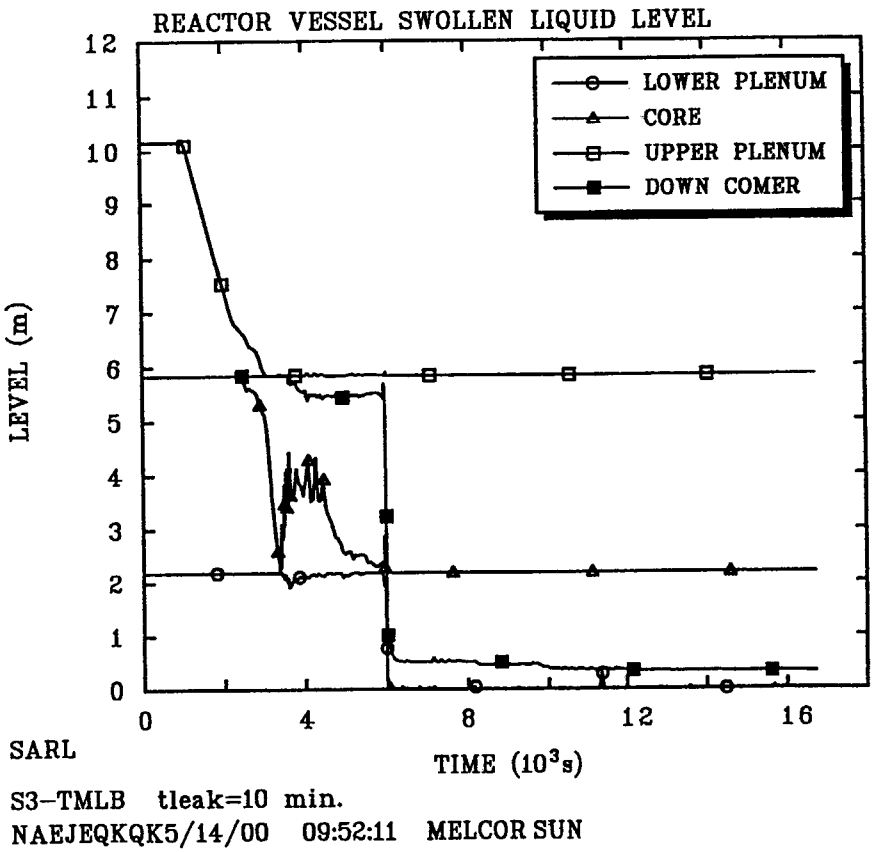

Figure 45. Run 2A: Swollen liquid level in reactor vessel.

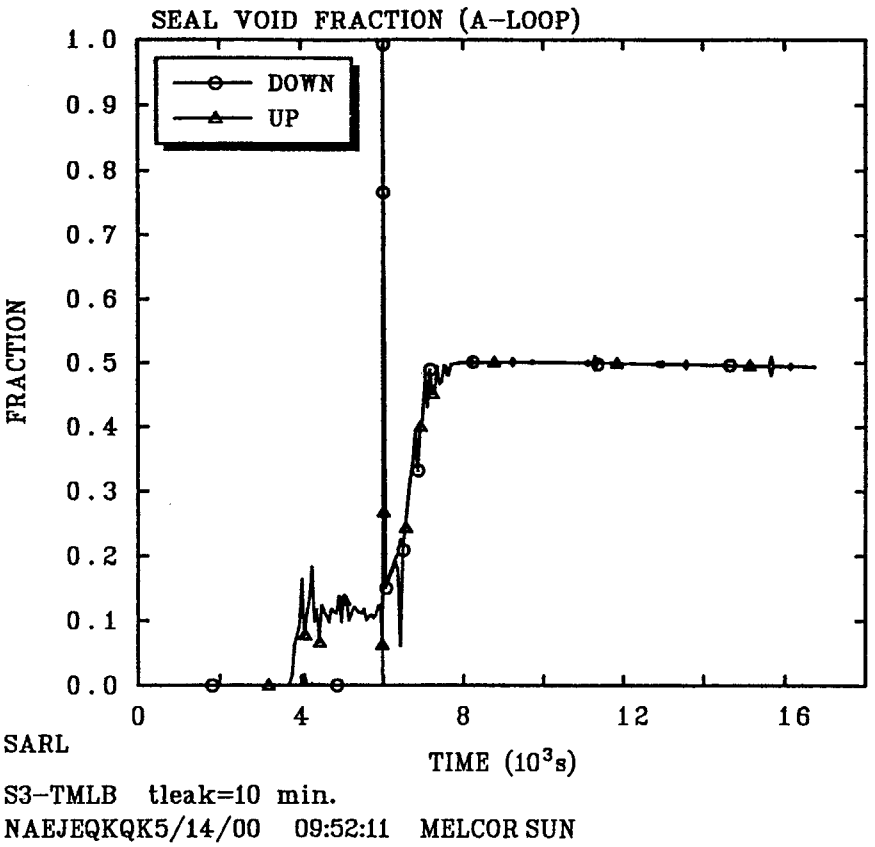

Figure 46. Run 2A: Loop seal void fraction of loop-A.

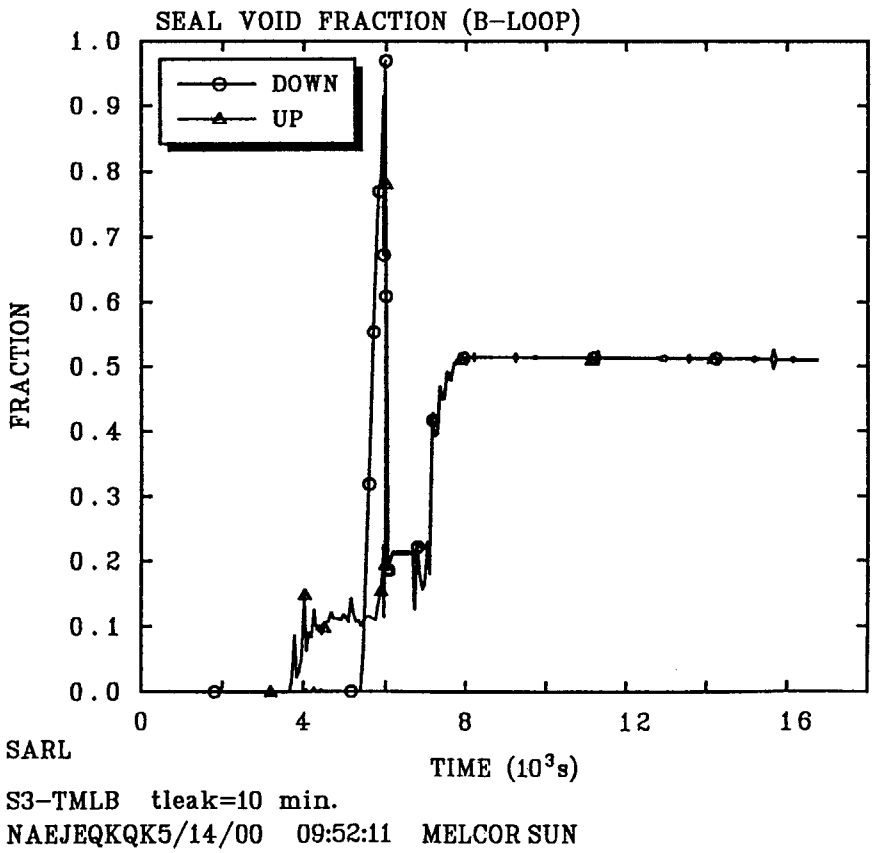

Figure 47. Run 2A: Loop seal void fraction of loop-B.

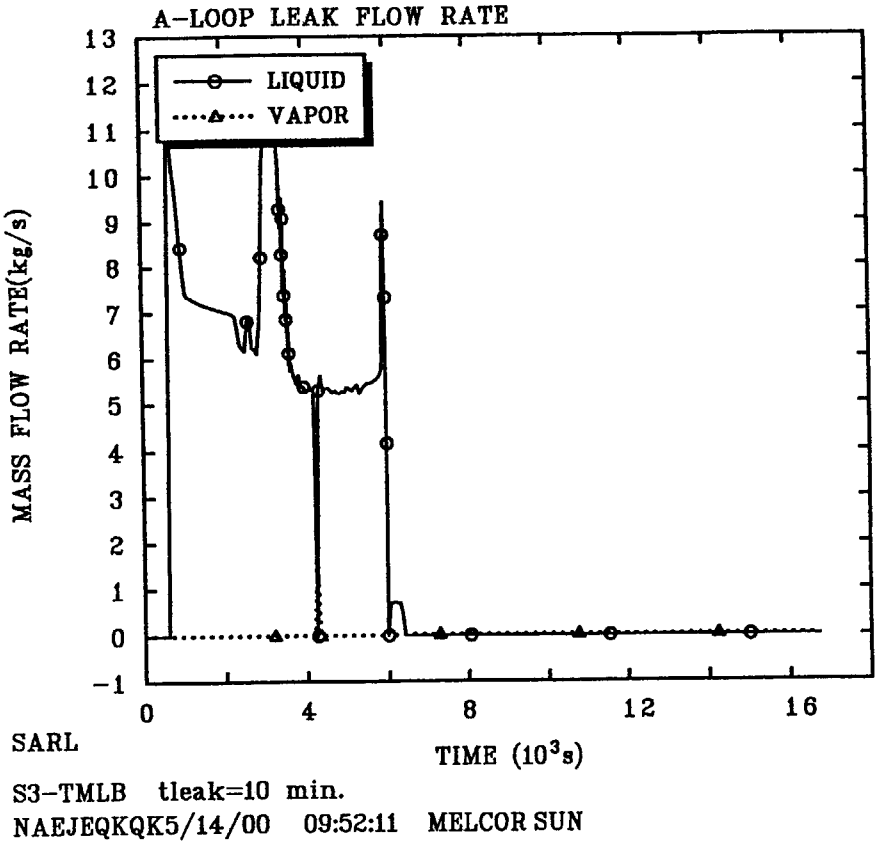

Figure 48. Run 2A: Coolant mass flow rate discharged from failed seal of loop-A.

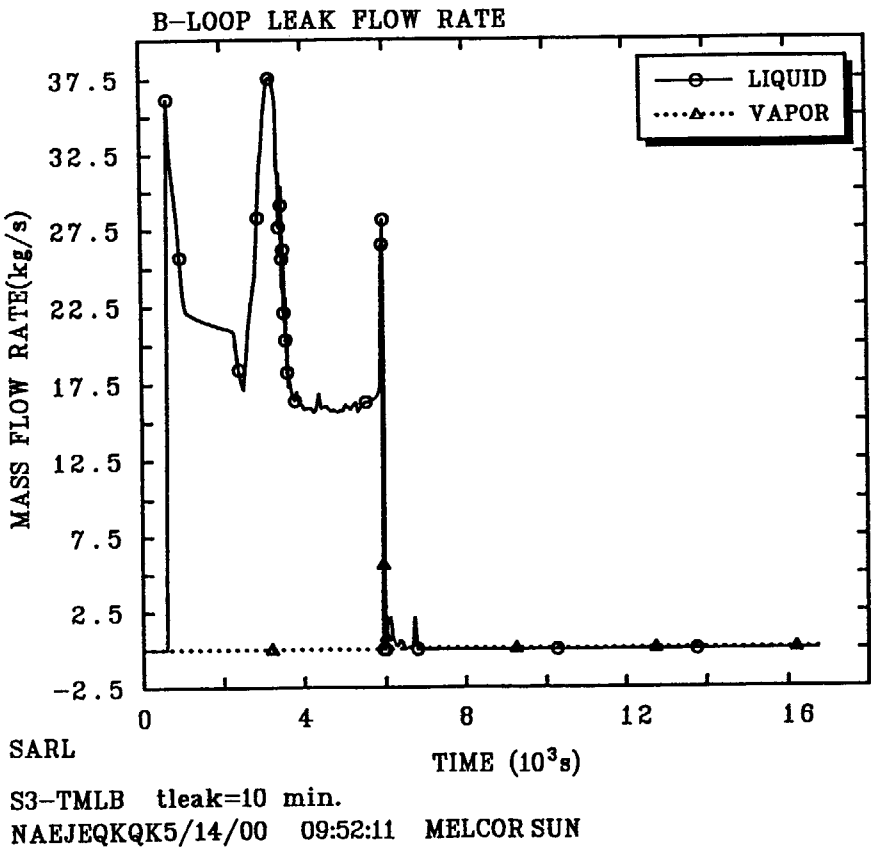

Figure 49. Run 2A: Coolant mass flow rate discharged from failed seal of loop-B.

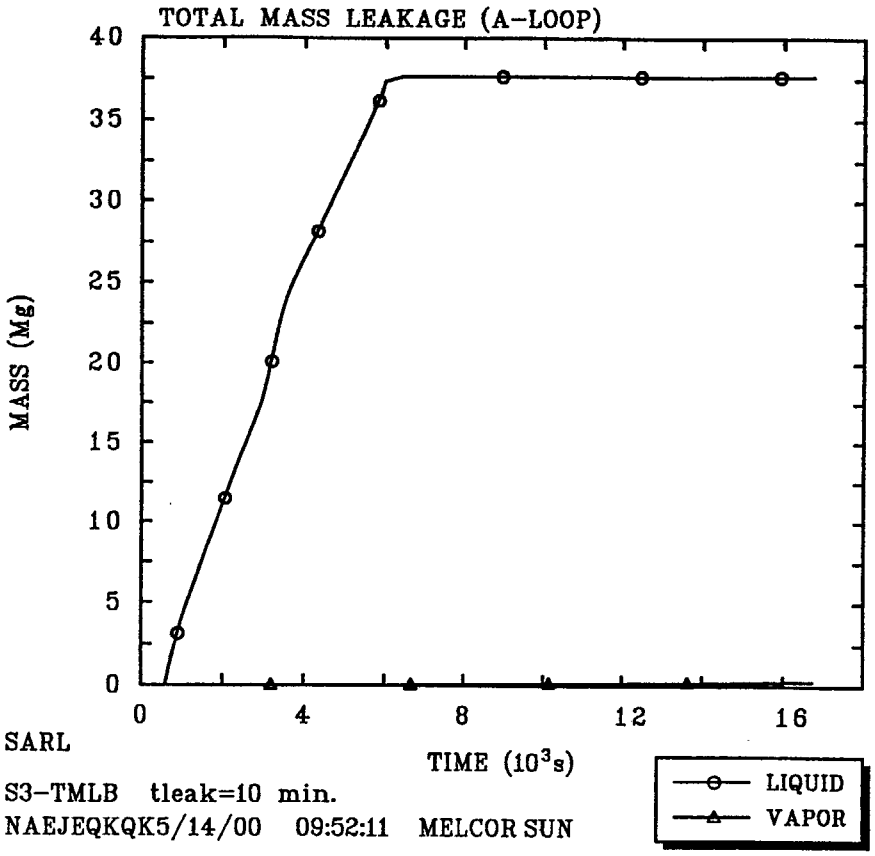

Figure 50. Run 2A: Total coolant mass discharged from failed seal of loop-A.

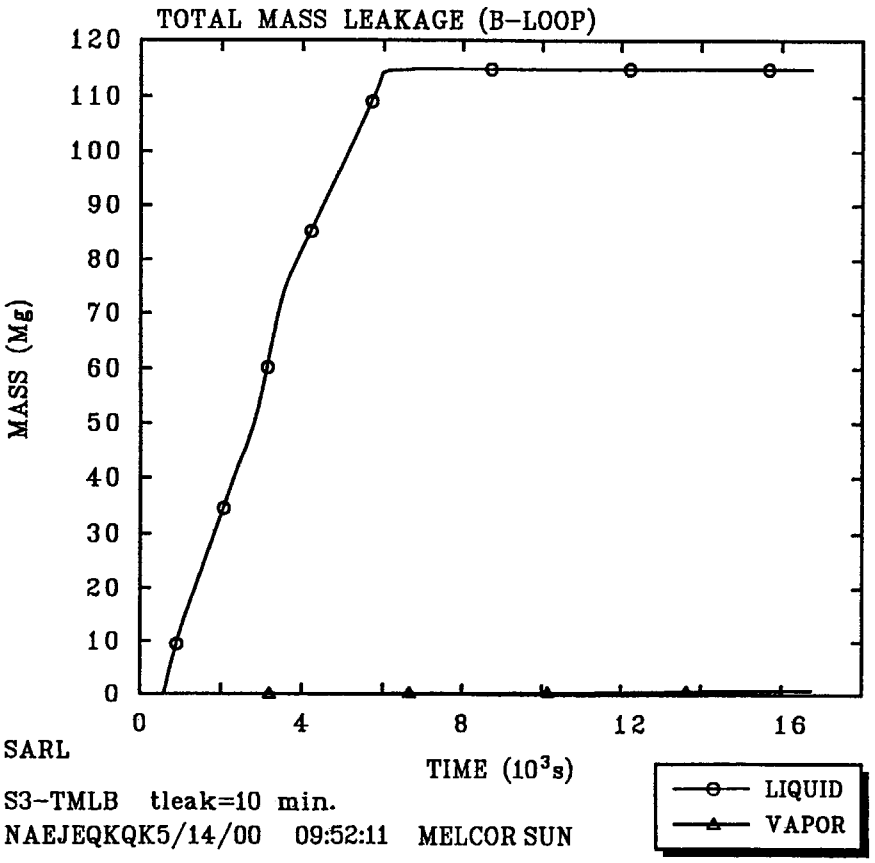

Figure 51. Run 2A: Total coolant mass discharged from failed seal of loop-B.

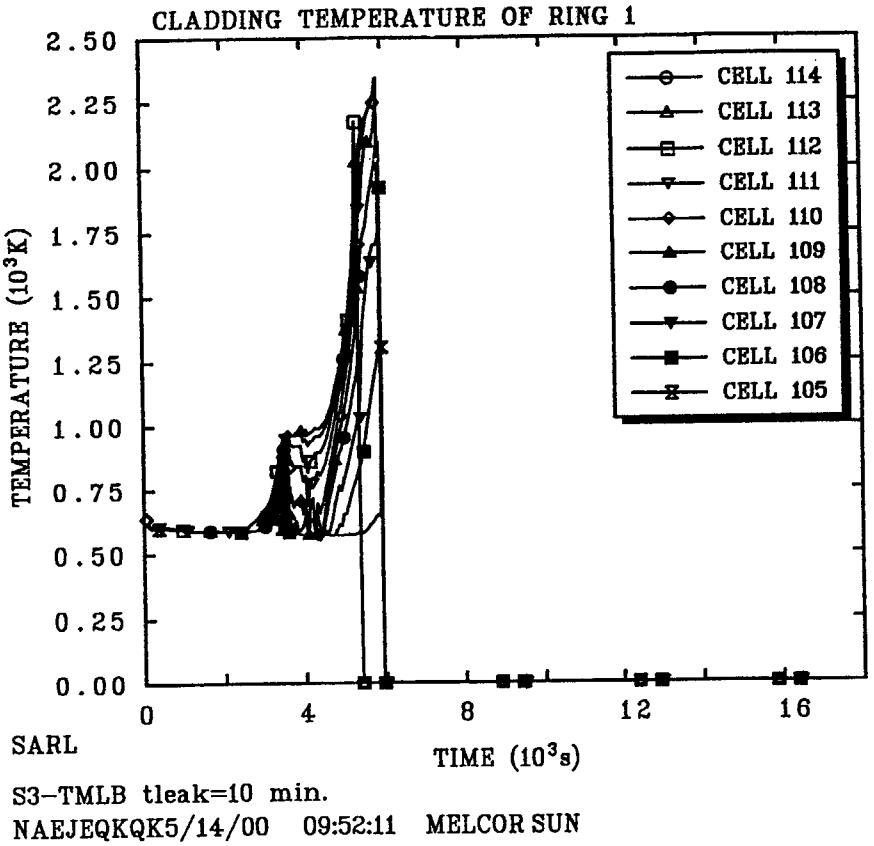

Figure 52. Run 2A: Cladding temperature in ring 1.

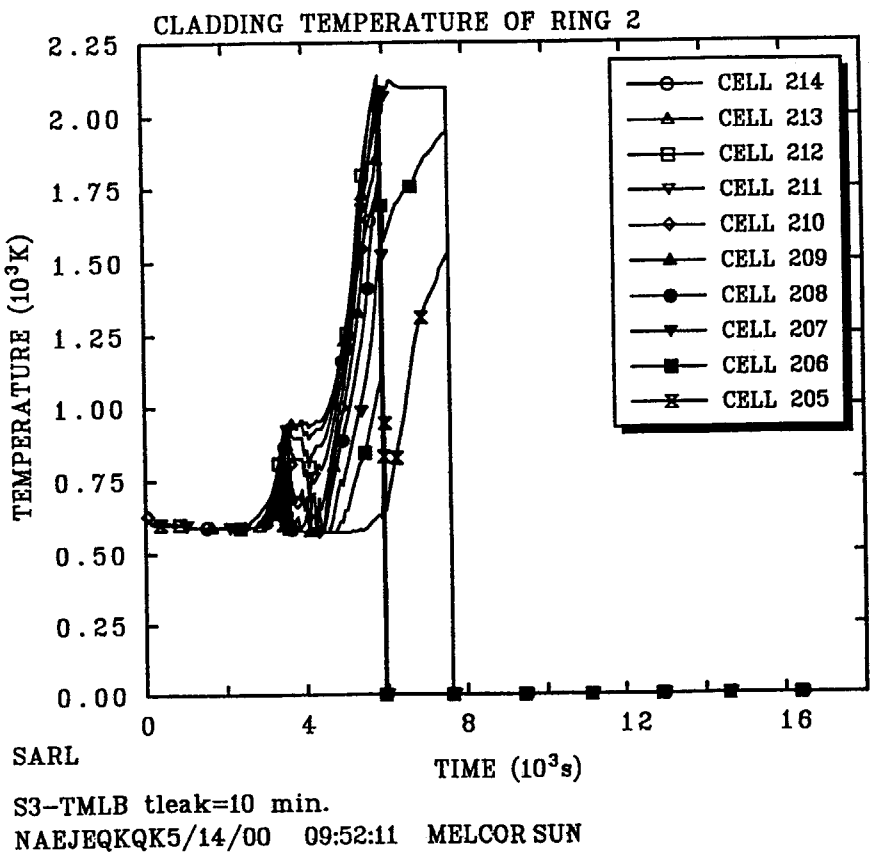

Figure 53. Run 2A: Cladding temperature in ring 2.

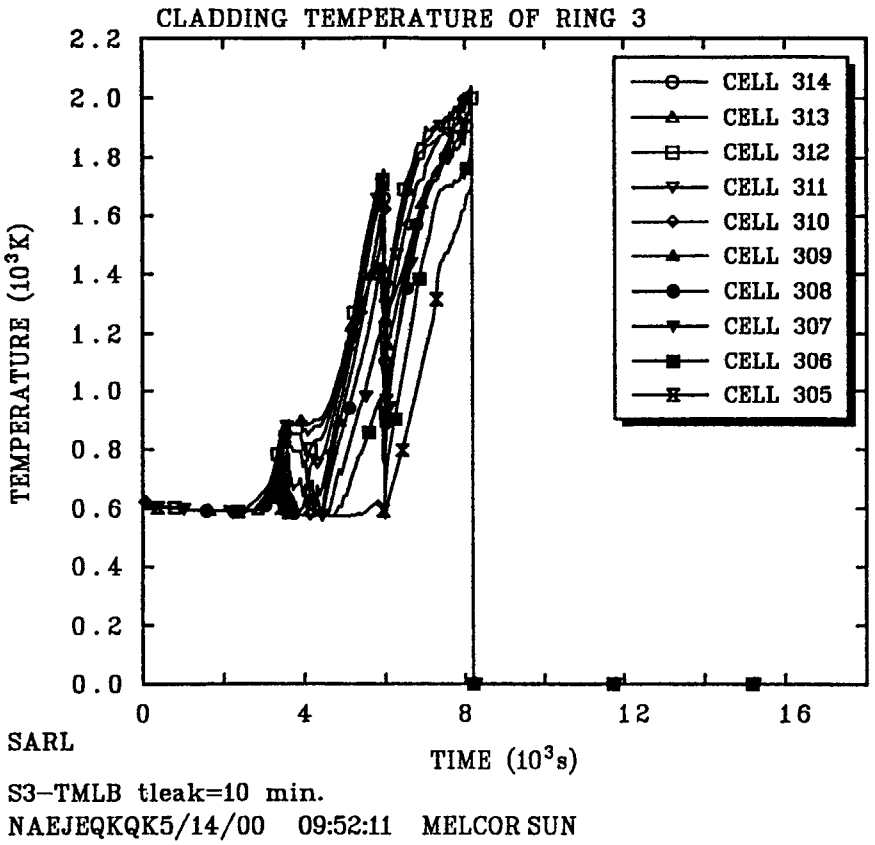

Figure 54. Run 2A: Cladding temperature in ring 3.

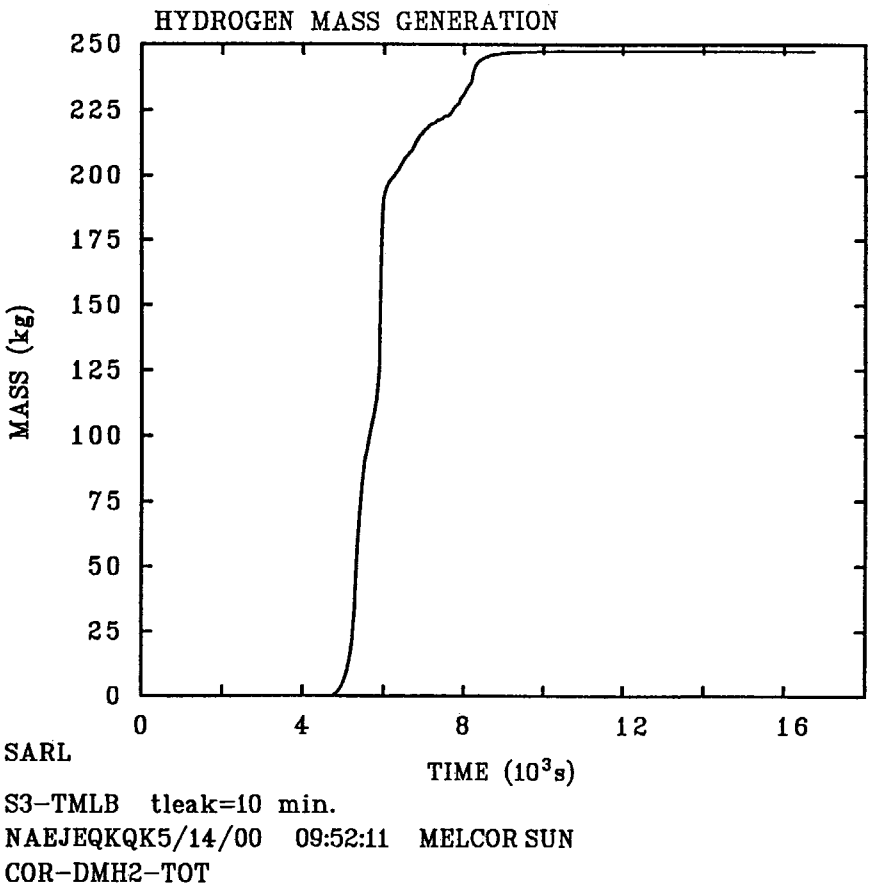

Figure 55. Run 2A: Hydrogen mass generated.

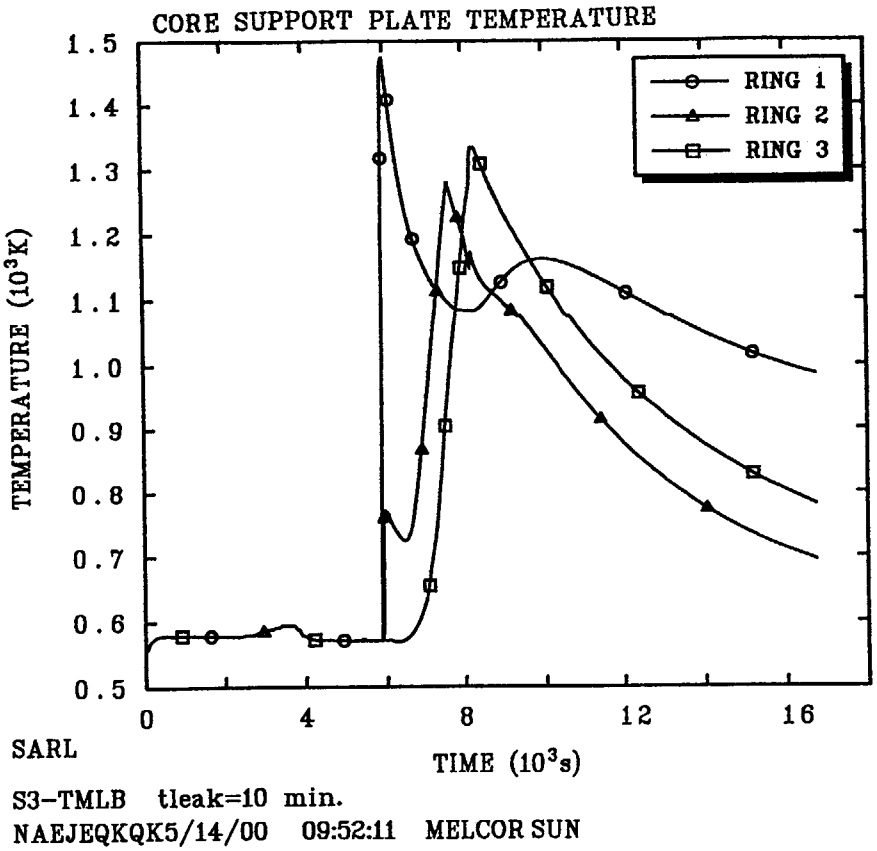

Figure 56. Run 2A: Core support plate temperature.

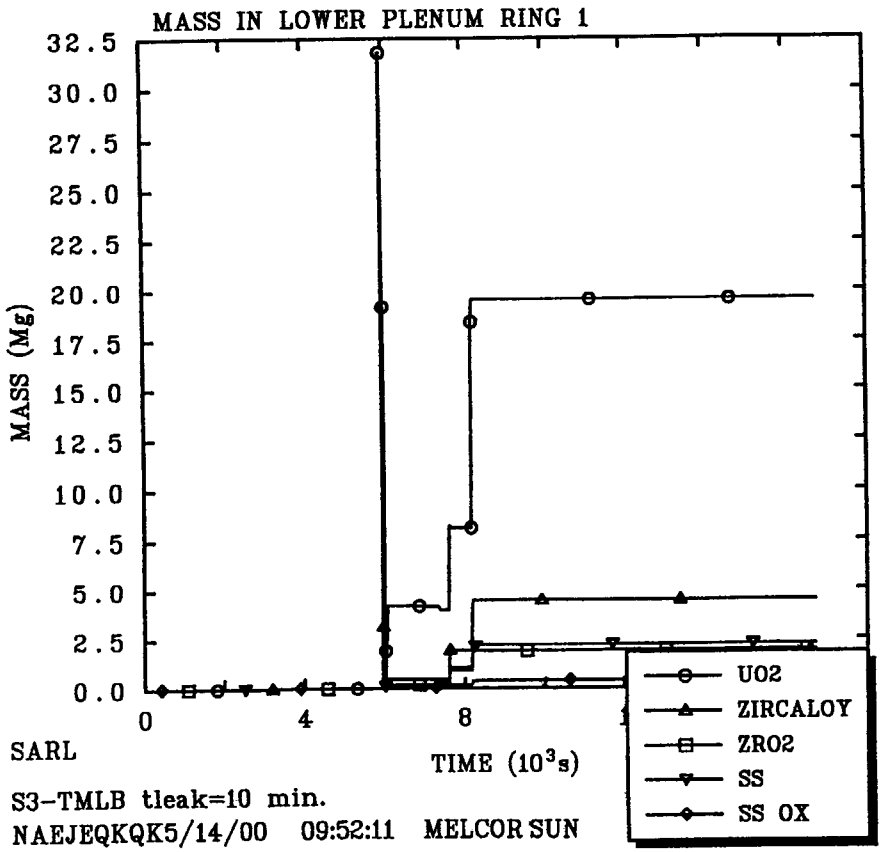

Figure 57. Run 2A: Debris mass in lower plenum ring 1.

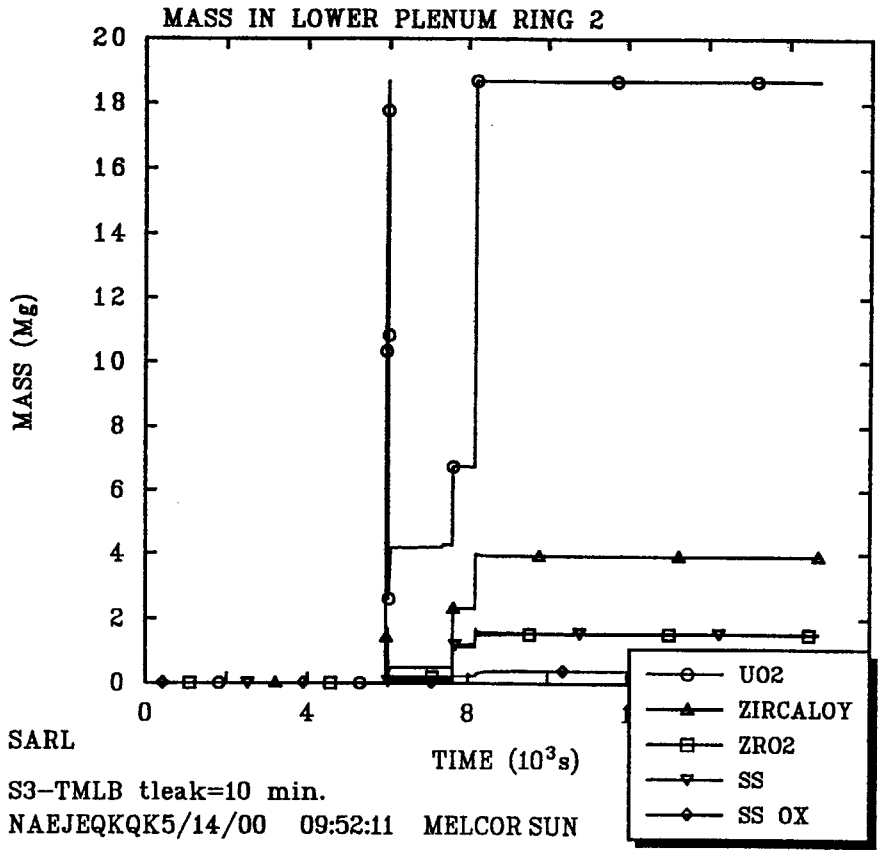

Figure 58. Run 2A: Debris mass in lower plenum ring 2.

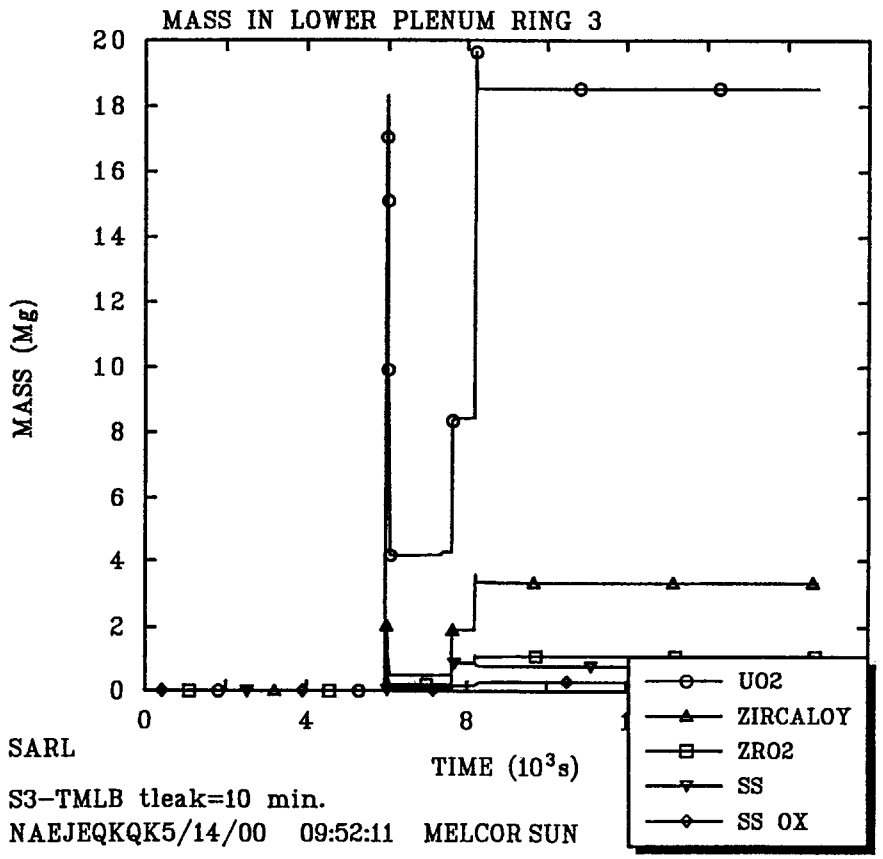

Figure 59. Run 2A: Debris mass in lower plenum ring 3.

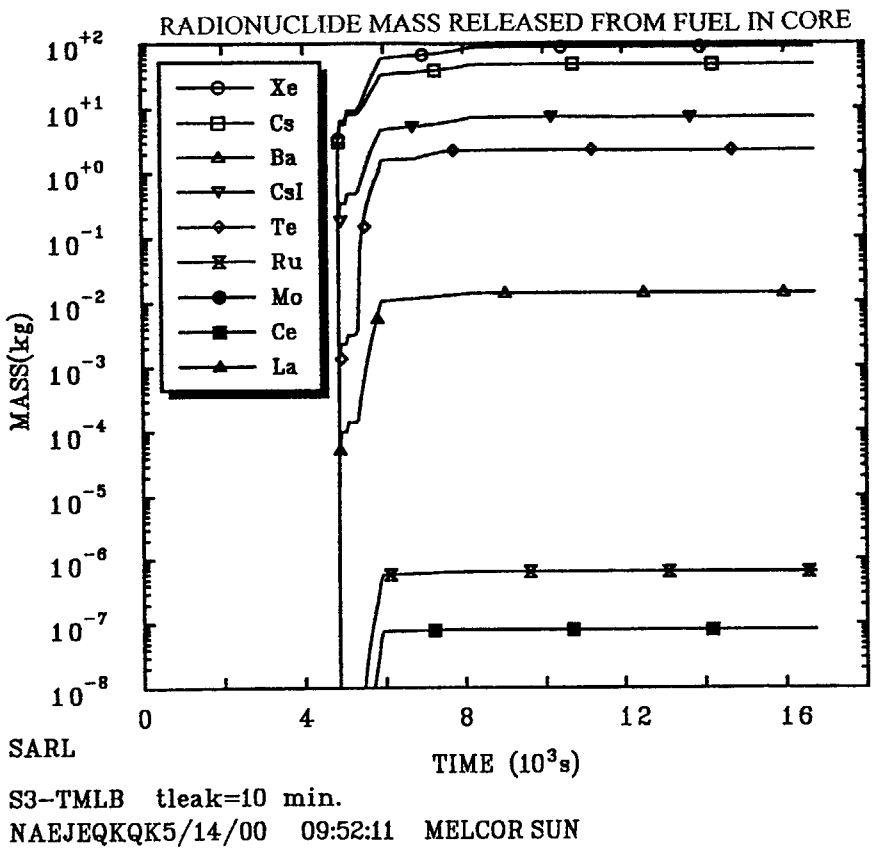

Figure 60. Run 2A: Radionuclide mass released from fuel in core.

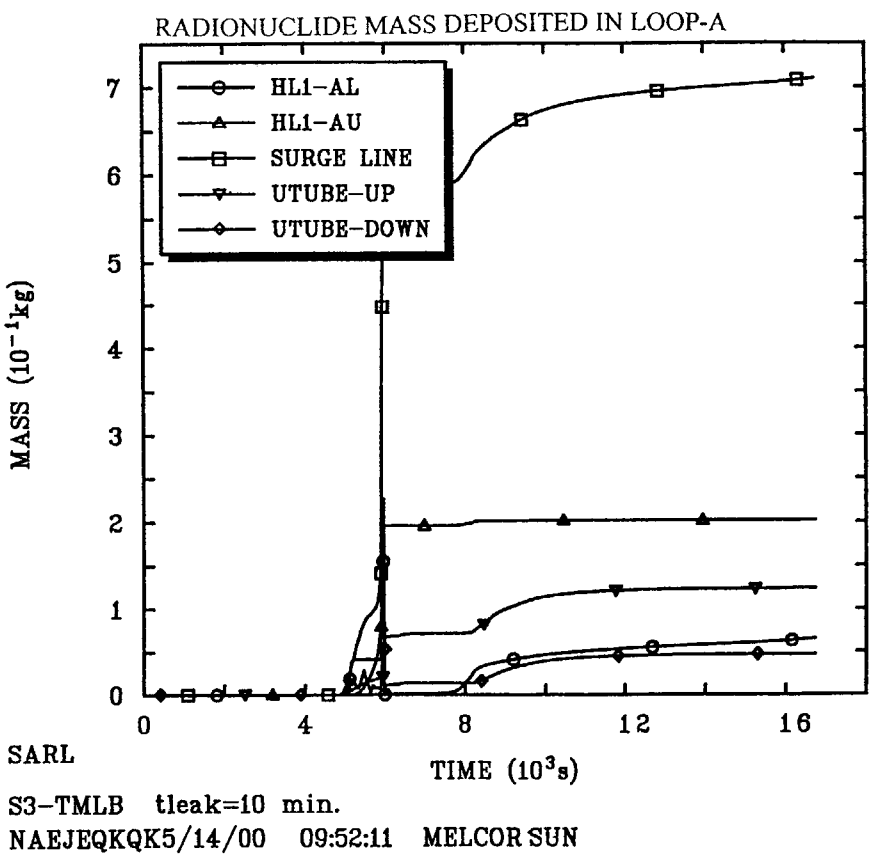

Figure 61. Run 2A: Deposited radionuclide mass.

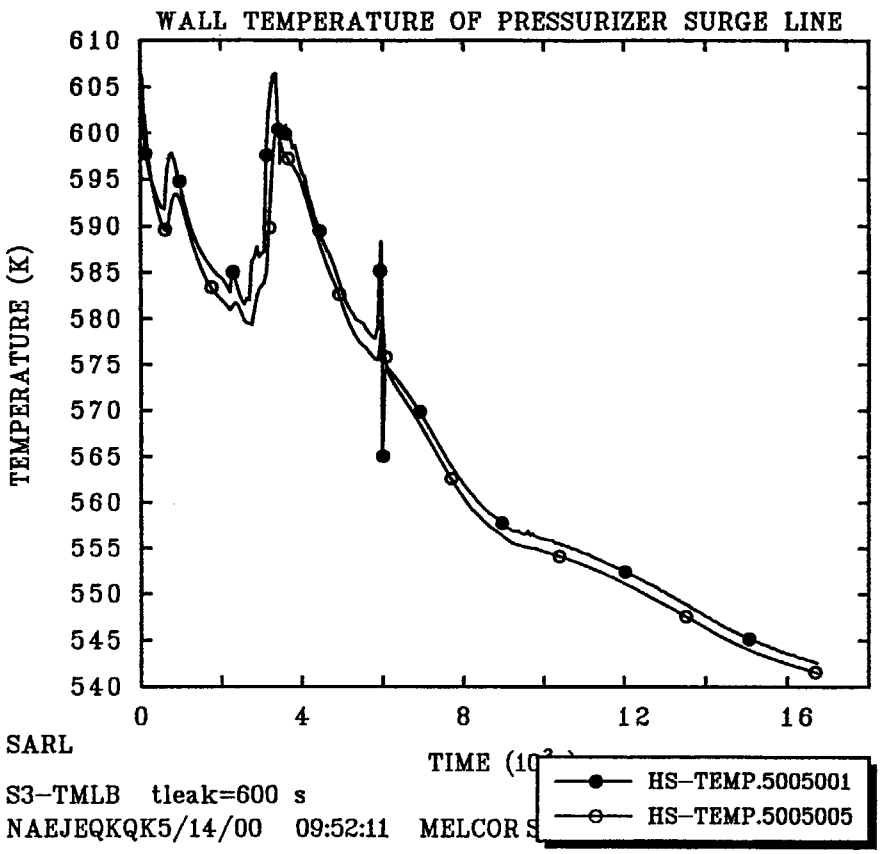

Figure 62. Run 2A: Wall temperature of surge line.

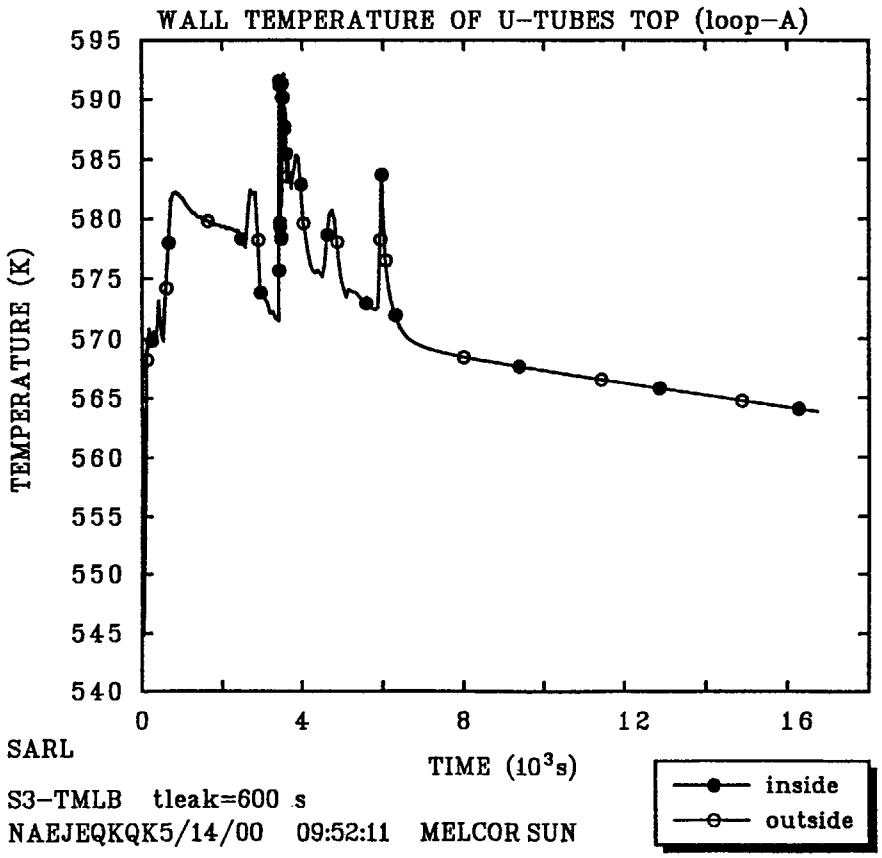

Figure 63. Run 2A: Wall temperature of SG-A U-tubes.

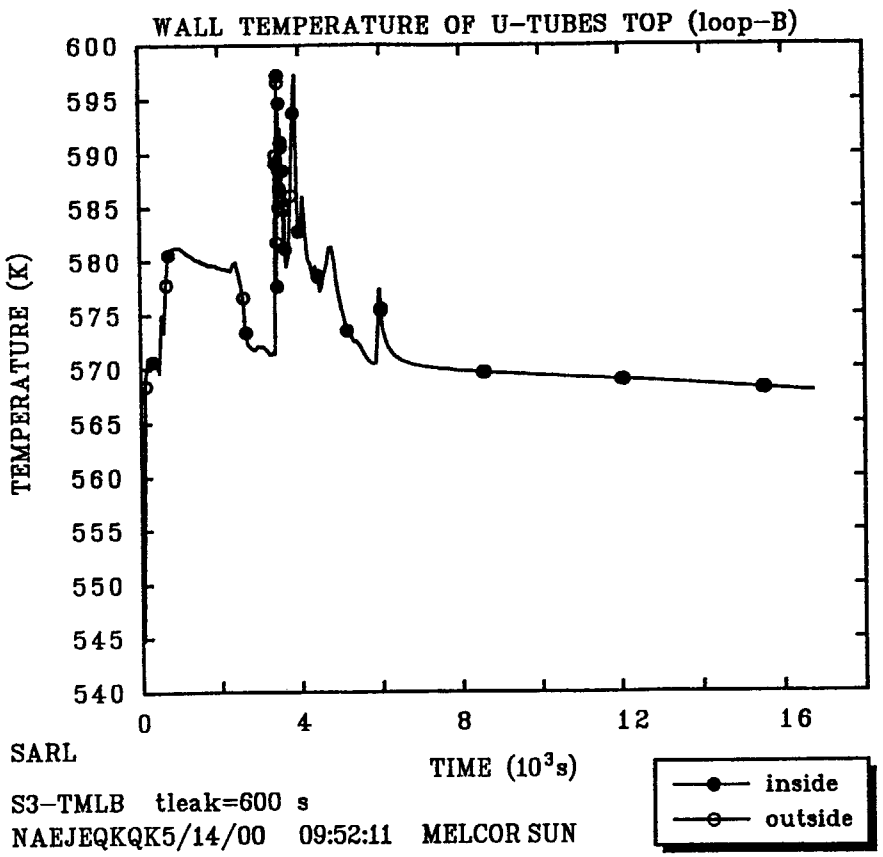

Figure 64. Run 2A: Wall temperature of SG-B U-tubes.

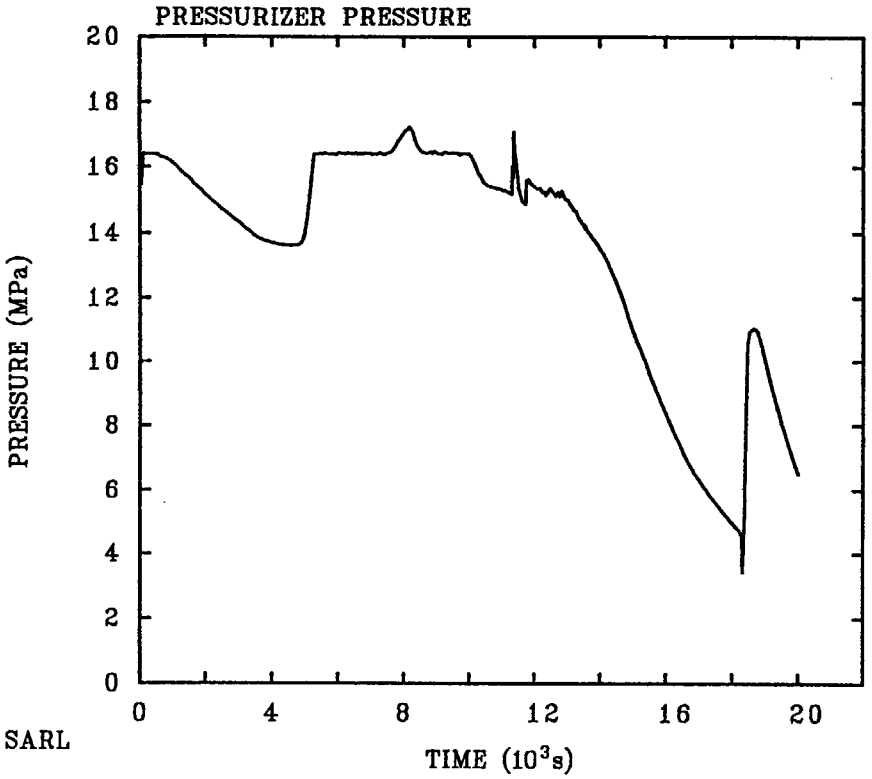

Figure 65. Run 2B: Pressurizer pressure.

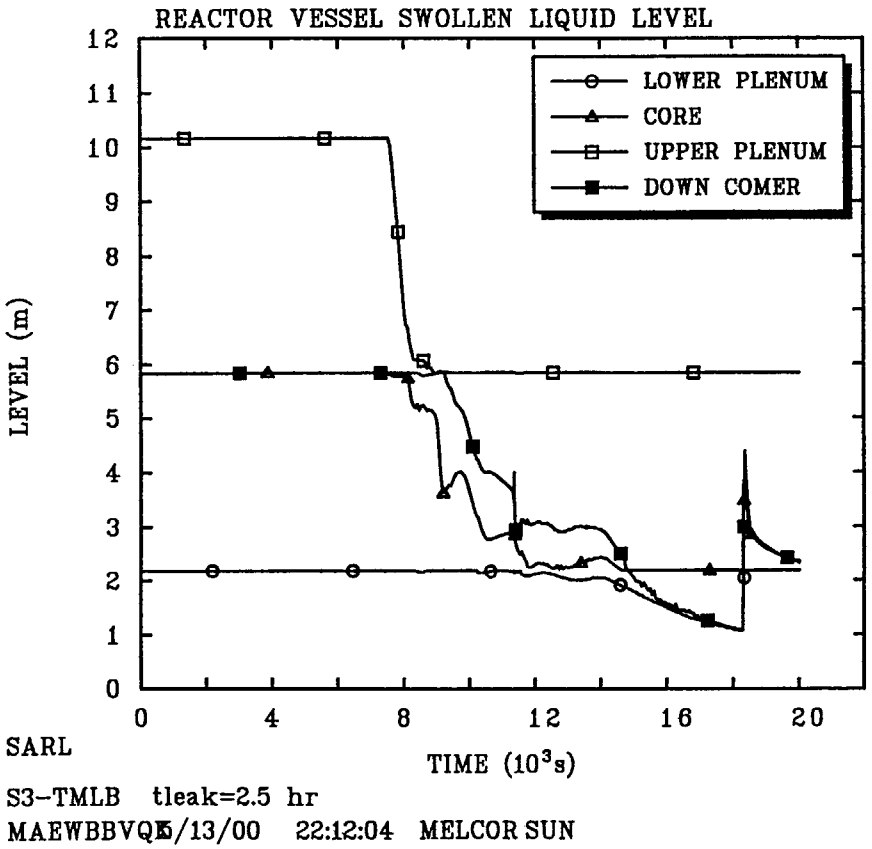

Figure 66. Run 2B: Swollen liquid level in reactor vessel.

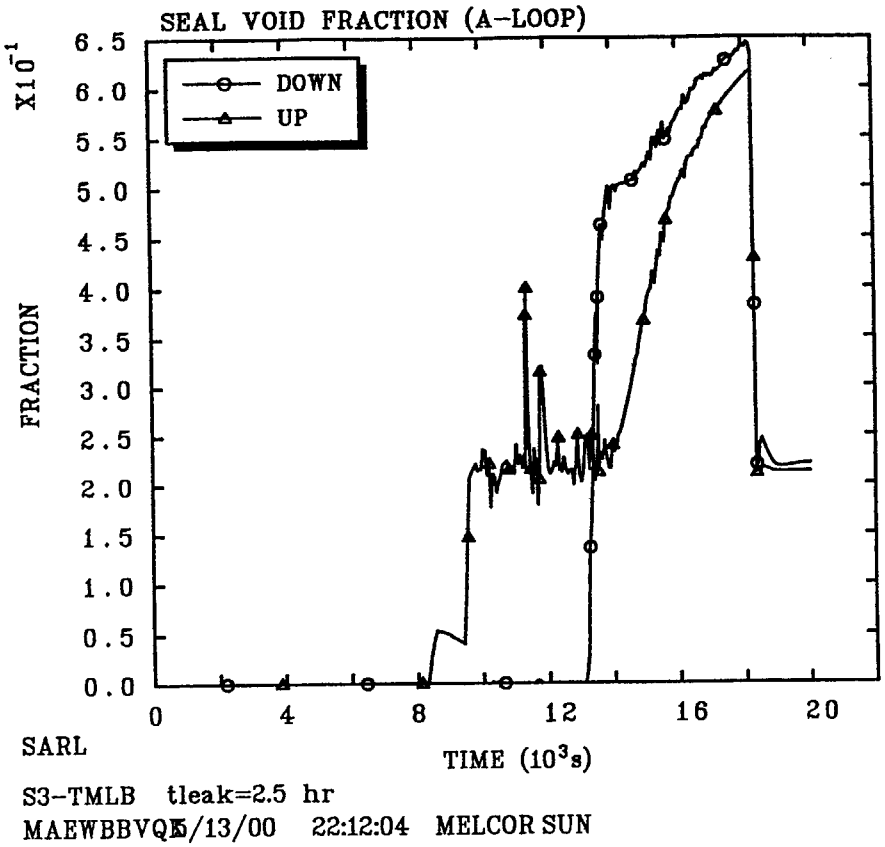

Figure 67. Run 2B: Loop seal void fraction of loop-A.

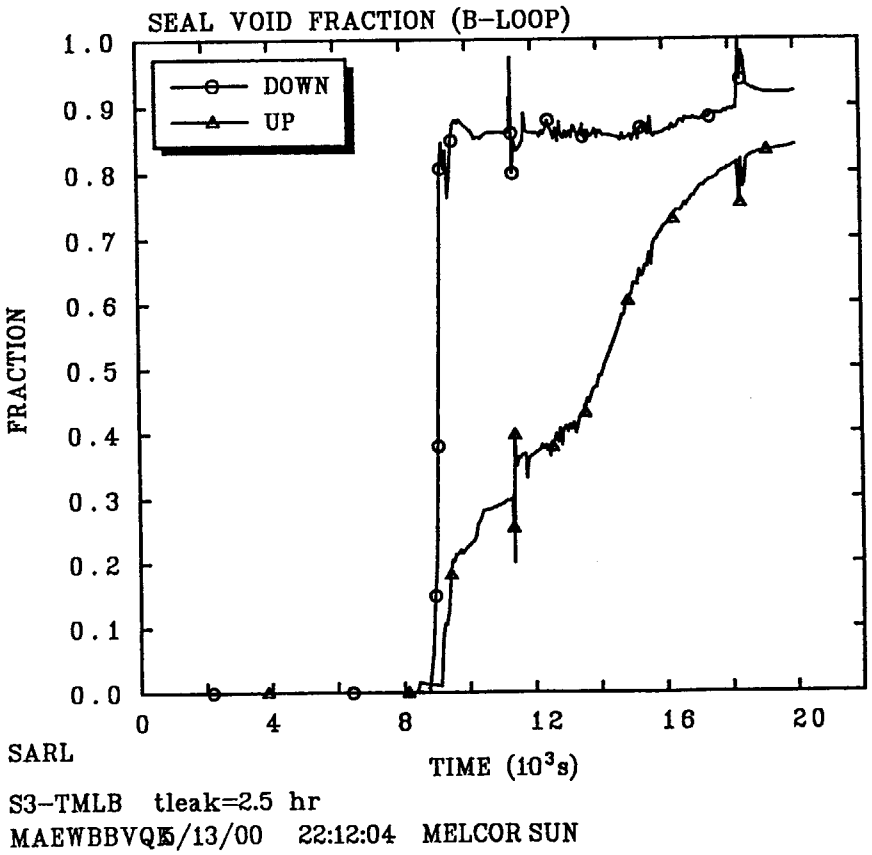

Figure 68. Run 2B: Loop seal void fraction of loop-B.

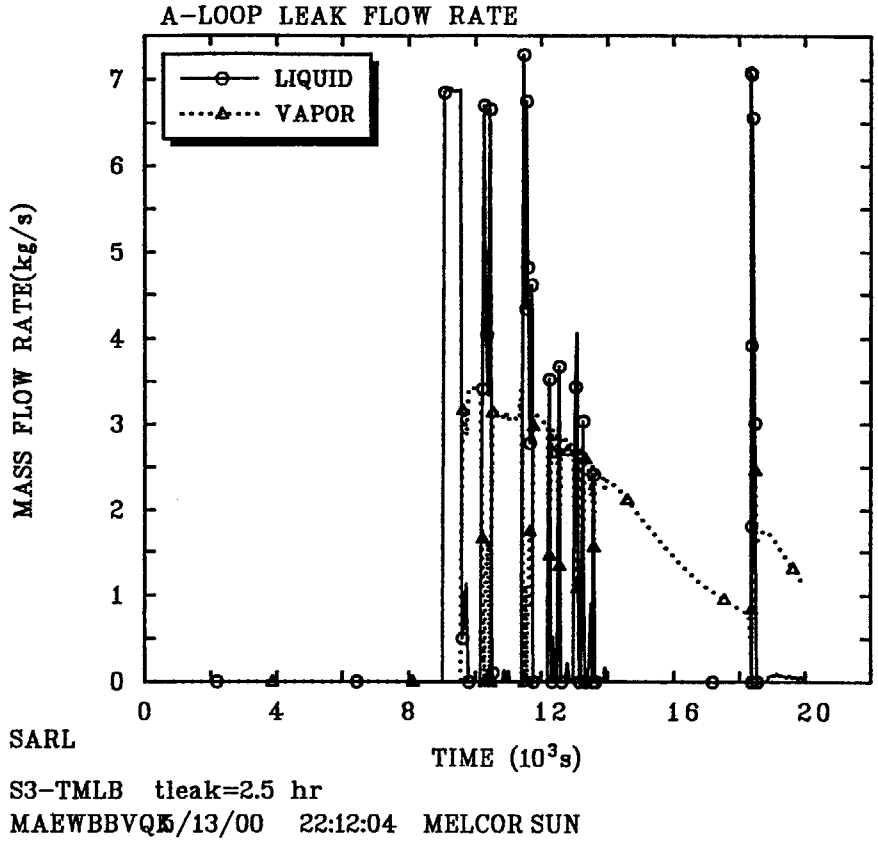

Figure 69. Run 2B: Coolant mass flow rate discharged from failed seal of loop-A.

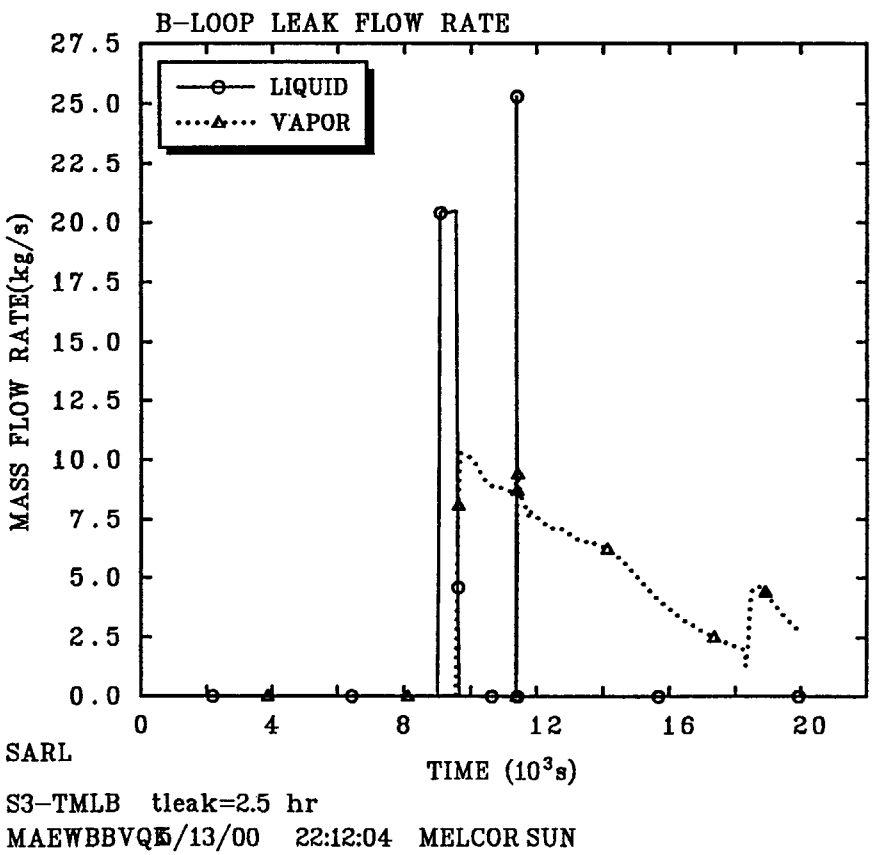

Figure 70. Run 2B: Coolant mass flow rate discharged from failed seal of loop-B.

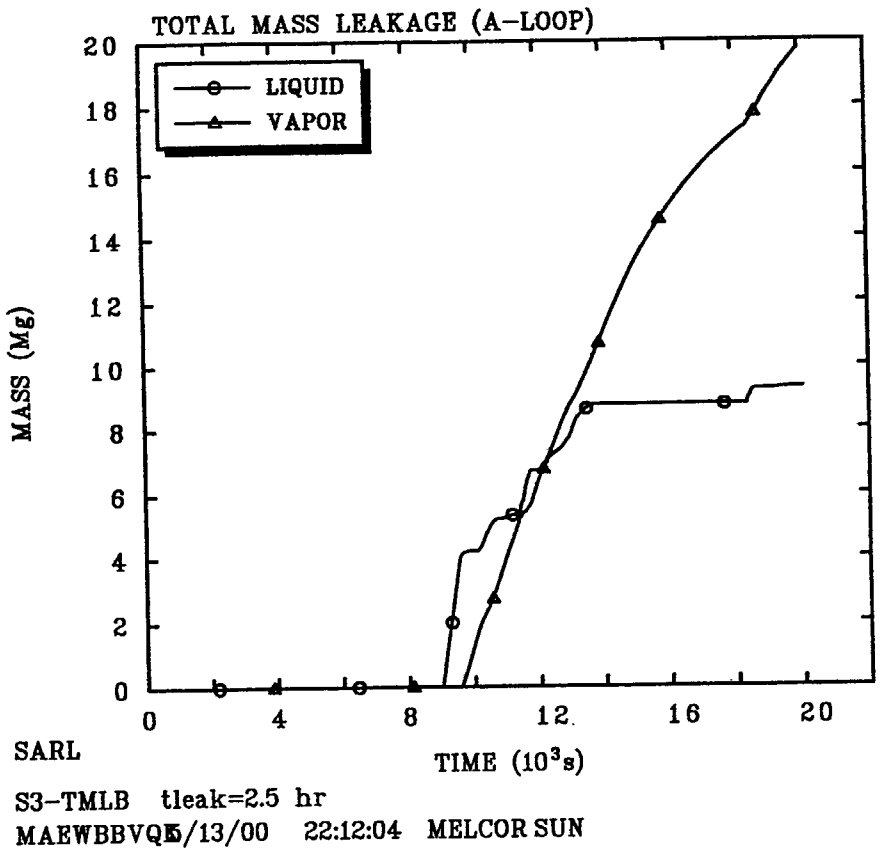

Figure 71. Run 2B: Total coolant mass discharged from failed seal of loop-A.

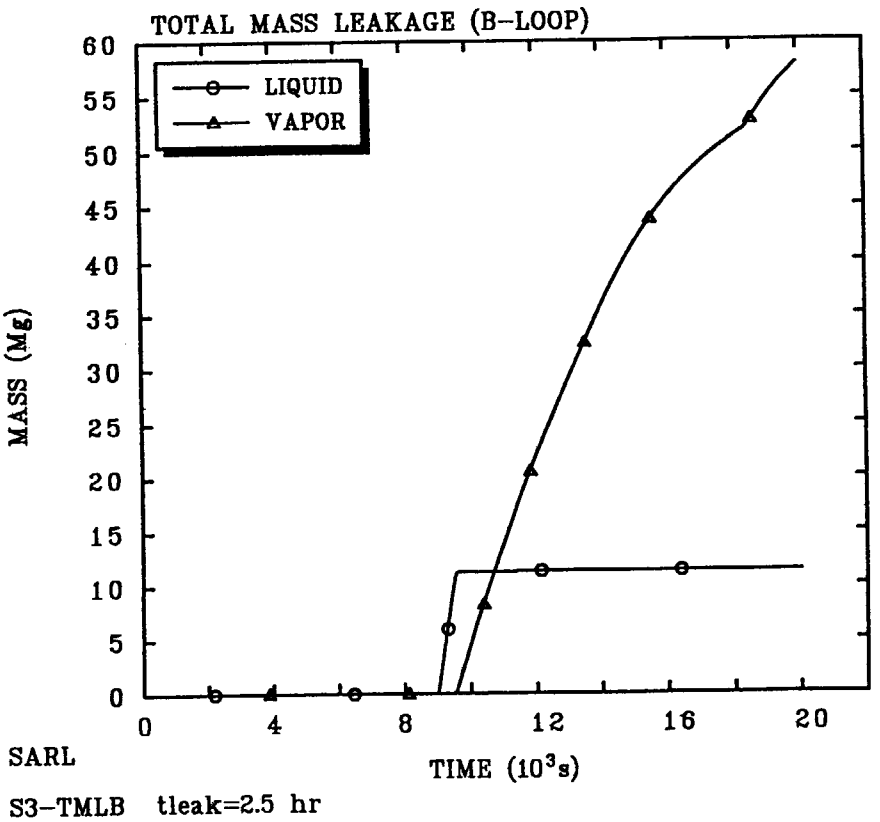

Figure 72. Run 2B: Total coolant mass discharged from failed seal of loop-B.

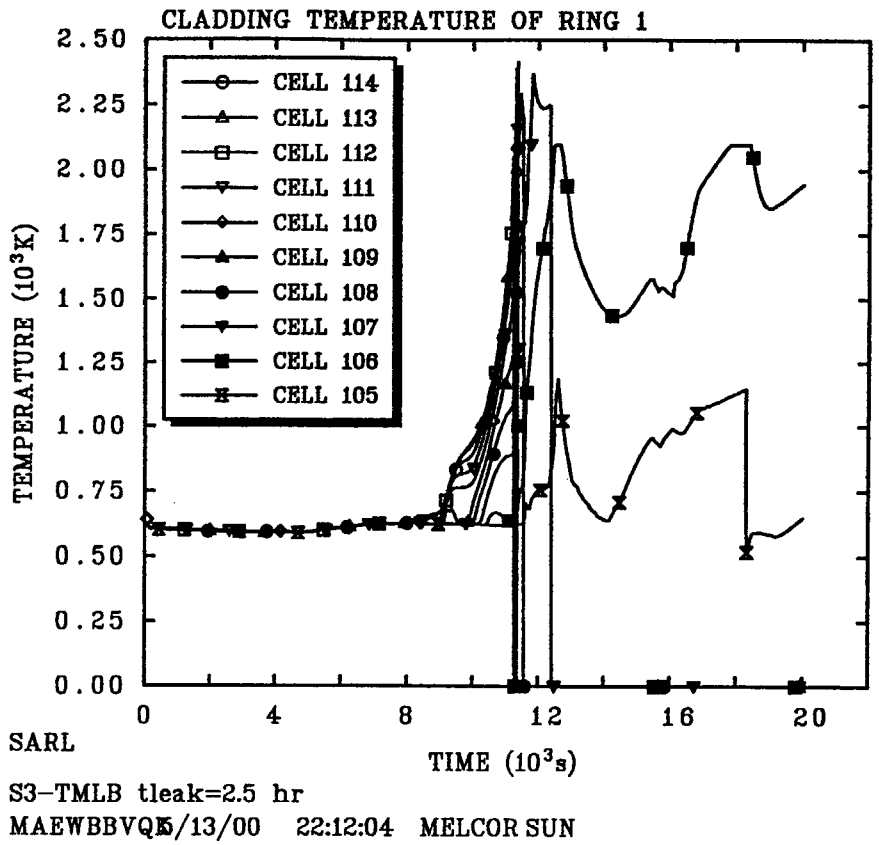

Figure 73. Run 2B: Cladding temperature in ring 1.

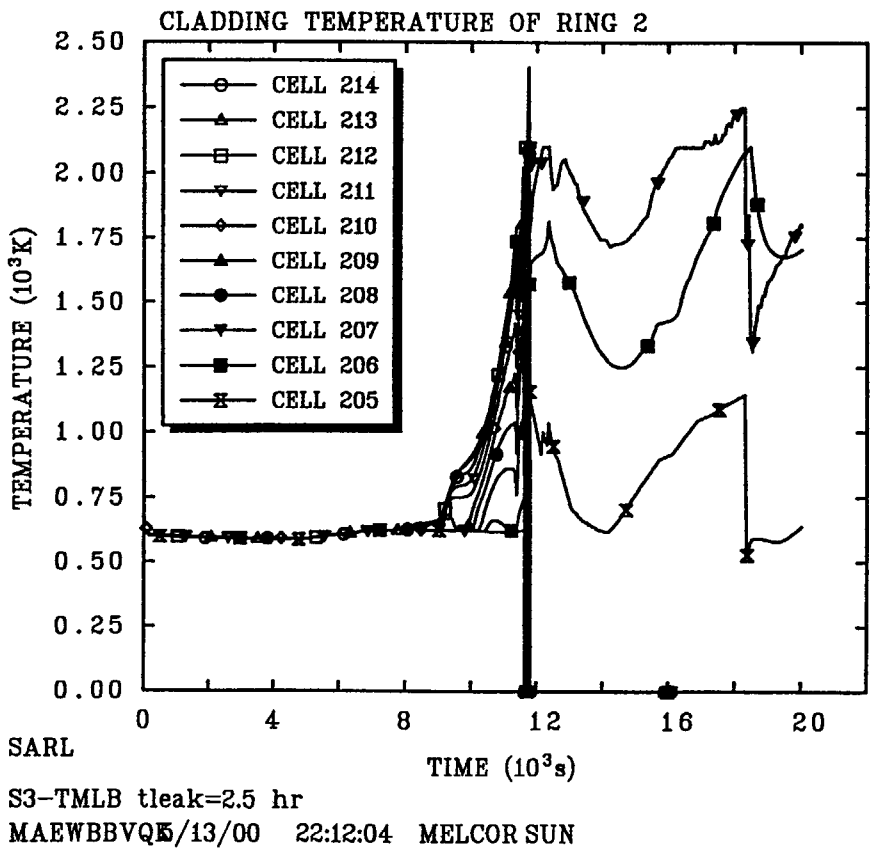

Figure 74. Run 2B: Cladding temperature in ring 2.

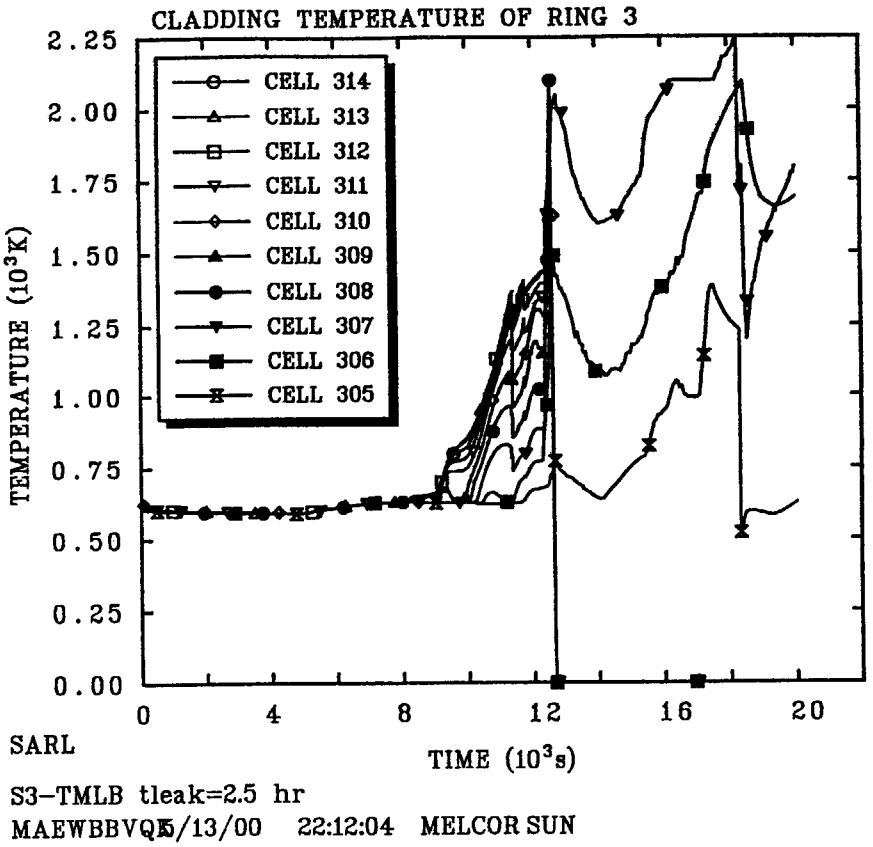

Figure 75. Run 2B: Cladding temperature in ring 3.

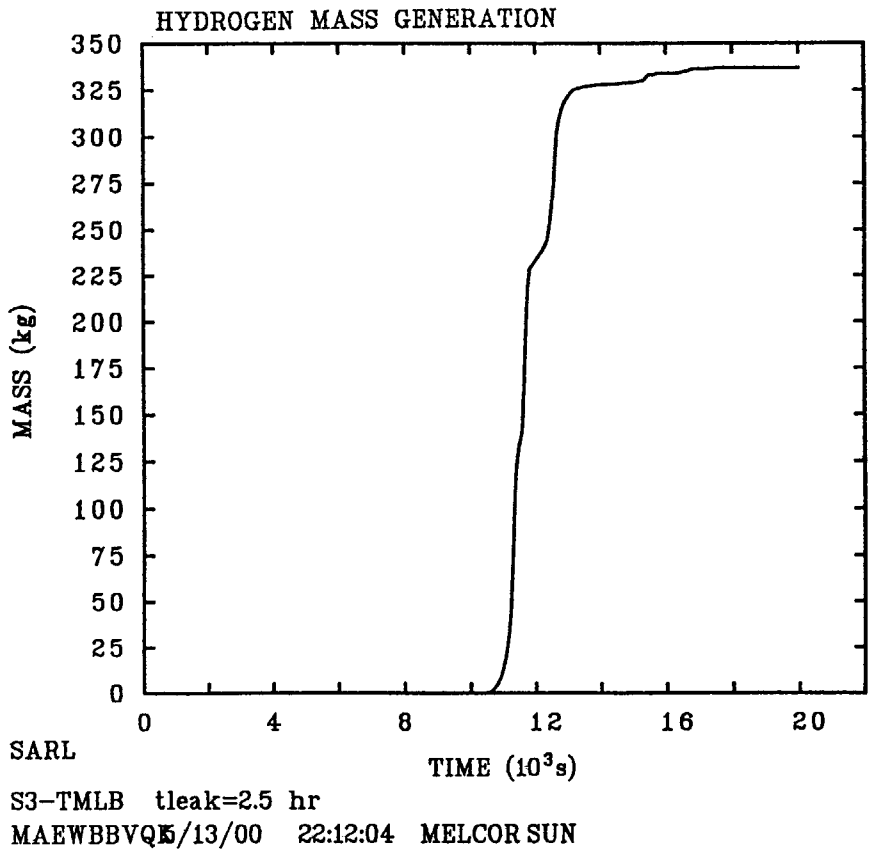

Figure 76. Run 2B: Hydrogen mass generated.

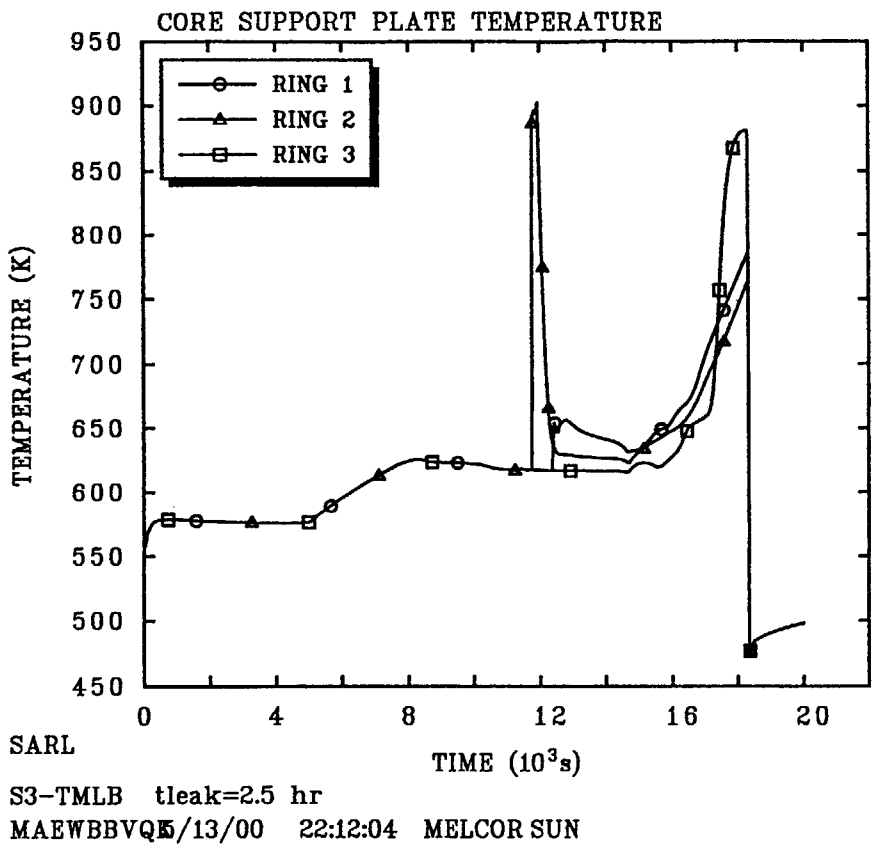

Figure 77. Run 2B: Core support plate temperature.

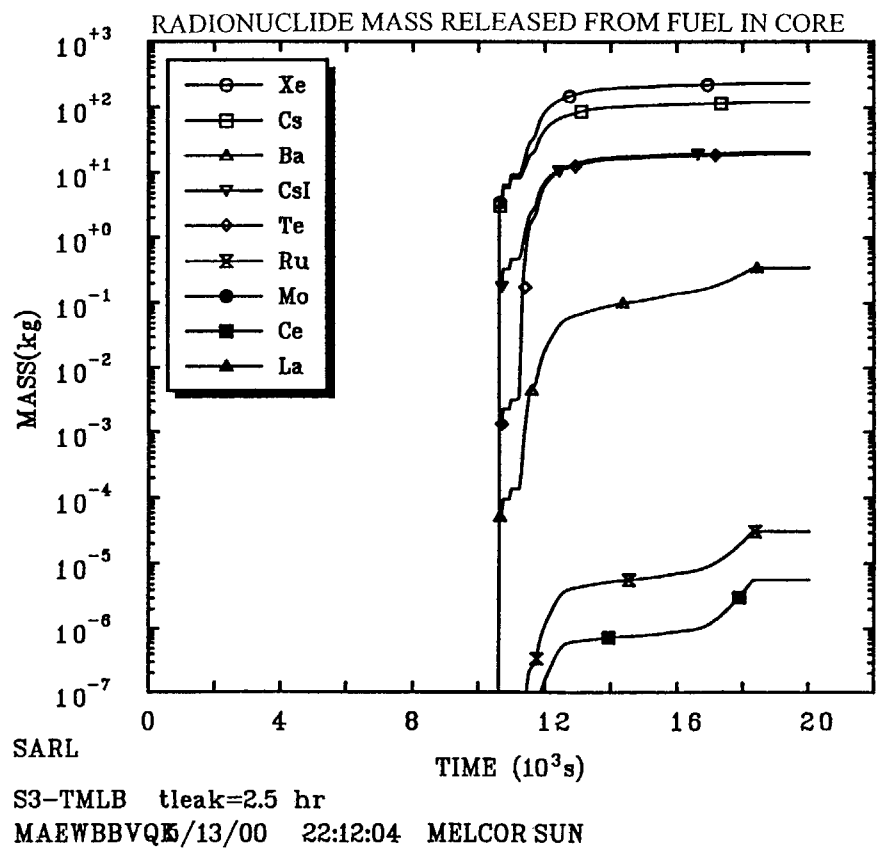

Figure 78. Run 2B: Radionuclide mass released from fuel in core.

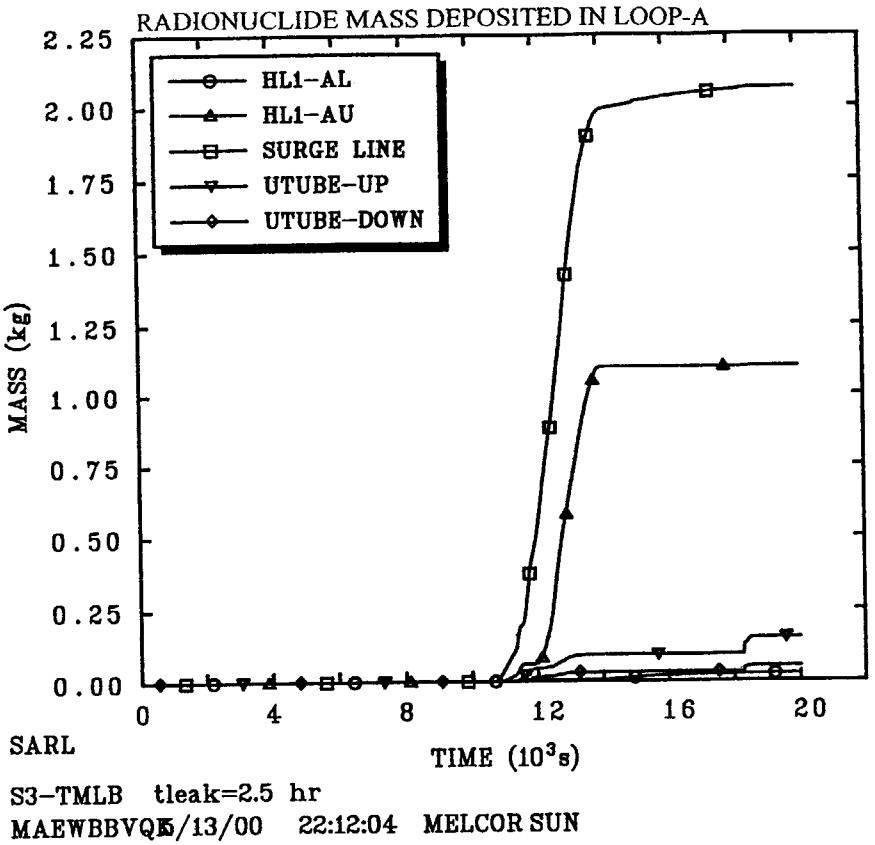

Figure 79. Run 2B: Deposited radionuclide mass.

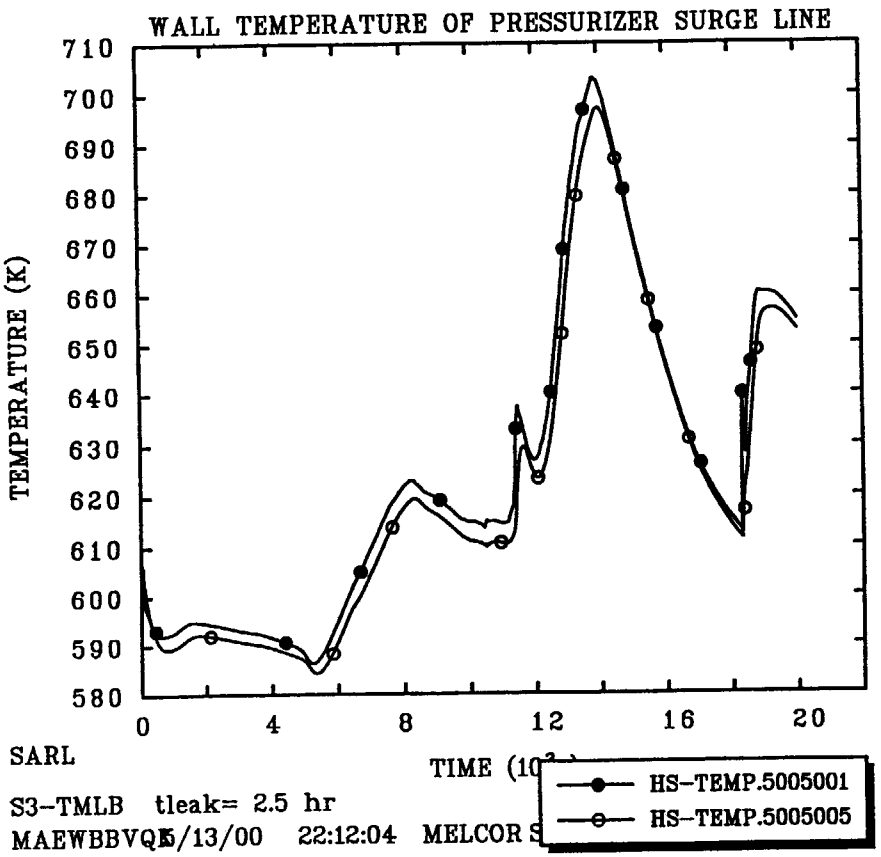

Figure 80. Run 2B: Wall temperature of surge line.

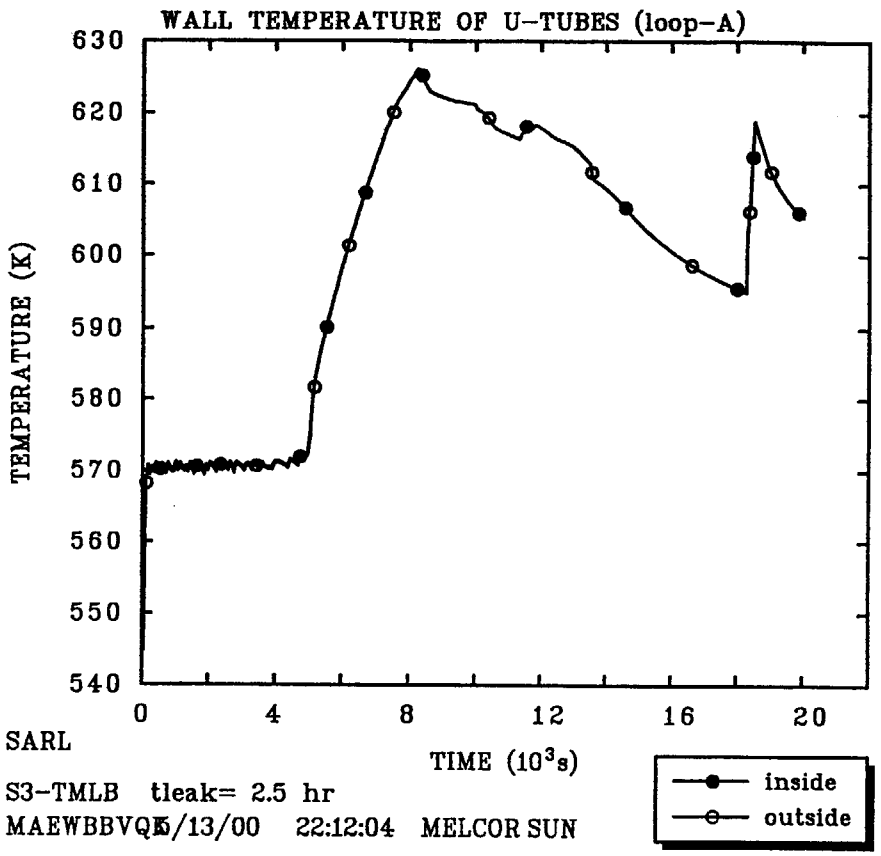

Figure 81. Run 2B: Wall temperature of SG-A U-tubes.

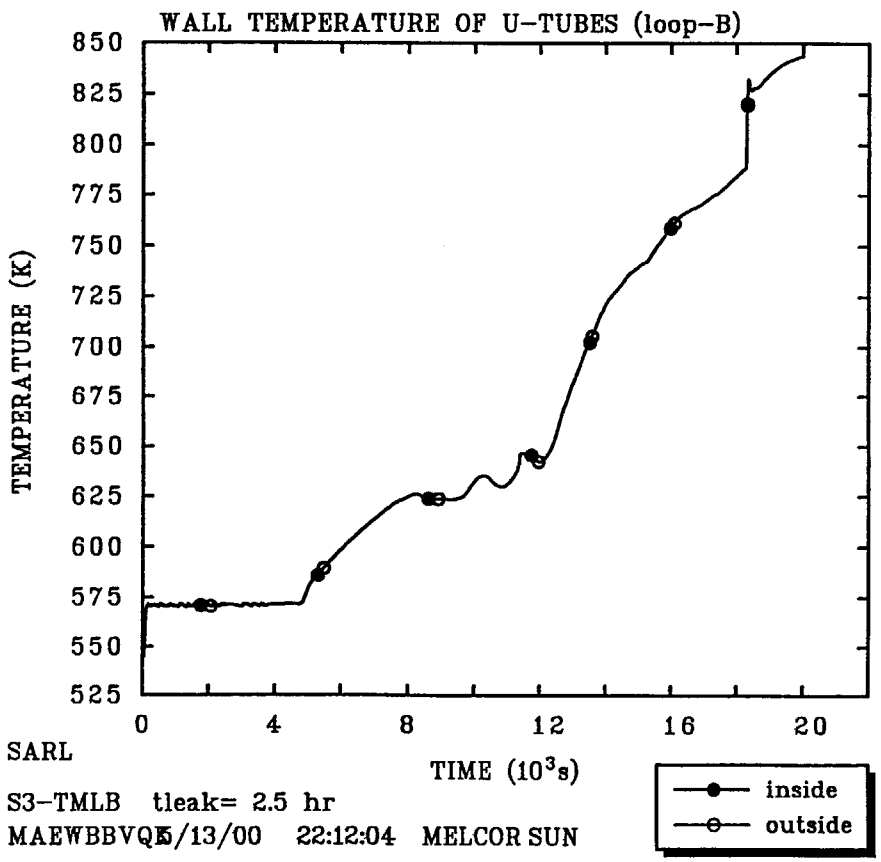

Figure 82. Run 2B: Wall temperature of SG-B U-tubes.

6.3. TMLB′ with RCS Depressurization (Run 3, 3A)

The analysis of accident sequence initiating by a total station blackout had shown the probability of core melt ejection to the containment while RCS was in a high pressure condition[4]. Such event known as High Pressure Melt Ejection (HPME) could challenge the containment integrity due to a direct containment heating (DCH) phenomenon. To avoid such kind of event, an intentional RCS depressurization is proposed as one of accident management measures. It is assumed that the operator will open pressurizer PORVs at some time during TMLB′ transient.

The intentional opening of PORVs is determined as ref. 10 proposed, i.e. the time when the exit core temperature reached 922 K. The reason of late depressurization is that it permits to more rapid RCS depressurization because the quality of the PORV discharge was higher.

In case of the PORVs depressurization capability was insufficient, the SRVs is assumed could be latched open together with PORVs, as also assumed in ref. 14, 15 and 16. The opening of SRVs would allow the faster depressurization due to increasing flow area. The run 3A calculates the accident sequence for such case. However, it must be noted that in real PWR only PORVs could be opened for intentional depressurization. So, this assumption must be considered as a numerical simulation breakthrough to overcome inadequacy of PORVs depressurization capability.

6.3.1. Run 3

(1) Accident Sequence

Table 6 gives the timing of key events predicted in run 3. As in TMLB′ sequence, because the RCS coolant inventory was continually being removed during PORVs opening and closing, the core eventually began to uncover at 7980 s. As the core became uncovered, the fuel rod cladding in the upper regions of the core became steam cooled. However, the steam flow rate past the cladding was inadequate to maintain an equilibrium temperature. When the fuel cladding temperature increase, the steam became superheated. At 11,180 s, the core exit steam temperature reached 922 K and the PORVs were latched open according to the intentional depressurization strategy.

After the PORVs were latched open, the RCS pressure began to decrease. During the time required to reduce the RCS pressure, the core structures continued to heat up. At about 12, 600 s, the upper region of the innermost ring

became debris. The relocation of the debris downward to the lower cell reached the core support plate. At 12,963 s, the core support plate failed allowing the debris to relocate into the vessel lower head. By 13,000 s, the lower head penetration in ring 1 failed. The coolant was discharged through the breach. At that time, the RCS pressure was about 11 MPa.

(2) System Response

1) Pressurizer pressure

Calculated pressurizer pressure is shown in Figure 83. The pressurizer pressure history before PORVs were latched open is identical with TMLB′ sequence. After PORVs were latched open at 11,180 s, the steam was discharged through the PORVs. The pressure decreased with the average rate of about 0.003 MPa/s until the lower head vessel failed at 13,000 s. A short peak at few seconds before the vessel failure was caused by the steam generation due to debris relocation into lower plenum. The pressure at the time of vessel failure was about 11 MPa. The Figures 85 and 86 show the mass flow rate, and total mass flow discharged from the PORVs, respectively.

2) Liquid level in reactor vessel

Figure 87 shows the swollen liquid level in the reactor vessel. At the time of PORVs latched open, the liquid level in the core was at about one-third of the core height. When PORVs were latched open, the liquid level in the downcomer decreased faster. At 11,500 s, the liquid level in the downcomer was lower than in the core. At about 12,900 s, the core was completely uncovered.

3) Core damage

Figures 88, 89 and 90 show the fuel rod cladding temperature history. During core uncovery, the uppermost core region heated up first, especially in ring 1 because of the most highest-powered. At about 10,600 s, the mid-height core began to heat up. Because the steam could not cooled sufficiently, the core heat up continued without interruption until the failure temperature limit of the cladding was exceeded.

The debris, which was relocated in the core support plate, caused the quick increase of temperature of the plate, and excess of the failed temperature (Figure 91). Once the plate failed, the debris relocated into the vessel lower head. The debris mass of core materials relocated in

the lower plenum are shown in Figures 92, 93 and 94. When the failure temperature of the penetration was exceeded, the breach occurred and the coolant began to be discharged from reactor vessel.

4) Radionuclide release

When the cladding failed, the gap release began to occur. Until the end of calculation, about 60 kg of Xe class, 40 kg of Cs class, 5 kg of CsI, and 2.5 kg of Te class were released from fuel in the core. In case of other radionuclide classes, the releases were very small. Figure 95 shows the radionuclide mass released in the core.

The deposited radionuclide mass is shown in Figure 96. Most of radionuclide mass was deposited in the upper part of the inner wall of loop-A hot leg pipe closest to the reactor vessel (denoted HL1-AU).

5) Wall temperature

Figure 97 shows the wall temperature of pressurizer surge line. Until the vessel failure, the temperature was kept relatively low. There are two peaks of temperature, first was 620 K reached after SGs secondaries dried out, at about 8000 s; the second peak was 630 K at 11,500 s which occurred due to the superheated steam generation.

The SG U-tubes wall temperature history was shown in Figures 98 and 99 for SG-A and SG-B, respectively. The temperature curves were similar to the TMLB' reference calculation. The maximum temperature was less than 630 K in all SGs.

6.3.2 Run 3A

(1) Accident Sequence

Table 7 shows the timing of the key events predicted in run 3A. Before valve latched opening, the sequence was identical with the above run 3. At the time of PORVs and SRVs latched opening, the pressure decreased quickly from PORVs set point to below the accumulator pressure set point. Then, after accumulator injection, the small pressure increase occurred due to steam generation. The increase was small because PORVs and SRVs all were opened, so hot steam passed easily, and RCS was not pressurized. The pressure was always below the accumulator set point allowing borated water was continuously injected until the borated water in accumulator tanks was depleted.

The injection of cold borated water from accumulator

flooded the core. The fuel temperature decreased except for the core uppermost region which continued to increase. Starting from about 12,000 s, gap release occurred. However, until 20,000s no substantial core damage occurred.

(2) System Response

1) Pressurizer pressure

The pressurizer pressure is shown in Figure 100. The pressure decreased rapidly, about 0.15 MPa/s, after the valves opening at 11,180 s. The coolant mass flow rate through SRVs was higher than in PORVs, and was dominated by vapor flow. Figure 101 and 102 show the coolant mass flow rate through PORVs and SRVs respectively. The total coolant mass flows are shown in Figures 103 and 104.

The pressure reached the accumulators pressure set point at 12,045 s. When the cold water was injected, the pressure decreased quickly to about 2.5 MPa, but then increased as a small peak pressure. After that several small peaks appeared due to steam generation in the core. The sharp peak at about 17,400 s occurred because of a large steam production when the liquid level in the core suddenly increased due to water supply from the downcomer. However, the pressure remained under 2.0 MPa.

2) Water level in reactor vessel

Figure 105 shows the swollen liquid level in the reactor vessel. At the time of valves opening, the liquid level in downcomer collapsed almost instantaneously due to the rapid pressure decrease. After 12,000 s, the water level increased up to 6 m high, but then decreased slower as the steam generation continued.

The core completely uncovered at about 11,800 s. Then, the liquid level in the lower plenum began to decrease due to evaporation. At 12,045 s, the water injection from accumulators flooded the core. The liquid level went up to mid-height. Until 20,000 s the core was half-filled by liquid.

3) Core damage

Figures 106, 107 and 108 show the cladding temperatures in rings 1, 2 and 3, respectively. The upper region of the core was actually heated up at about 9000 s. After that, at about 10,000 s the temperature increase was reduced due to an effective steam cooling when the liquid in downcomer decreased; during that time, the temperature was almost constant. Then, at 10,620 s, the temperature

began to increase again. But, a large quantity of steam produced at the beginning valves latched open at 11,860 s caused temporal decrease of the temperature.

As the liquid level in core decreased again, the temperature increased, especially in the upper region. However, the cold borated water injection from accumulators at 12,045 s reduced the temperature again. Only at the uppermost region, the temperature continued to increase. When the temperature exceeded 1000 K, the oxidation of the cladding in the upper region began as could be seen in Hydrogen generation shown in Figure 109. Because limited oxidation, the Hydrogen mass generated was also low.

The cladding failure occurrence at 12,618 s in ring 1, at 15,609 s in ring 2, and 19,625 s in ring 3 caused the fission product gap release. Until 20,000 s, all core materials were kept intact, no debris was produced.

4) Radionuclide release

The radionuclide release until 20,000 s was low as could be seen in Figure 110. The most important release of Xe class and Cs class were only about 8 kg each. Most of deposited radionuclide mass was found in the pressurizer surge line wall as shown in Figure 111.

5) Wall temperature

Calculated wall temperature of pressurizer surge line is shown in Figure 112. Until initiation of accumulator injection, the wall temperature of pressurizer surge line was always below 625 K. After about 14,800 s, The temperature increase of pressurizer surge line occurred without interruption. This is because the hot steam flowed through the pressurizer surge line to escape to containment via PORVs and SRVs which were latched open.

On the other hand, the wall temperatures of SGs U-tubes did not increase significantly. They reached the maximum when SGs secondary dried out. After that they tended to decrease continuously. Figure 113 shows the wall temperature of SG-A U-tubes. The temperature of SG-B is practically similar and is shown in Figure 114.

6.3.3. Discussions

The calculation results showed that the intentional PORVs latched open during TMLB′ sequence was not able to mitigate or delay the severe core damage progression. The depressurization was not so fast to reach the accumulator set point prior to the reactor vessel failure.

To evaluate the PWR's capability to depressurize, ref. 10 defines PORV ratio which is the ratio of normalized PORV capacity to RCS volume given by:

$$\text{PORV Ratio} = \frac{(G_{PORV} / V_{RCS})_{study}}{(G_{PORV} / V_{RCS})_{base}}$$

where

G_{PORV} = PORV mass flow rate of study and base PWRs

V_{RCS} = RCS volume of study and base PWRs

Using the Surry NPP as the base plant, the PORV ratio of Indian point 3 is 0.78.

Still based on the ref. 10, the analysis of the same sequence for Sequoyah plant, which has PORV ratio of 0.75, showed that the depressurization could delay the accident progression. According to this, as Indian Point 3 has greater PORVs Ratio, so it could be expected that the depressurization would succeed to delay the core damage progression. But, the current calculation did not show that. The reasons for the discrepancies might be attributed, among others, to the RCS nodalization. In Sequoyah analysis, the one lumped loop model was used.

The other way to increase the depressurization capability is to open SRVs as well. The run 3A showed that this strategy worked well. The depressurization occurred rapidly, and the accumulator set point was reached only in 800 s (13.3 minutes) after opening the valves. The SRVs, which has about 2.3 times total flow area of PORVs, have provided bigger coolant mass flow rate discharged from RCS to the containment.

Table 6. Timing Key Events of TMLB'with RCS depressurization: Run 3.

Events	Time ,s	/(hr)
Station blackout initiation	0	(0)
SG dried out	4981	(1.38)
Core coolant at saturation	7408	(2.06)
Start of core uncovery	7980	(2.22)
PORVs latched open	11,180	(3.11)
Start of oxidation	11,400	(3.17)
Gap release		
Ring 1	11,628	(3.23)
Ring 2	11,813	(3.28)
Ring 3	12,216	(3.39)
Core completely uncovered	12,900	(3.58)
Core support plate failure		
Ring 1	12,963	(3.60)
Ring 2	14,522	(4.03)
Ring 3	15,217	(4.23)
Lower head penetration failure		
Ring 1	13,000	(3.61)
Ring 2	13,031	(3.62)
Ring 3	13,040	(3.62)
Debris ejection	16,165	(4.49)

Table 7. Timing Key Events of TMLB'with RCS depressurization: Run 3A

Events	Time ,s	/(hr)
Station blackout initiation	0	(0)
SG dried out	4981	(1.38)
Core coolant at saturation	7408	(2.06)
Start of core uncovery	7980	(2.22)
PORVs and SRVs latched open	11,180	(3.11)
Core completely uncovered	11,820	(3.28)
Accumulator opens	12,045	(3.36)
Start of oxidation	12,360	(3.43)
Gap release		
Ring 1	12,618	(3.51)
Ring 2	15,609	(4.34)
Ring 3	19,625	(5.45)
Core support plate failure		
Ring 1	> 20,000	(> 5.55)
Ring 2	> 20,000	(> 5.55)
Ring 3	> 20,000	(> 5.55)
Lower head penetration failure		
Ring 1	> 20,000	(> 5.55)
Ring 2	> 20,000	(> 5.55)
Ring 3	> 20,000	(> 5.55)
Debris ejection	> 20,000	(> 5.55)

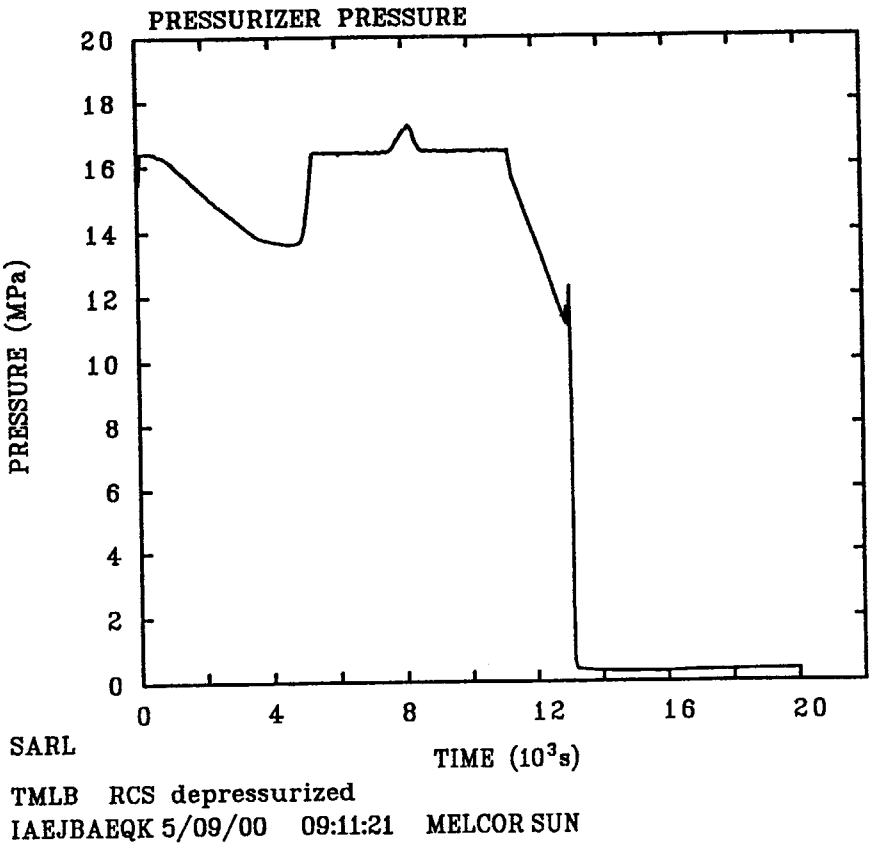

Figure 83. Run 3: Pressurizer pressure.

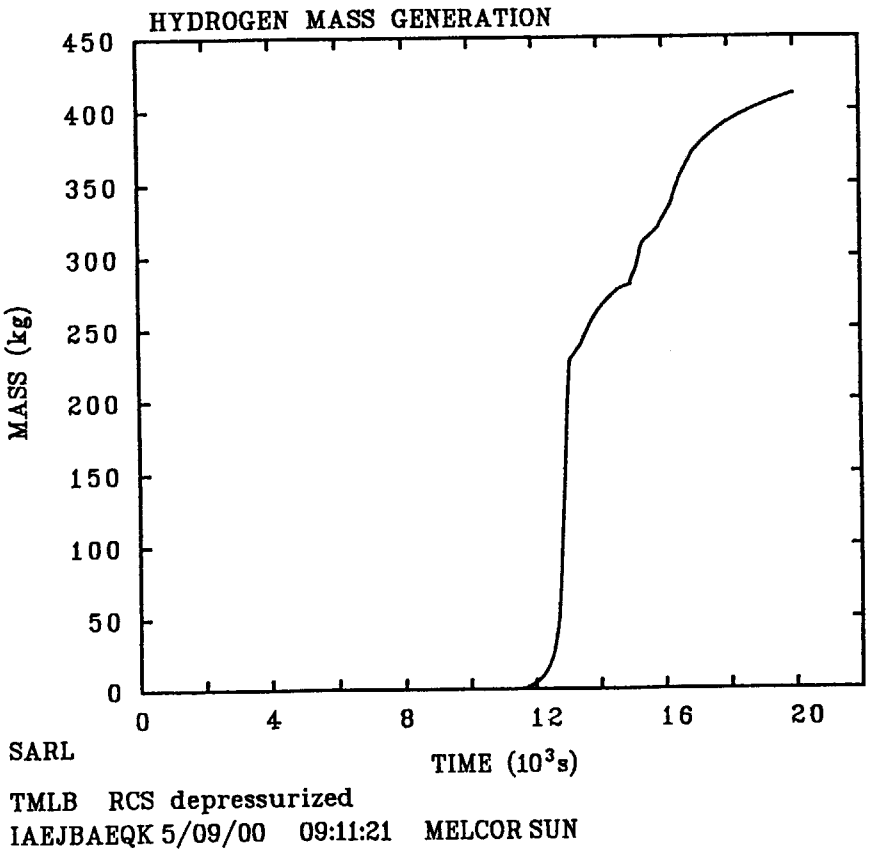

Figure 84. Run 3: Hydrogen mass produced.

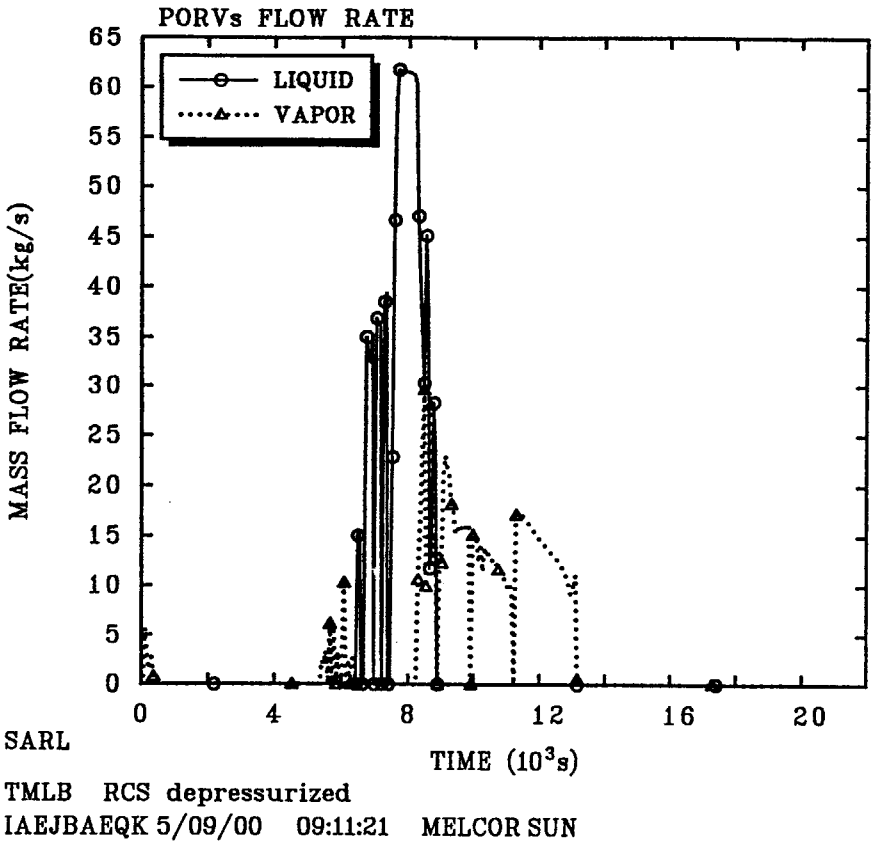

Figure 85. Run 3: Coolant mass flow rate discharged from PORVs.

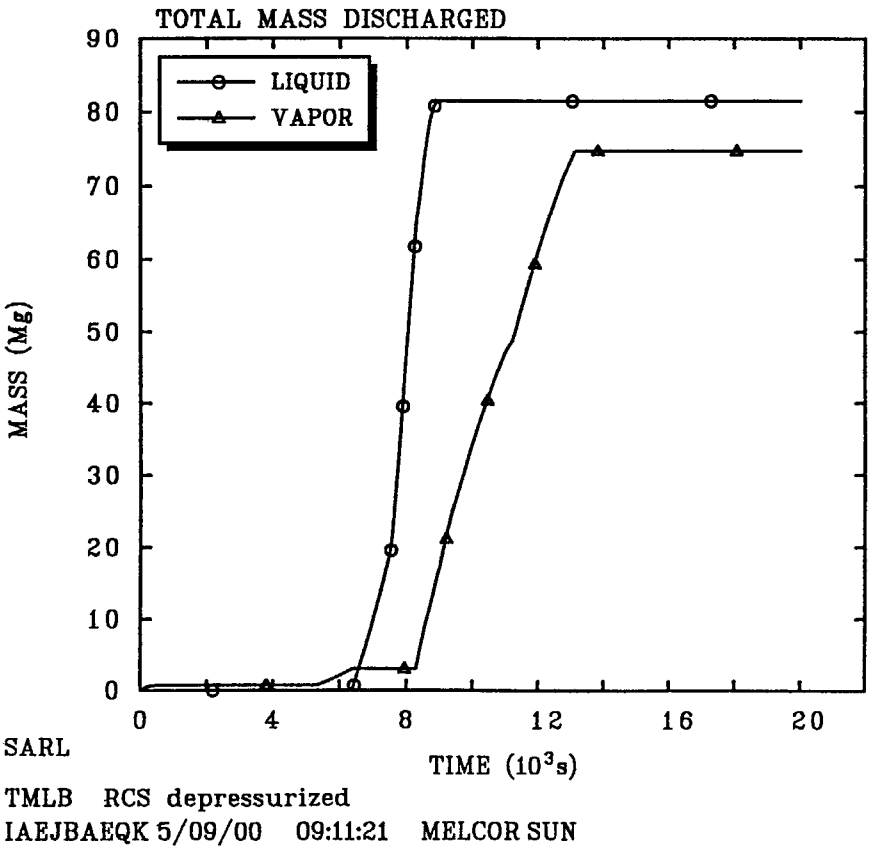

Figure 86. Run 3: Total coolant mass discharged from PORVs.

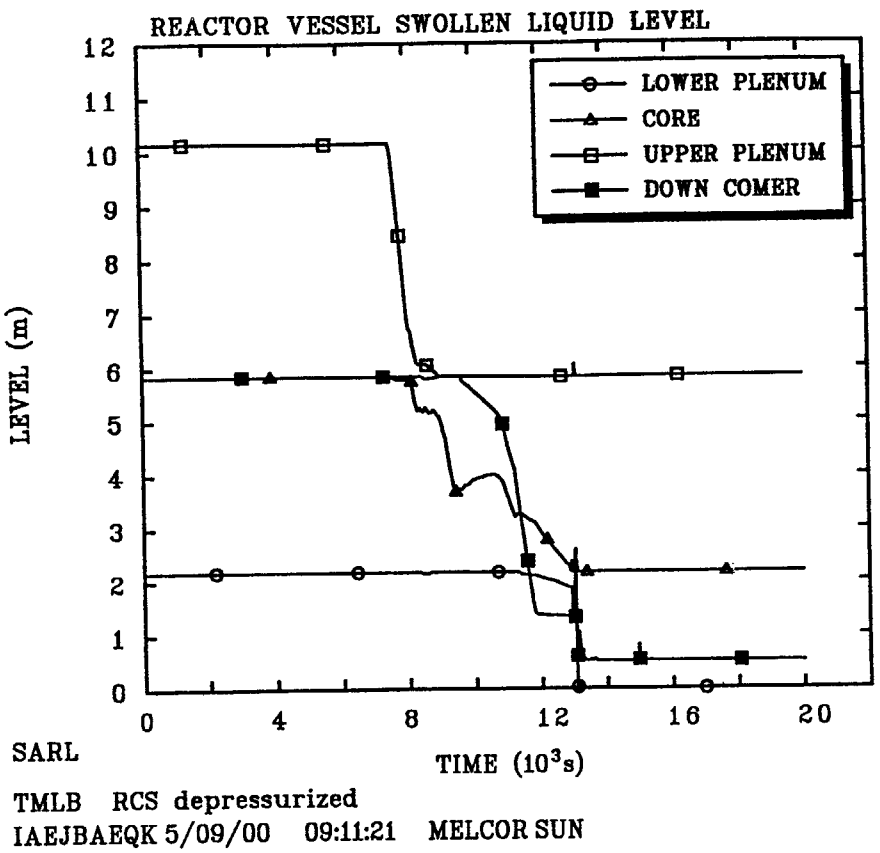

Figure 87. Run 3: Swollen liquid level in reactor vessel.

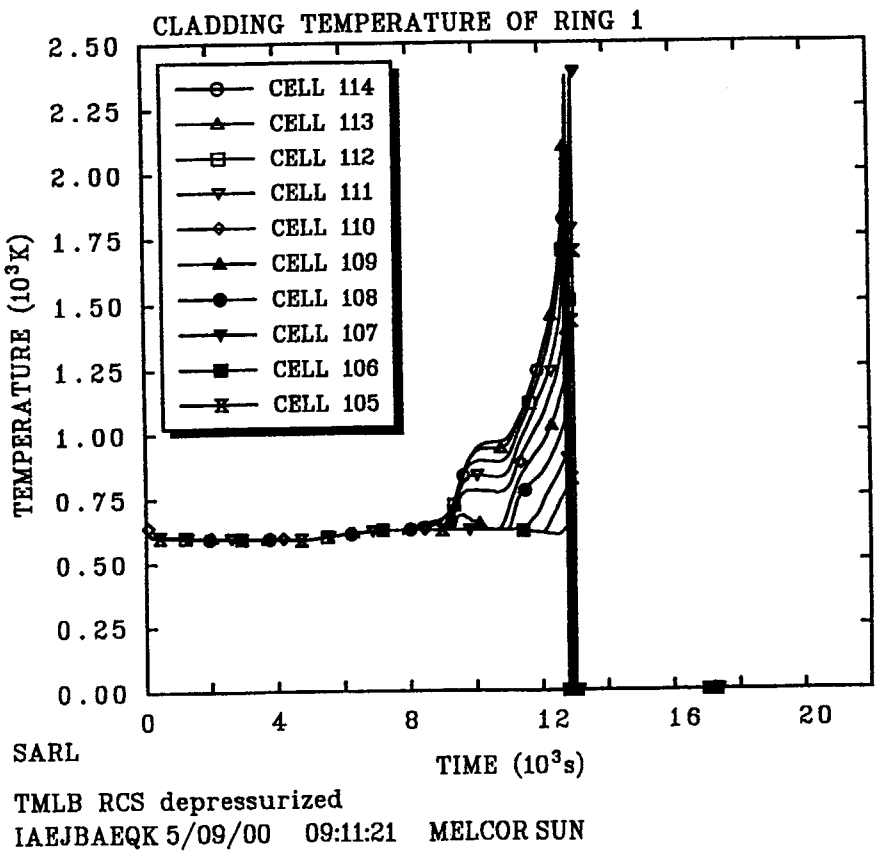

Figure 88. Run 3: Cladding temperature in ring 1.

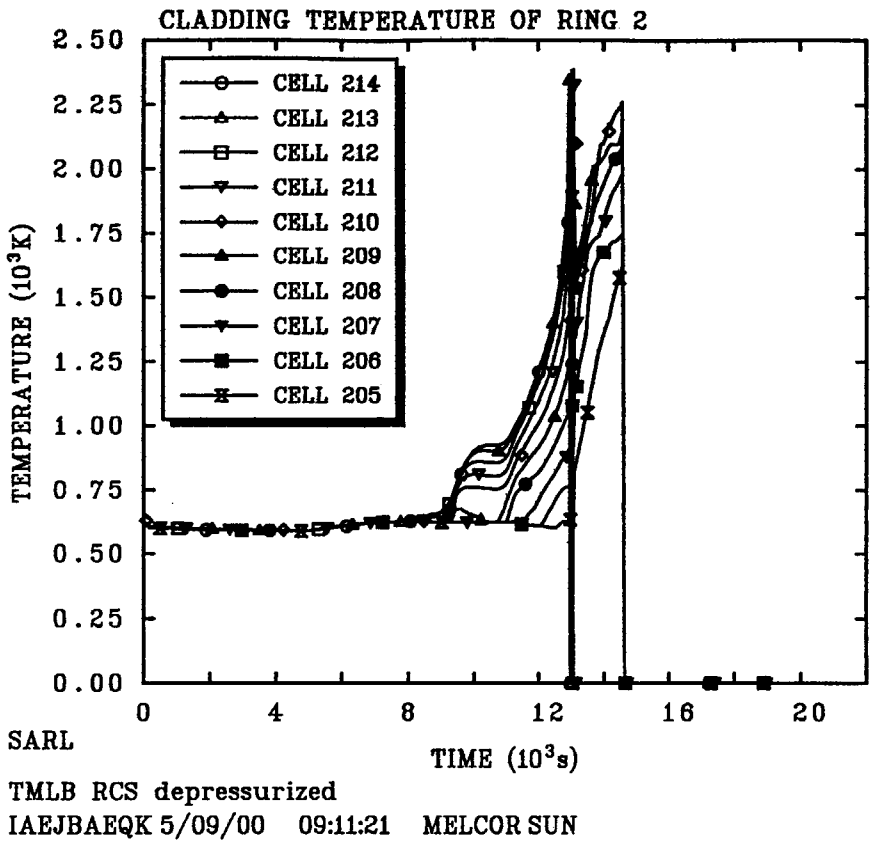

Figure 89. Run 3: Cladding temperature in ring 2.

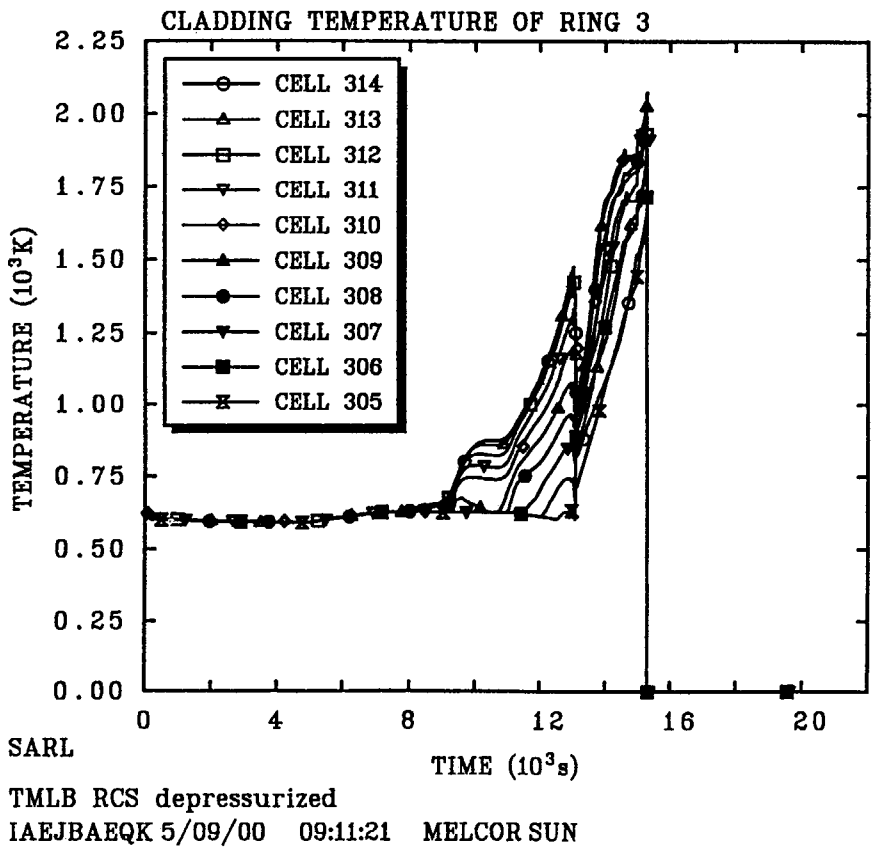

Figure 90. Run 3: Cladding temperature in ring 3.

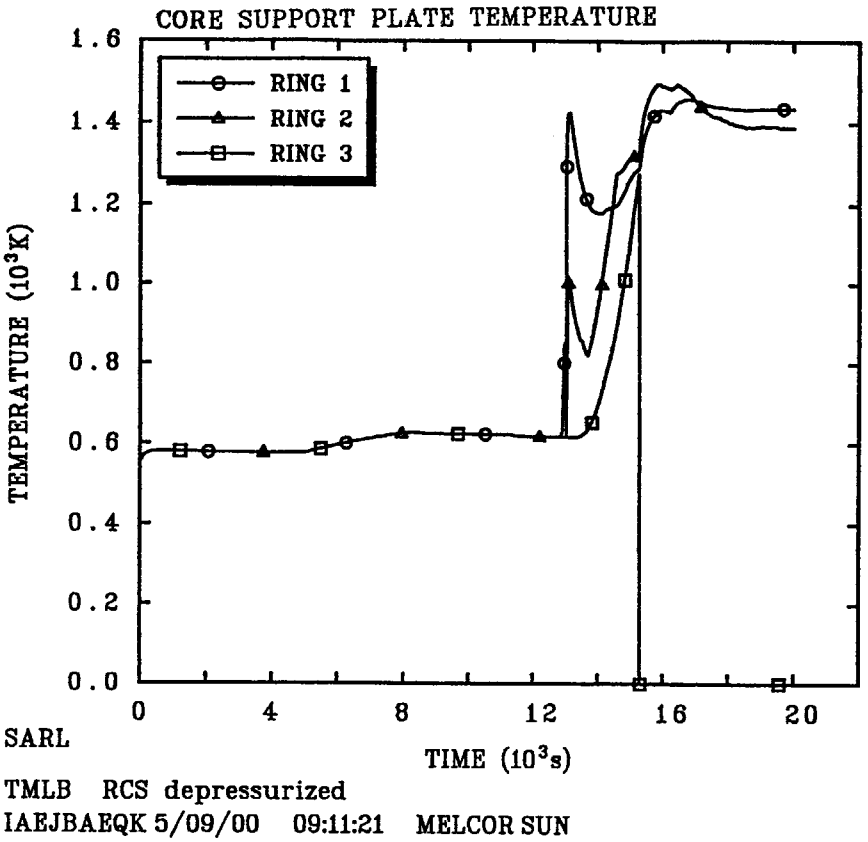

Figure 91. Run 3: Core support plate temperature.

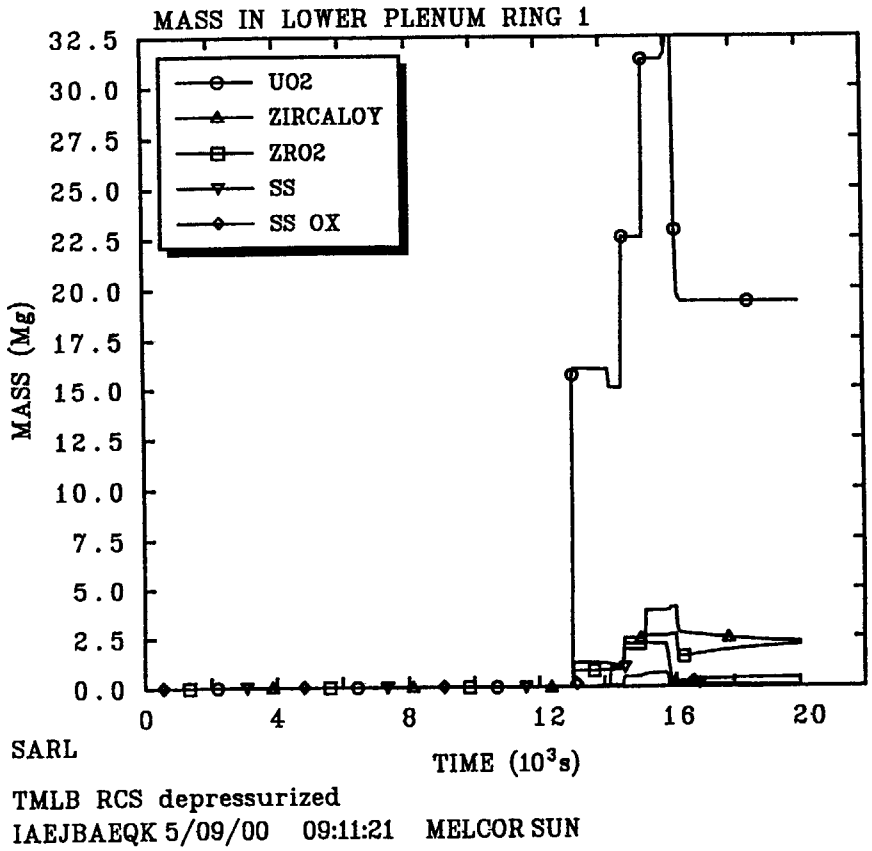

Figure 92. Run 3: Debris mass in lower plenum ring 1.

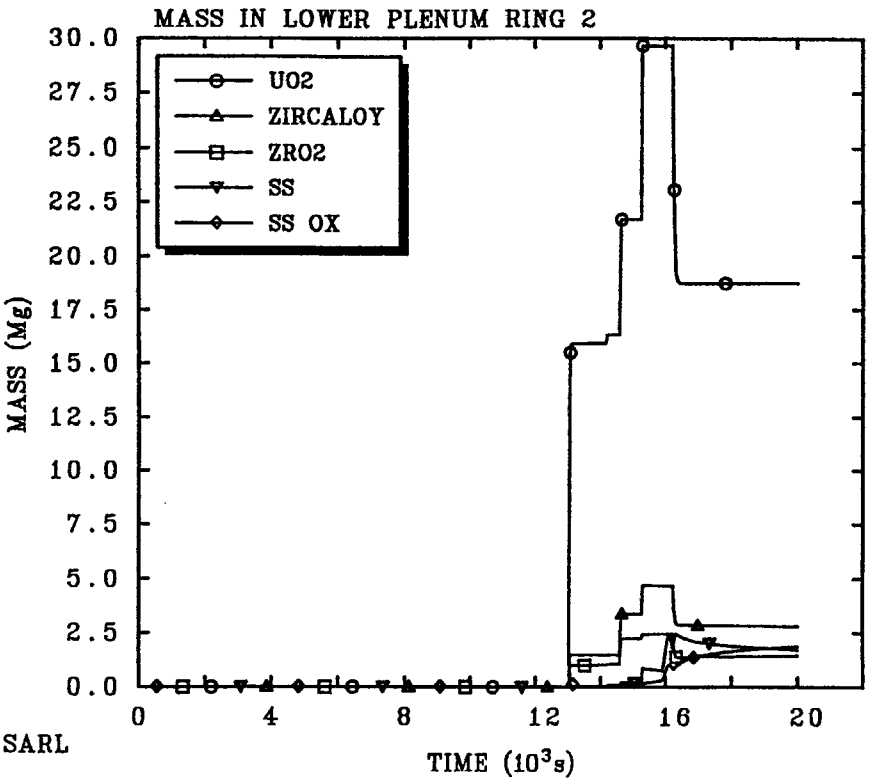

Figure 93. Run 3: Debris mass in lower plenum ring 2.

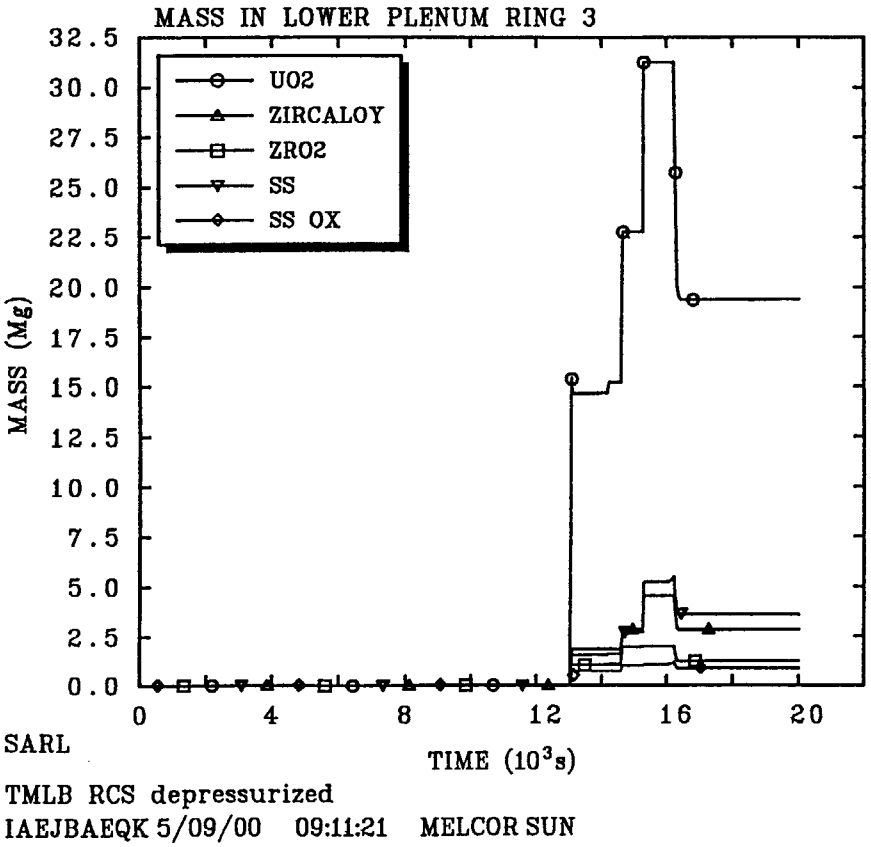

Figure 94. Run 3: Debris mass in lower plenum ring 3.

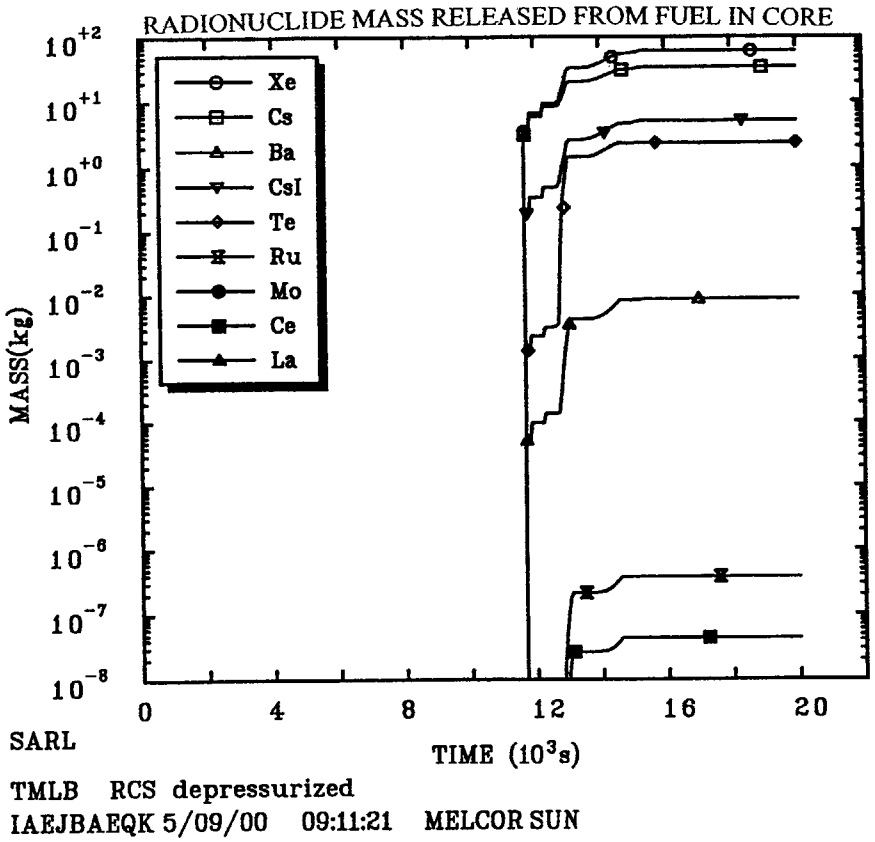

Figure 95. Run 3: Radionuclide mass release from fuel in core.

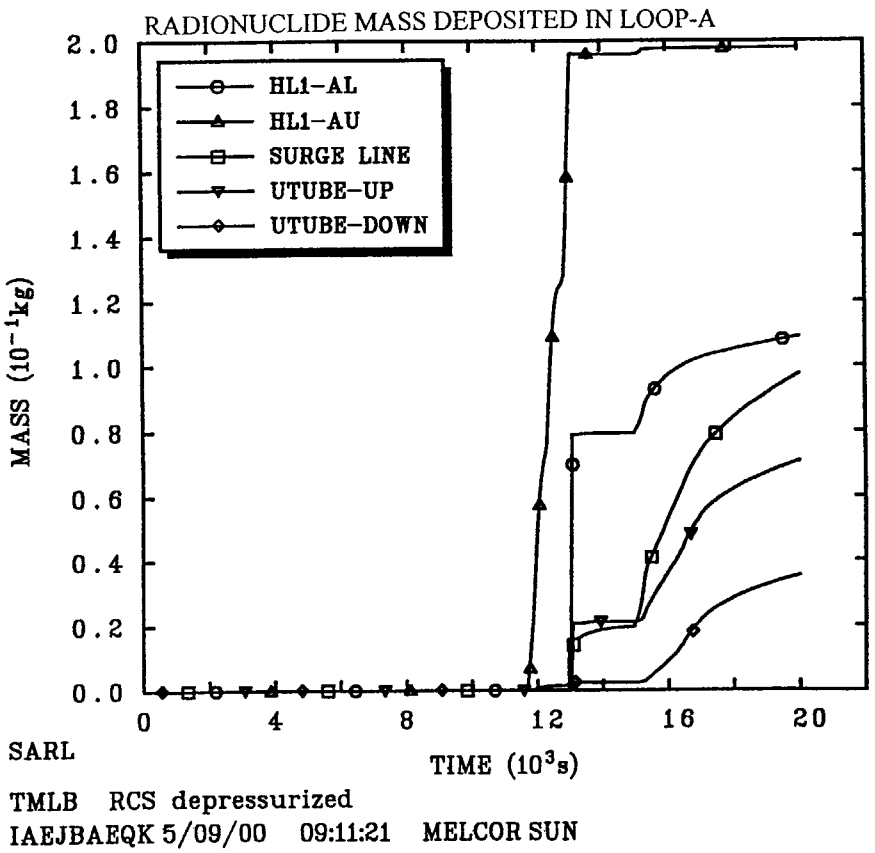

Figure 96. Run 3: Deposited radionuclide mass.

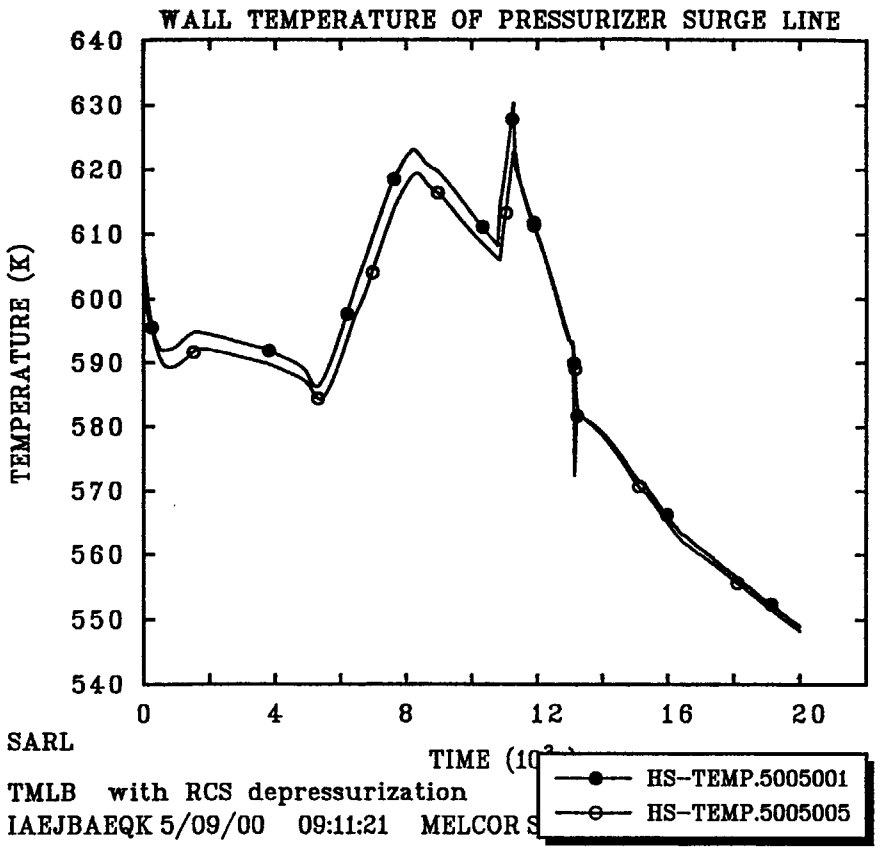

Figure 97. Run 3: Wall temperature of pressurizer surge line.

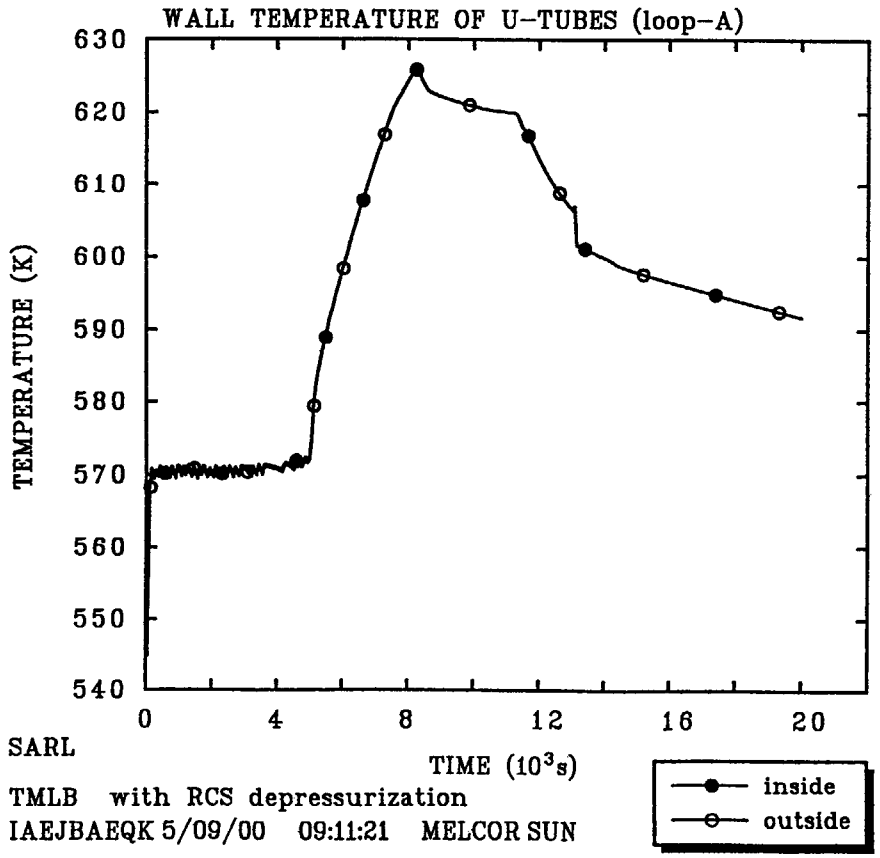

Figure 98. Run 3: SG-A U-tubes wall temperature.

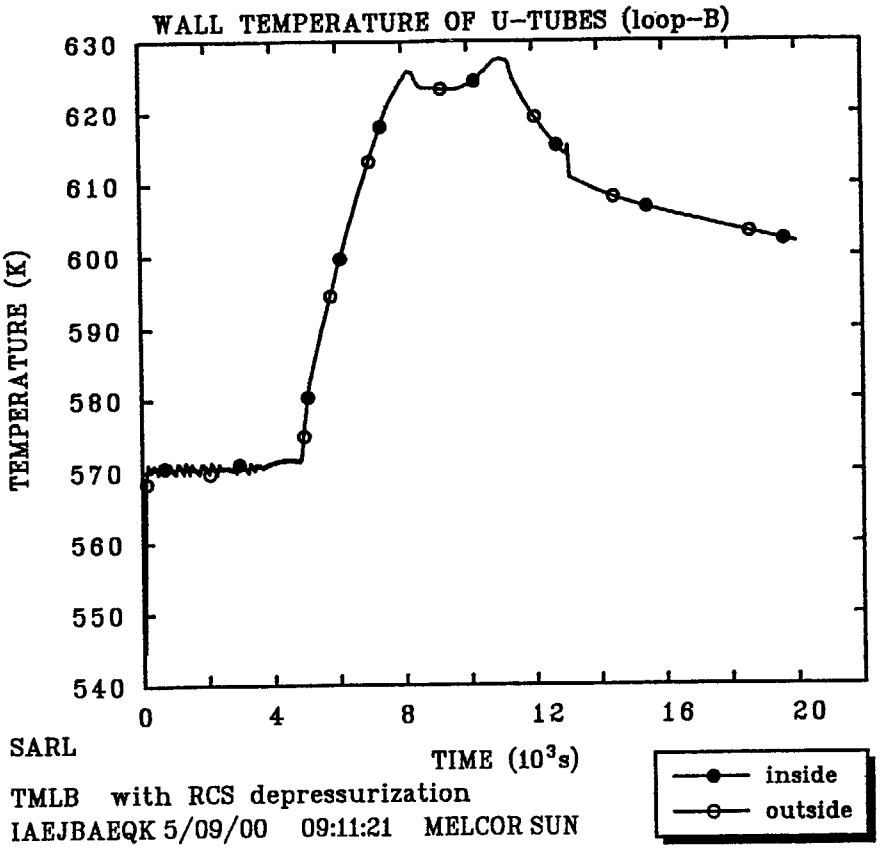

Figure 99. Run 3: SG-B U-tubes wall temperature.

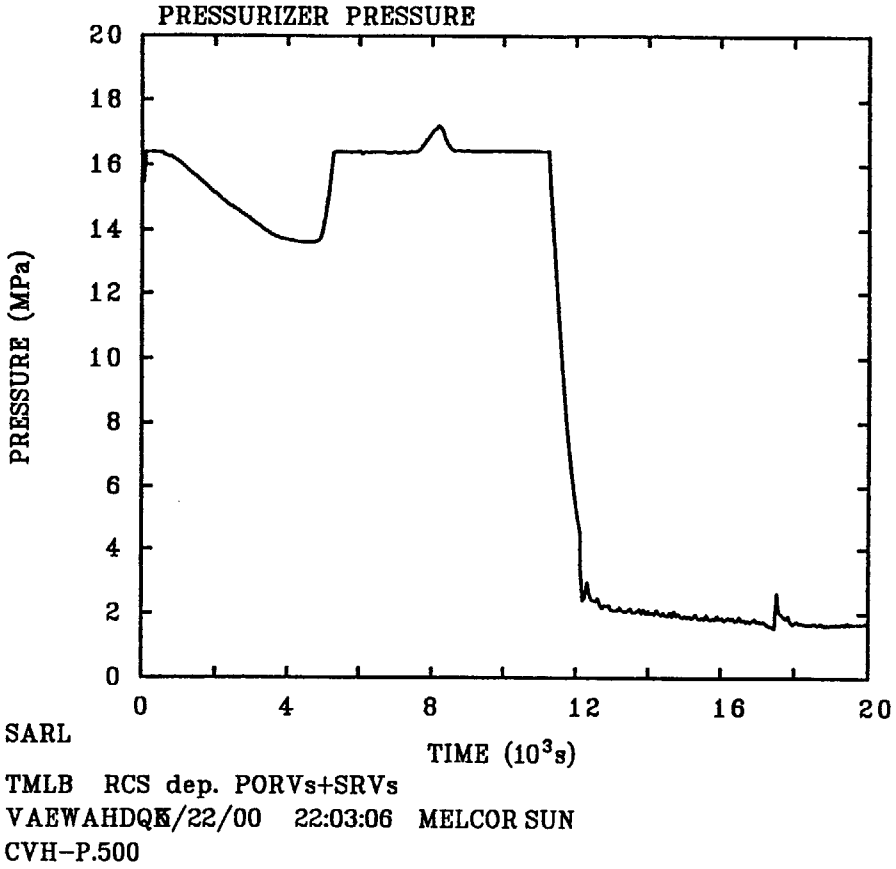

Figure 100. Run 3A: Pressurizer pressure.

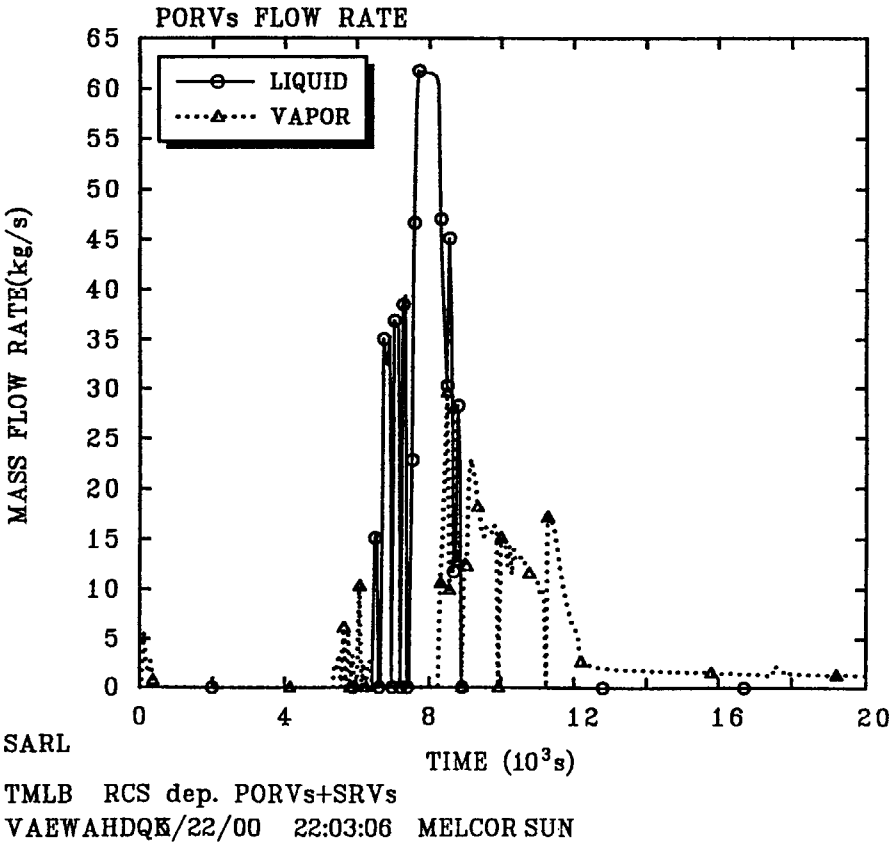

Figure 101. Run 3A: PORVs coolant mass flow rate.

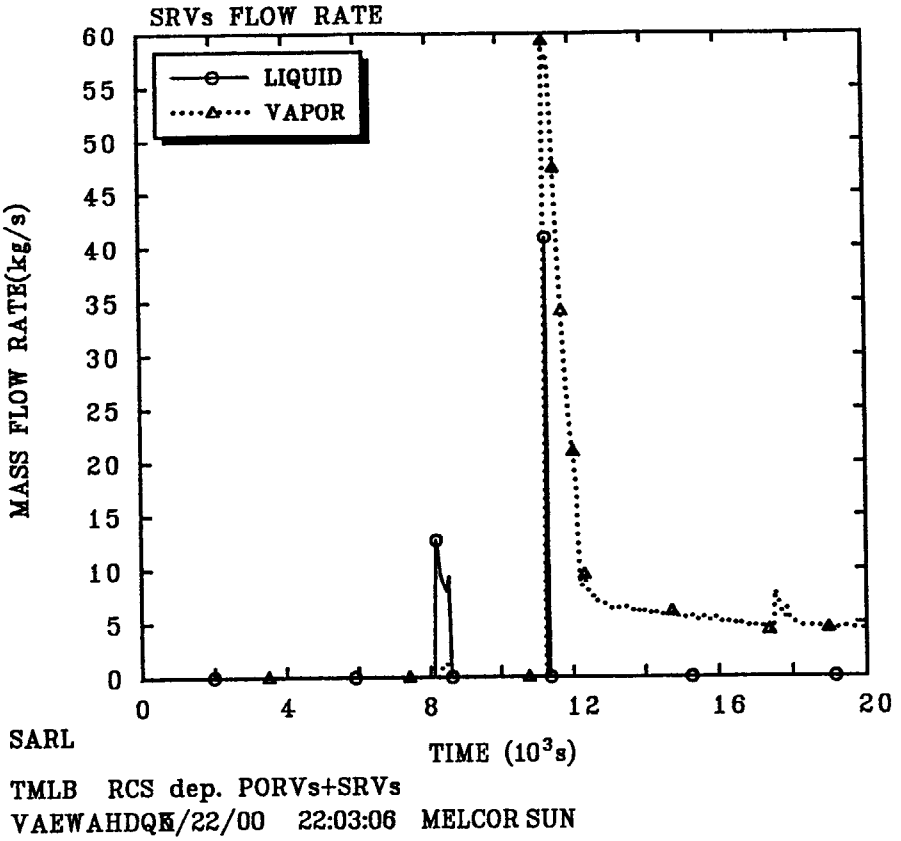

Figure 102. Run 3A: SRVs coolant mass flow rate.

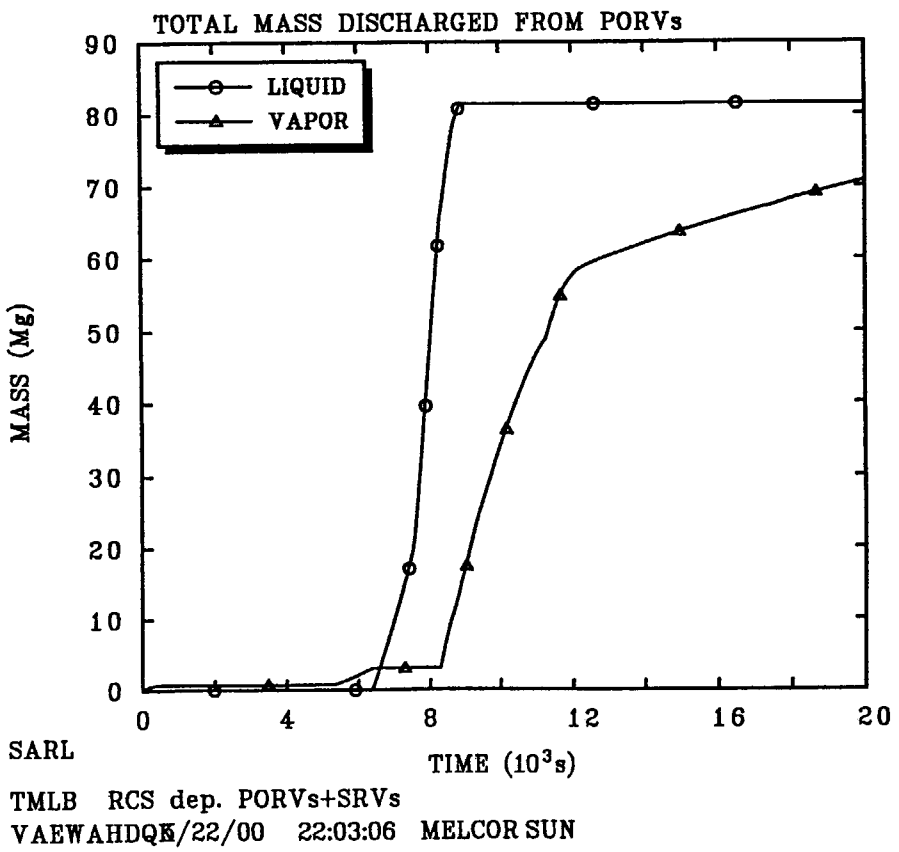

Figure 103. Run 3A: PORVs total coolant mass flow.

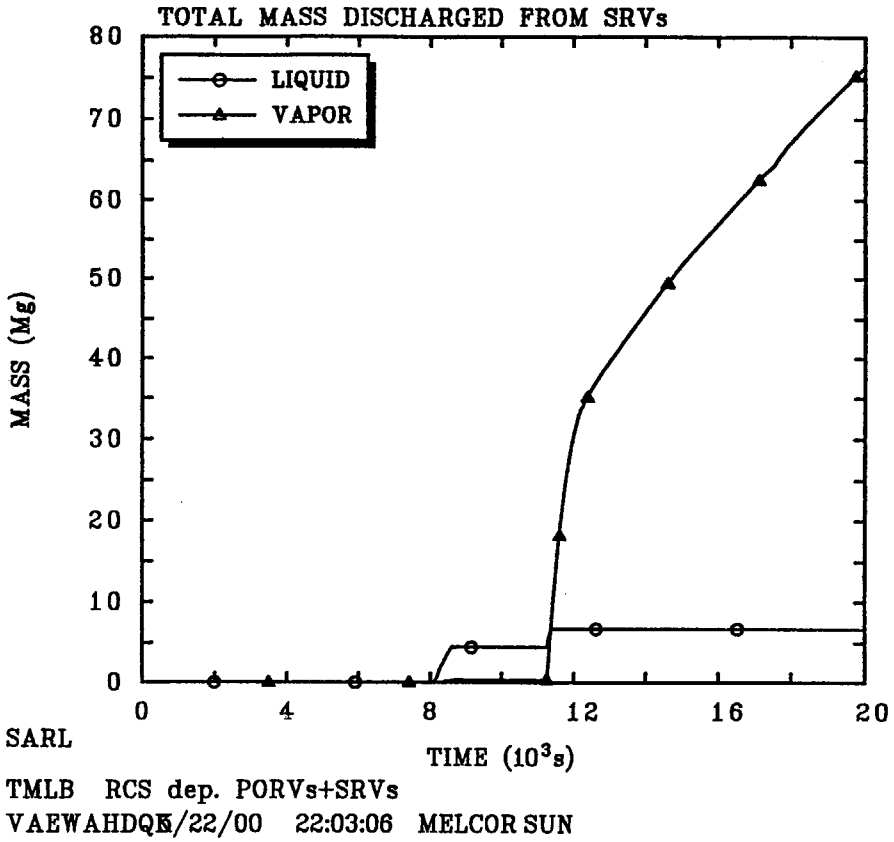

Figure 104. Run 3A: SRVs total coolant mass flow.

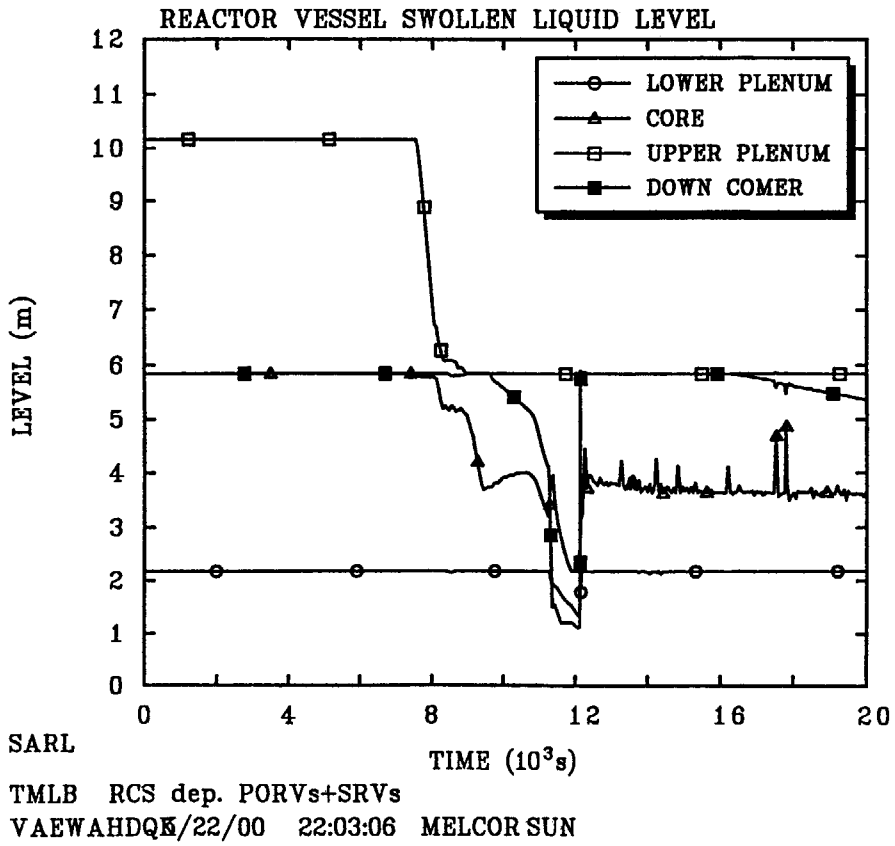

Figure 105. Run 3A: Swollen liquid level in reactor vessel.

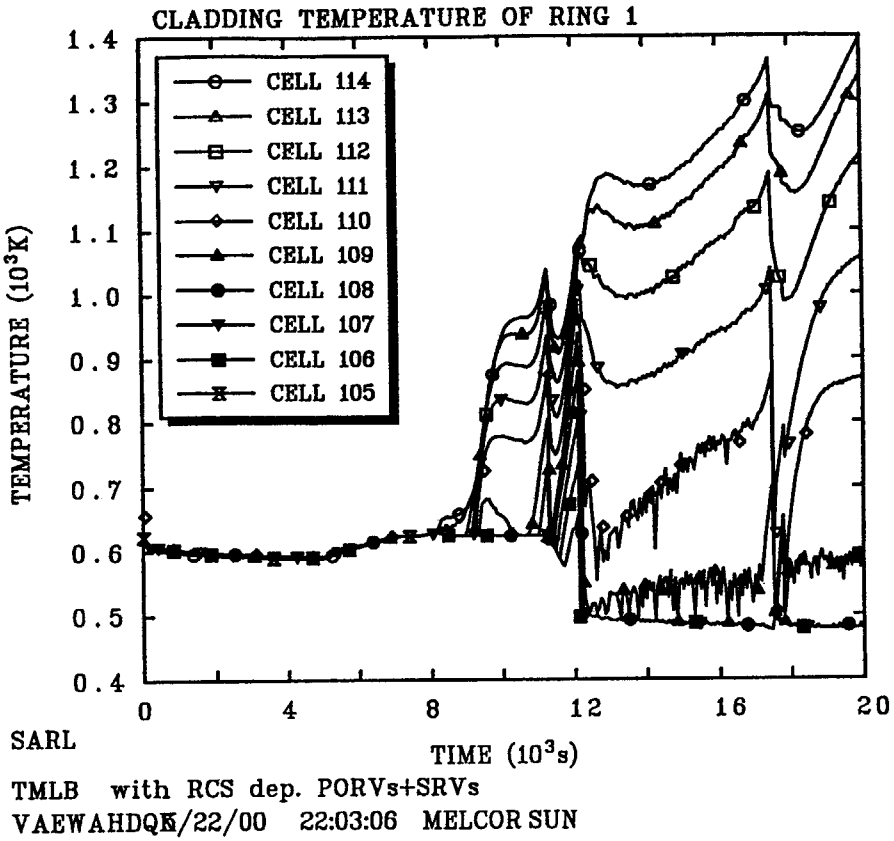

Figure 106. Run 3A: Cladding temperature in ring 1.

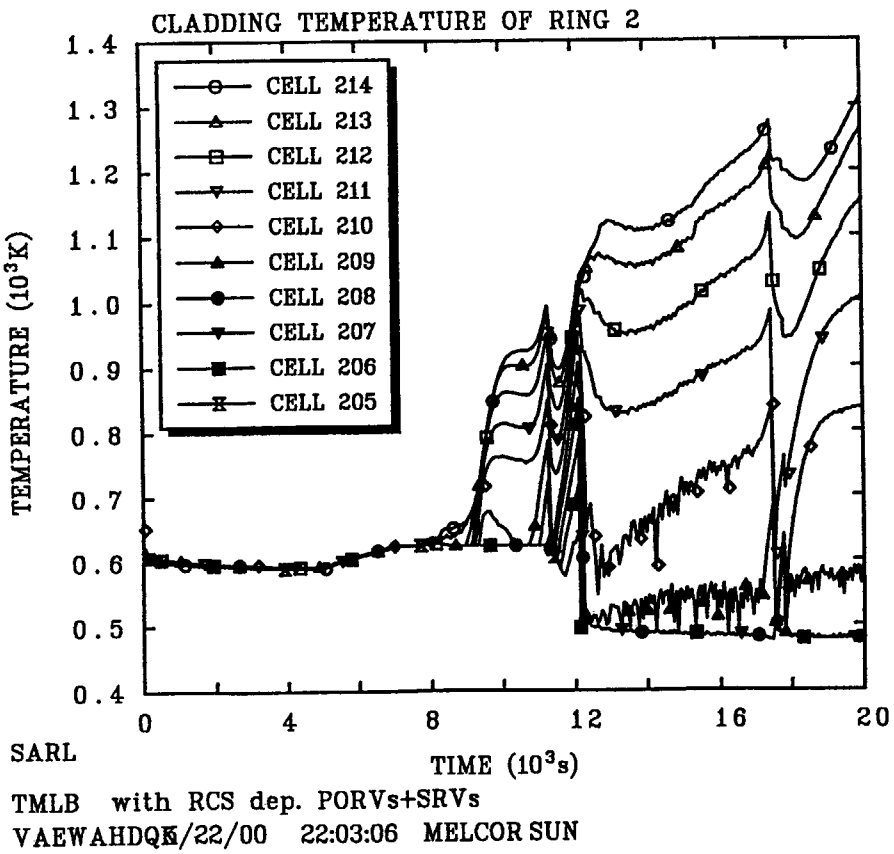

Figure 107. Run 3A: Cladding temperature in ring 2.

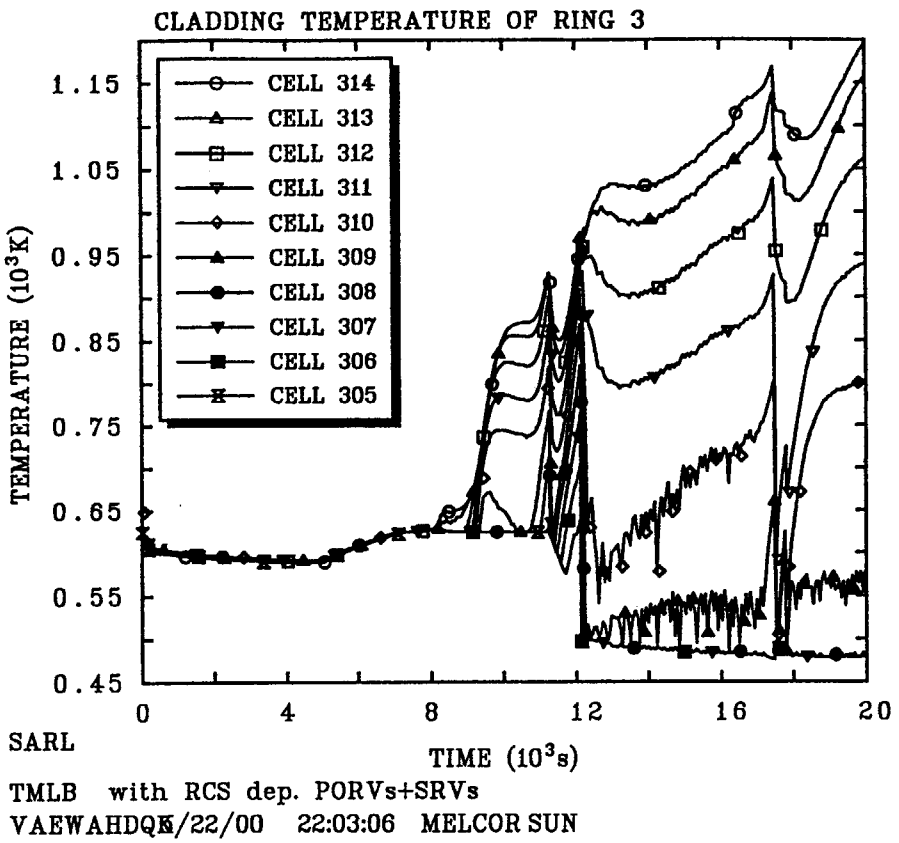

Figure 108. Run 3A: Cladding temperature in ring 3.

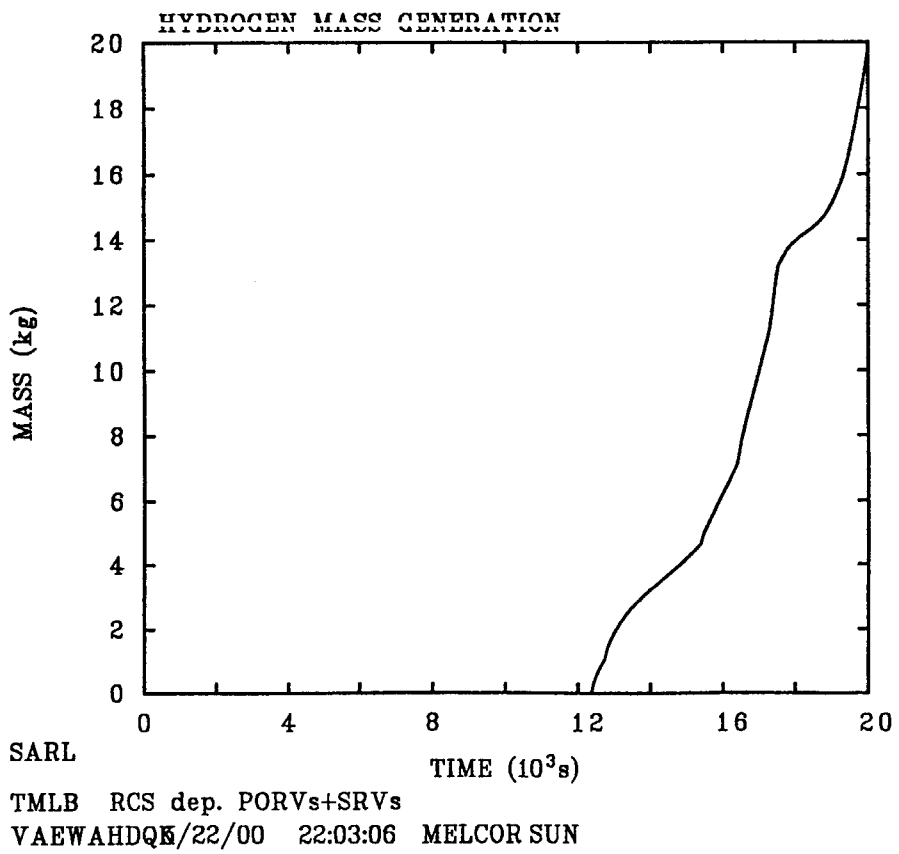

Figure 109. Run 3A: Hydrogen mass generated.

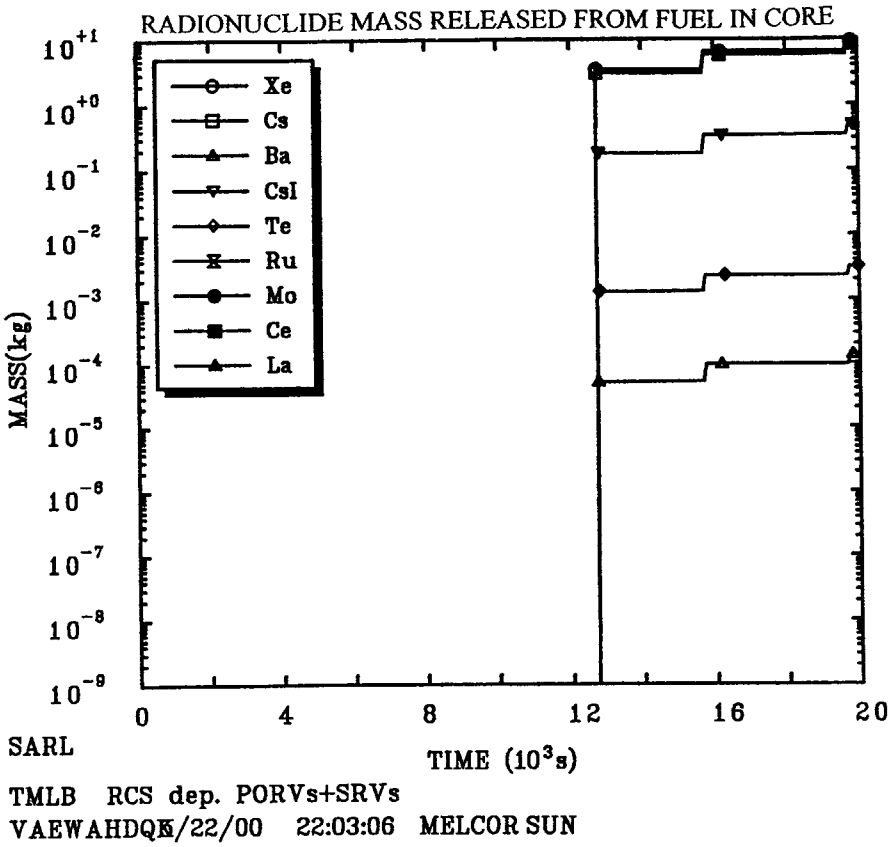

Figure 110. Run 3A: Radionuclide mass release from fuel in core.

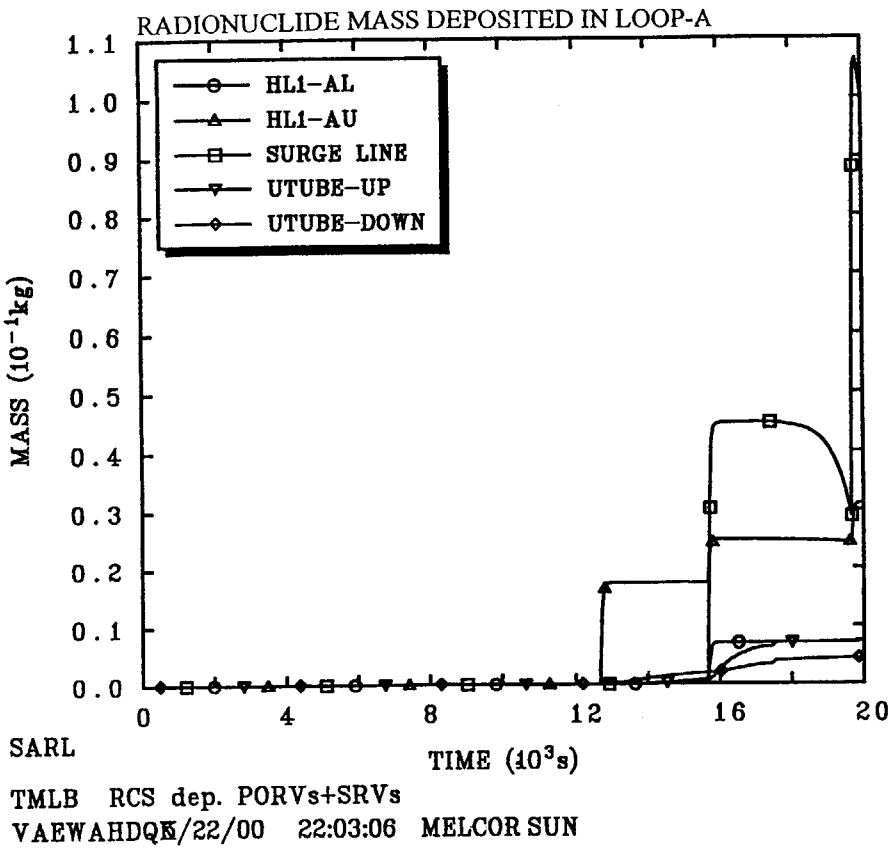

Figure 111. Run 3A: Deposited radionuclide mass.

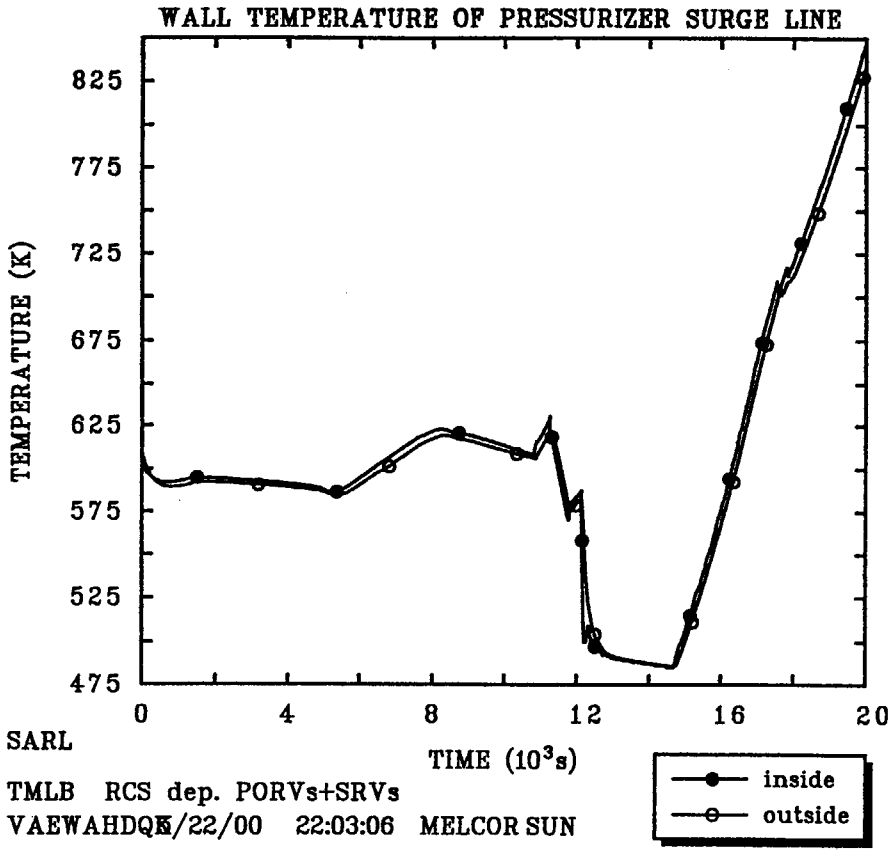

Figure 112. Run 3A: Wall temperature of surge line.

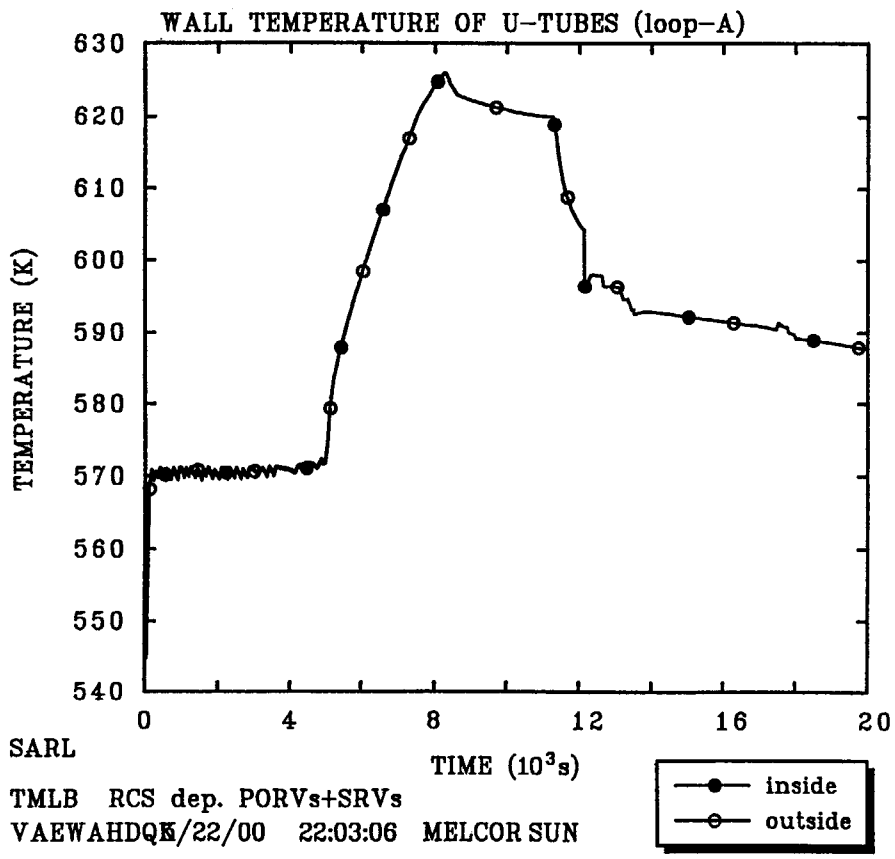

Figure 113. Run 3A: SG-A U-tubes wall temperature.

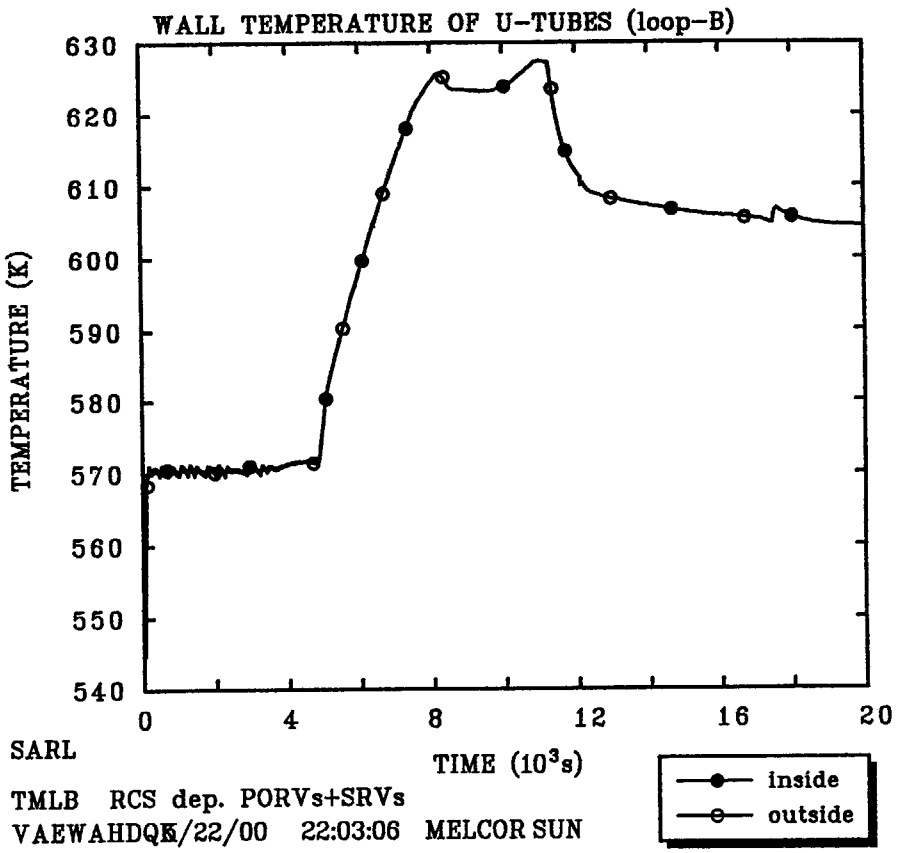

Figure 114. Run 3A: SG-B U-tubes wall temperature.

6.4 S3-TMLB′ With Intentional RCS Depressurization

The previous TMLB′ with intentional RCS depressurization showed that to mitigate or delay the core damage progression, both the PORVs and SRVs must be latched open. Based on this result, the same strategy will be applied to the S3-TMLB′ accident sequence. In this calculation, run 4, the RCP seal LOCAs is assumed to occur when the coolant in the core region reaches the saturation temperature (see also run 2). The timing of PORVs and SRVs latched open is determined at the timing of core exit vapor temperature arrival at 922 K (see also run 3A).

6.4.1. Accident Sequence

Table 8 shows the timing of key events predicted in run 4. Until the time of PORVs and SRVs latched open, the sequence was similar as run 2. The core exit temperature of 922 K was reached at about 10,500 s. At that time all pressurizer valves were latched open. The pressure decreased quickly. When the pressure dropped below the accumulator set point, cold borated water was injected from accumulator tanks.

A part of the water injected was discharged from seal break holes. Even though, most part of it flooded the core allowing the cooling of the hot core materials. However, as result of a large amount of coolant discharged from pressurizer valves and seal break holes, the core rapidly uncovered again. As consequence, the core continued to heat up, degraded and finally caused the lower head vessel failure at about 19,000 s.

6.4.2. System Response

(1) Pressurizer pressure

Calculated pressurizer pressure is shown in Figure 115. After valves opening, the pressure decreased quickly until reaching the accumulators set point at about 11,200 s. When the cold water from accumulator tanks was injected, the pressure decreased suddenly to about 2.2 MPa. A small peak pressure rose due to steam generation in the core. After that, the pressure continued to decrease slowly. At the time of reactor vessel failure, the pressure was at about 0.8 MPa.

(2) Water level in reactor vessel

Figure 116 shows the liquid level in reactor vessel.

Due to fast decrease of pressure at the time of pressurizer valves latched open, the liquid level decreased also quickly. The core was completely uncovered at about 200 s later. But, it was not for a long duration, because the injected cold water from accumulators flooded the core, and the level went up to about mid-height of the core. Since the pressure was low, the steam generation was high, and the coolant was continuously discharged from pressurizer valves and seal break holes, the liquid level decreased again.

At about 17,250 s, the core was completely uncovered again. Then, the water in accumulator tanks had already been depleted. So, the liquid level in the lower plenum was decreasing until the lower head failed.

(3) Core damage

Figures 117, 118 and 119 show the cladding temperature in rings 1, 2 and 3, respectively. From about 8,500 s, the uppermost cell of the core began to heat up, following the core uncovery. When the core was flooded by injected water from accumulators, the upper region was not sufficiently cooled, as consequence the temperature continued to increase. At 11,975 s the gap release due to cladding failure occurred in ring 1. It was followed by gap release of ring 2 and ring 3 at 13,449 s and 13,919 s, respectively.

At about 12,500 s, the cladding temperature increased quickly. At about 14,800 s, the uppermost region in ring 1 became debris, and candled downward. The core degradation was continued in ring 2 and the other rings at upper region. At about 15,000 s, the upper half core region in rings 1 and 2 became debris. The debris relocated to the lower cells. The relocation reached the core support plate in ring 1. The plate was failed when the failure temperature was exceeded (Figure 120).The debris fell down and relocated in the lower plenum as shown in Figure 121, 122 and 123. The hot debris caused the lower head penetration failure followed by coolant discharge from reactor vessel. At the time, the pressure in secondary side was almost kept at SGs MSRVs set point.

(4) Radionuclide release

The radionuclide mass released from fuel during core degradation up to vessel failure is shown in Figure 124. About 200 kg of Xe class, 120 kg of Cs class, 20 kg of CsI class and 20 kg of Te class were released in core. The other radionuclide release represented minor release.

The deposited radionuclide mass in loop-A is shown in Figure 125. The most radionuclide deposition was found in the pressurizer surge line.

(5) Wall temperature

Calculated wall temperature of pressurizer surge line is shown in Figure 126. The temperature reached 1000 K at about 17,000 s. While, the wall temperature of SGs U-tubes was lower as shown in Figures 127 and 128 for loop-A and loop-B, respectively. A larger quantity of hot steam was vented through PORVs and SRVs bypassing SGs.

6.4.3. Discussions

As shown in the above results, the intentional RCS depressurization through PORVs and SRVs latched open applied to S3-TMLB′ sequence had delayed the core damage progression compared to the S3-TMLB′ without such strategy. The calculated delay was about 3000 s (50 minutes).

Comparing to the application of such strategy to the TMLB′ accident, the delay was shorter. The injected cold water from accumulator tanks had flooded the core and delayed the core degradation for a while. The accumulators injection was initiated rapidly. A part of the injected water was discharged from RCS through seal break holes. Then the liquid in the core also decreased quickly and it caused the core heat up and damaged.

It is also noted that the sequence showed a high pressure difference between primary and secondary sides. At the time of vessel failure, the primary side was about 0.8 MPa and the secondary side was about 8.1 MPa.

Table 8. Timing Key Events of S3-TMLB'with RCS depressurization: Run 4

Events	Time ,s	/(hr)
Station blackout initiation	0	(0)
SG dried out	4981	(1.38)
Core coolant at saturation	7408	(2.06)
Pump seals failure	7408	(2.06)
Start of core uncovery	7980	(2.22)
PORVs and SRVs latched open	10,637	(2.954)
Accumulator opens	11,580	(3.22)
Start of oxidation	11,750	(3.26)
Gap release		
Ring 1	11,975	(3.33)
Ring 2	13,449	(3.74)
Ring 3	13,919	(3.87)
Core completely uncovered	17,250	(4.79)
Core support plate failure		
Ring 1	18,807	(5.22)
Ring 2	18,906	(5.25)
Ring 3	18,950	(5.26)
Lower head penetration failure		
Ring 1	18,844	(5.23)
Ring 2	18,880	(5.24)
Ring 3	18,882	(5.24)
Debris ejection	18,844	(5.23)

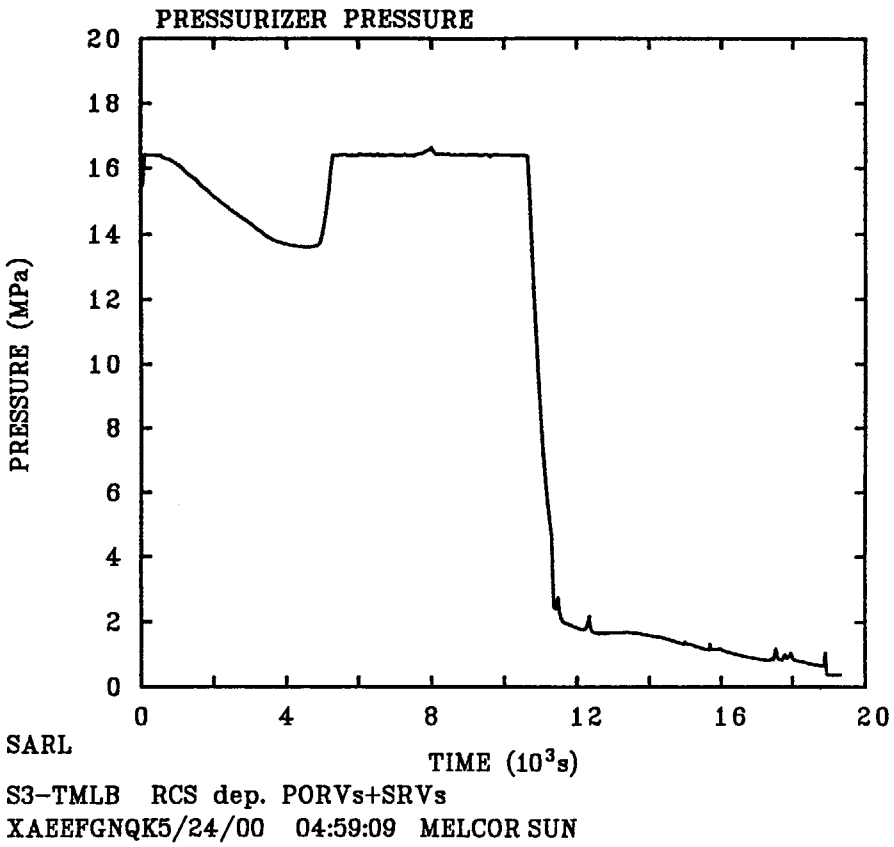

Figure 115. Run 4: Pressurizer pressure.

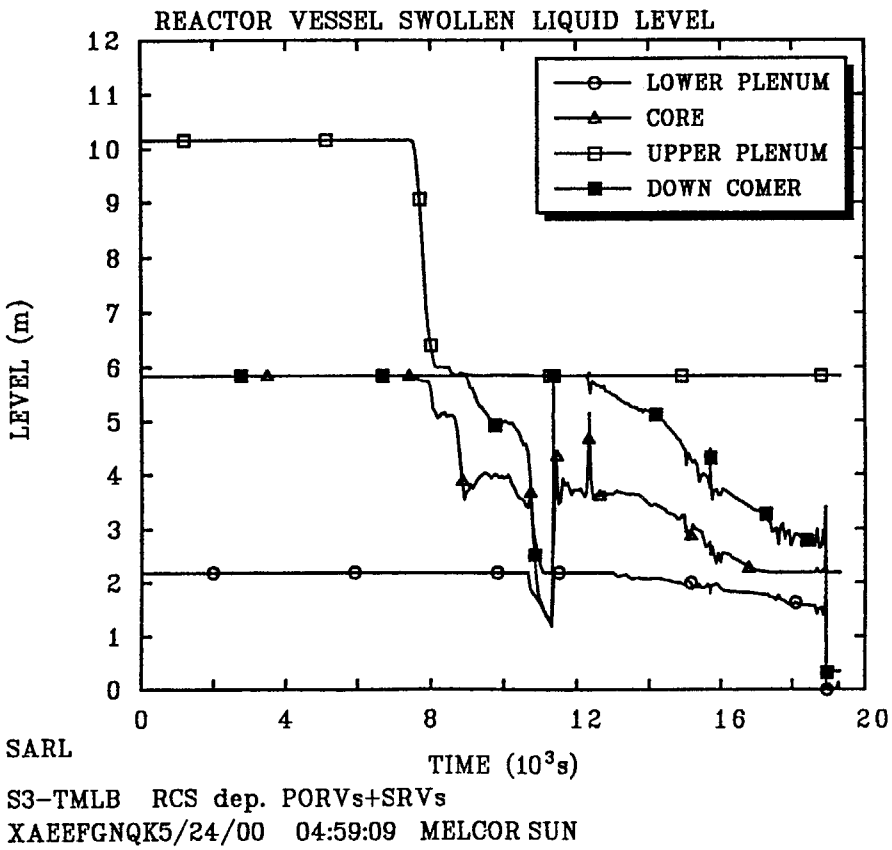

Figure 116. Run 4: Swollen liquid level in reactor vessel.

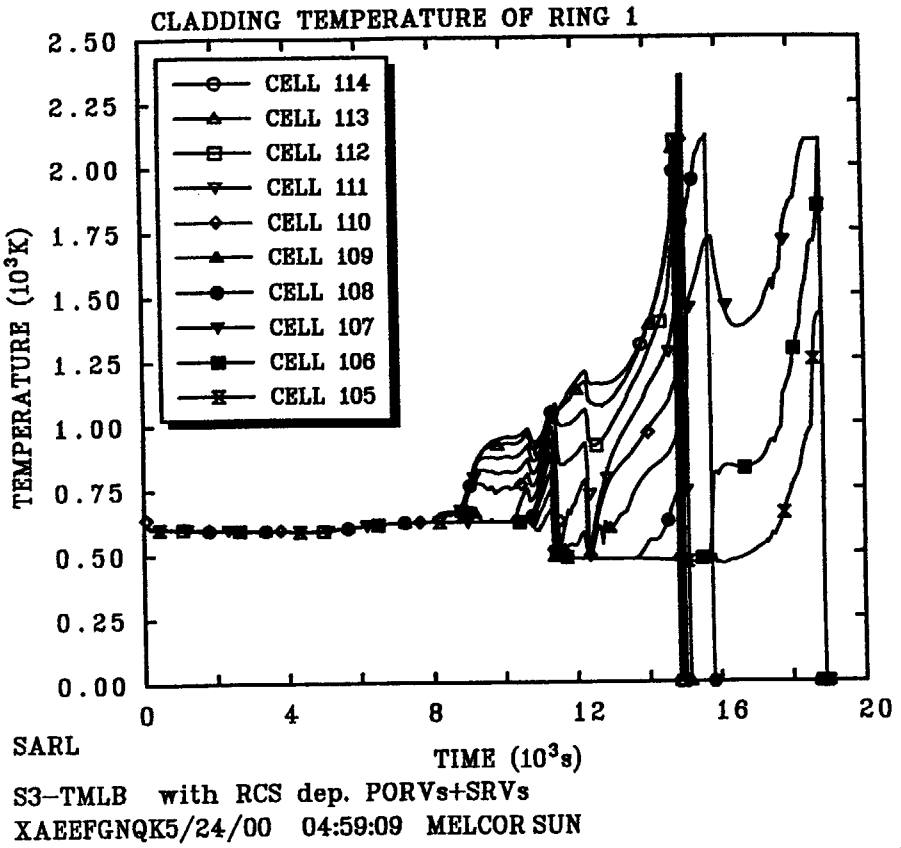

Figure 117. Run 4: Cladding temperature in ring 1.

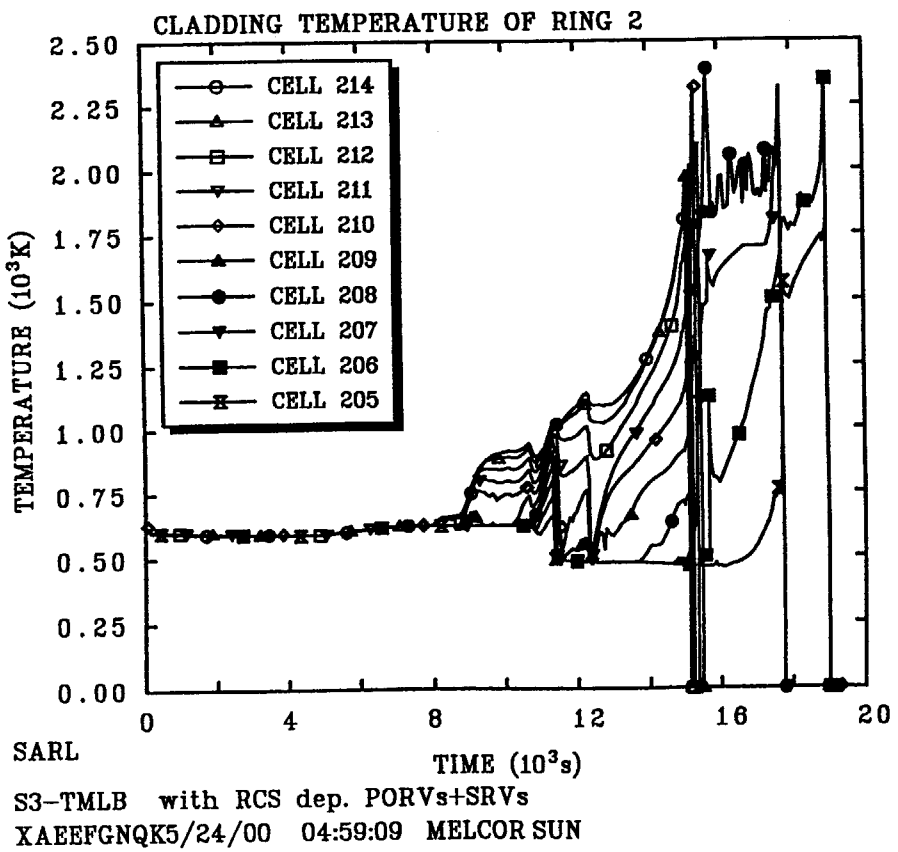

Figure 118. Run 4: Cladding temperature in ring 2.

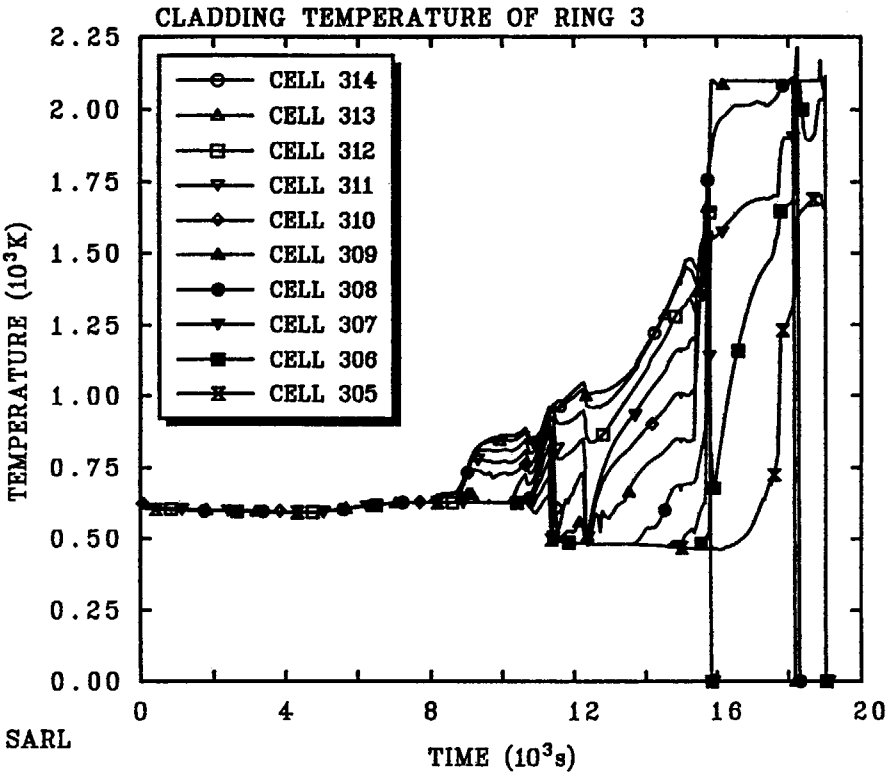

Figure 119. Run 4: Cladding temperature in ring 3.

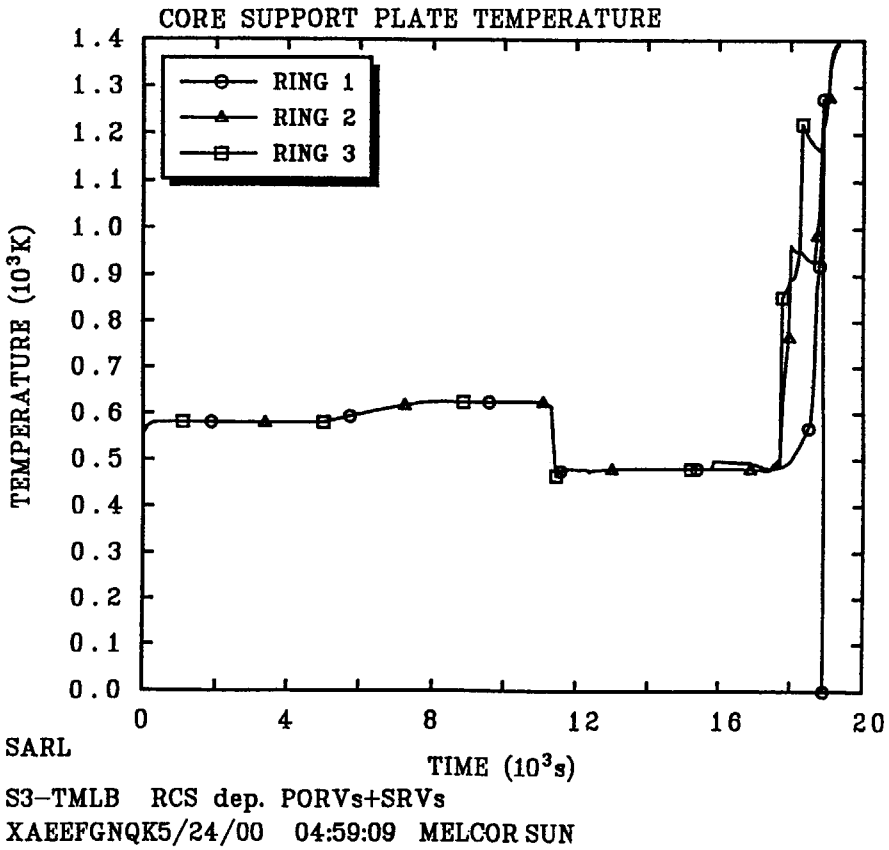

Figure 120. Run 4: Core support plate temperature.

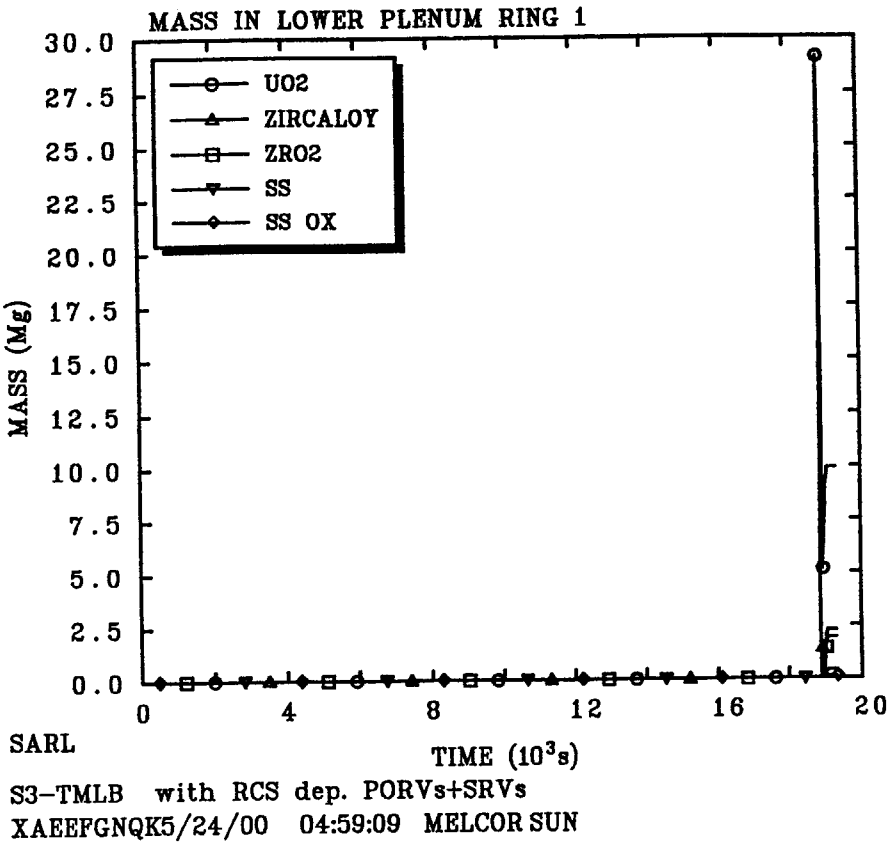

Figure 121. Run 4: Debris mass in lower plenum ring 1

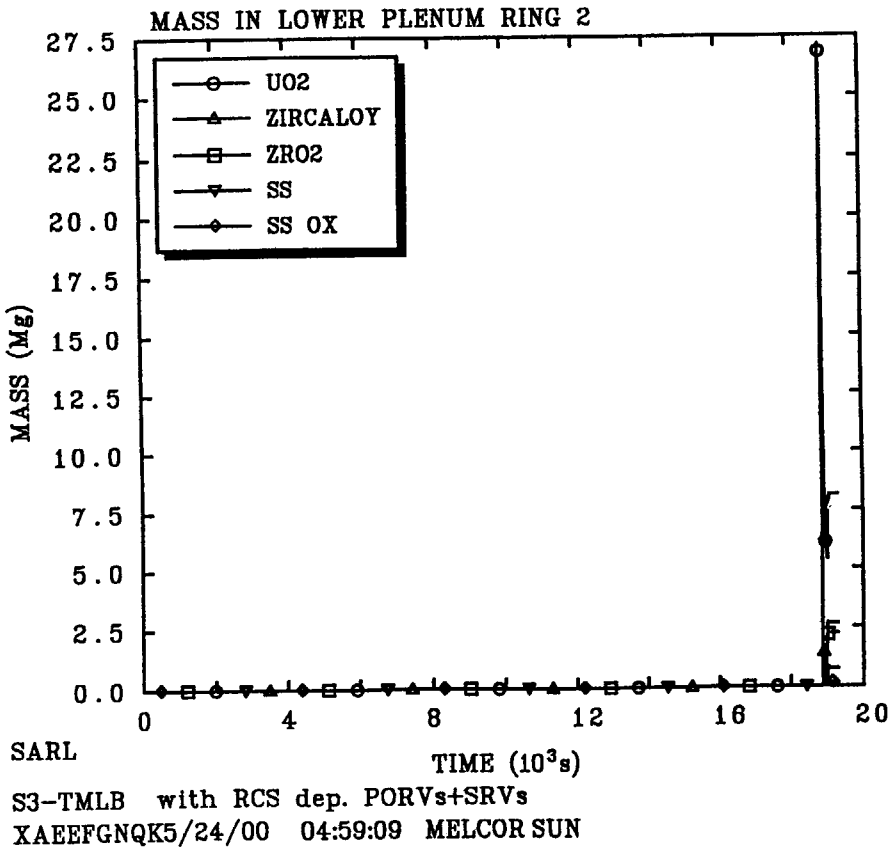

Figure 122. Run 4: Debris mass in lower plenum ring 2

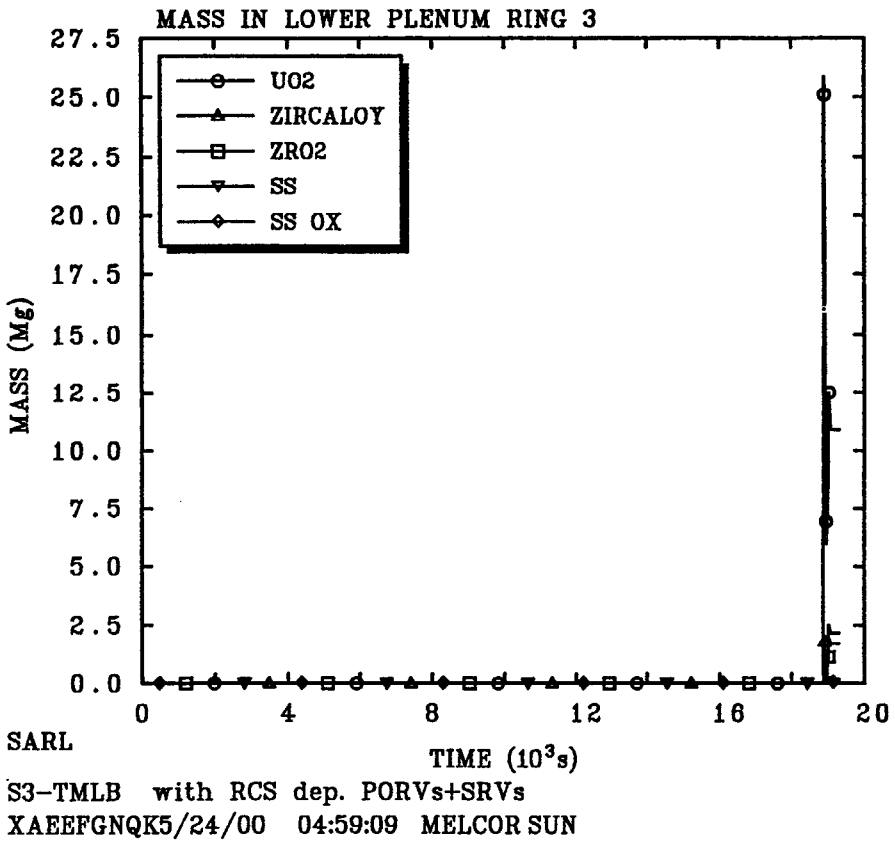

Figure 123. Run 4: Debris mass in lower plenum ring 3

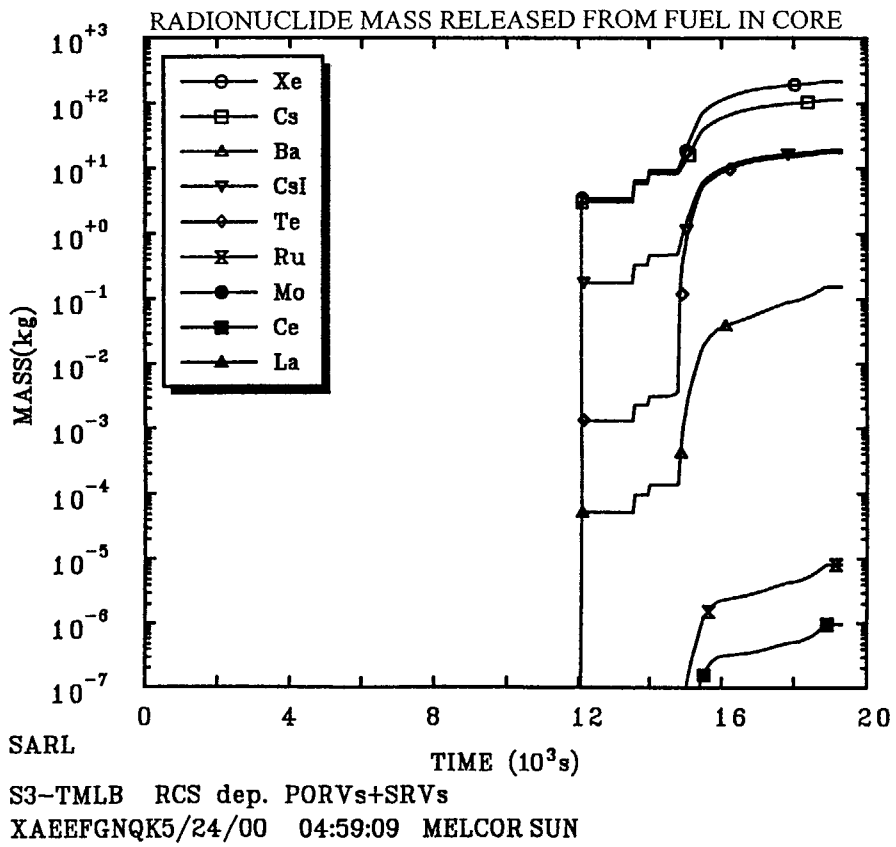

Figure 124. Run 4: Radionuclide mass release from fuel in core.

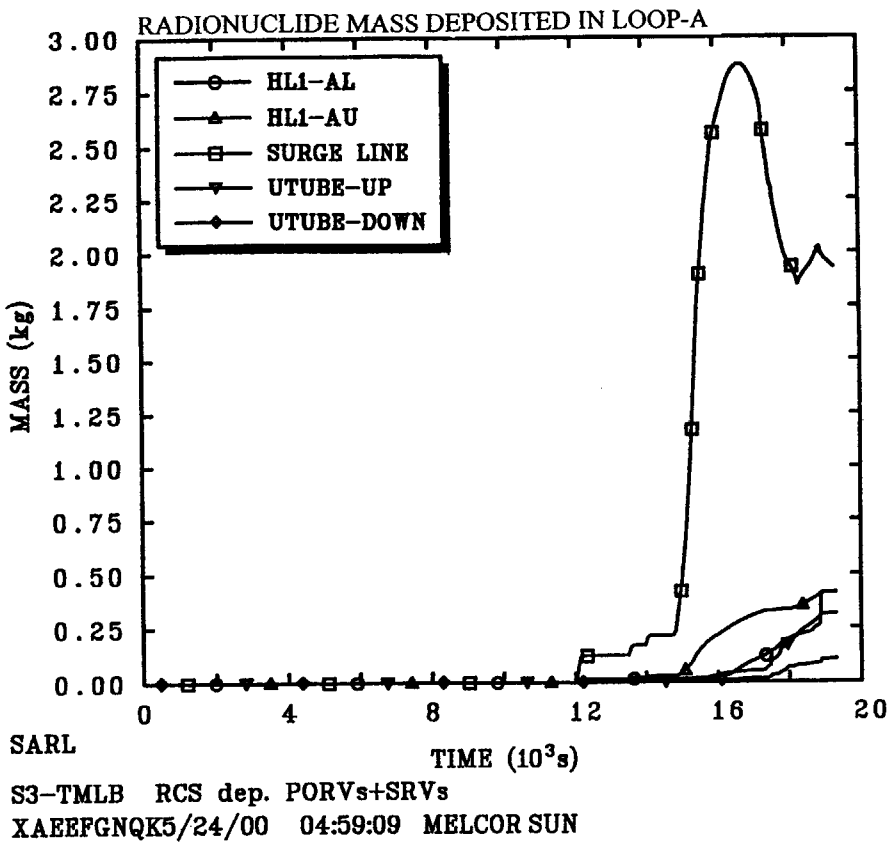

Figure 125. Run 4: Deposited radionuclide mass.

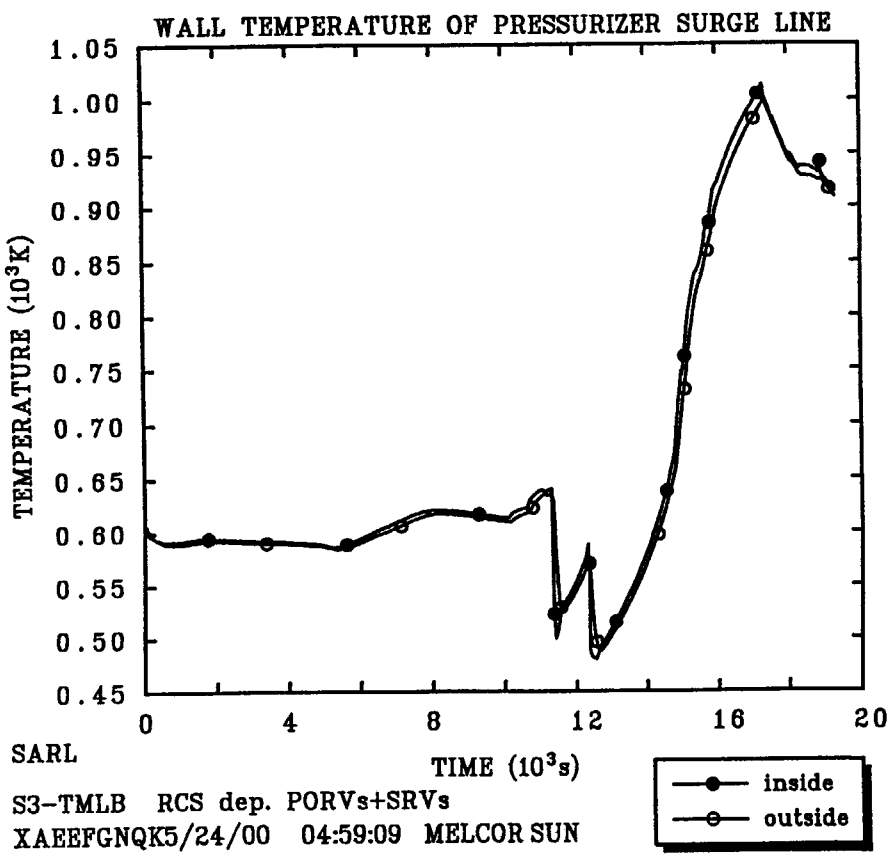

Figure 126. Run 4: Wall temperature of surge line.

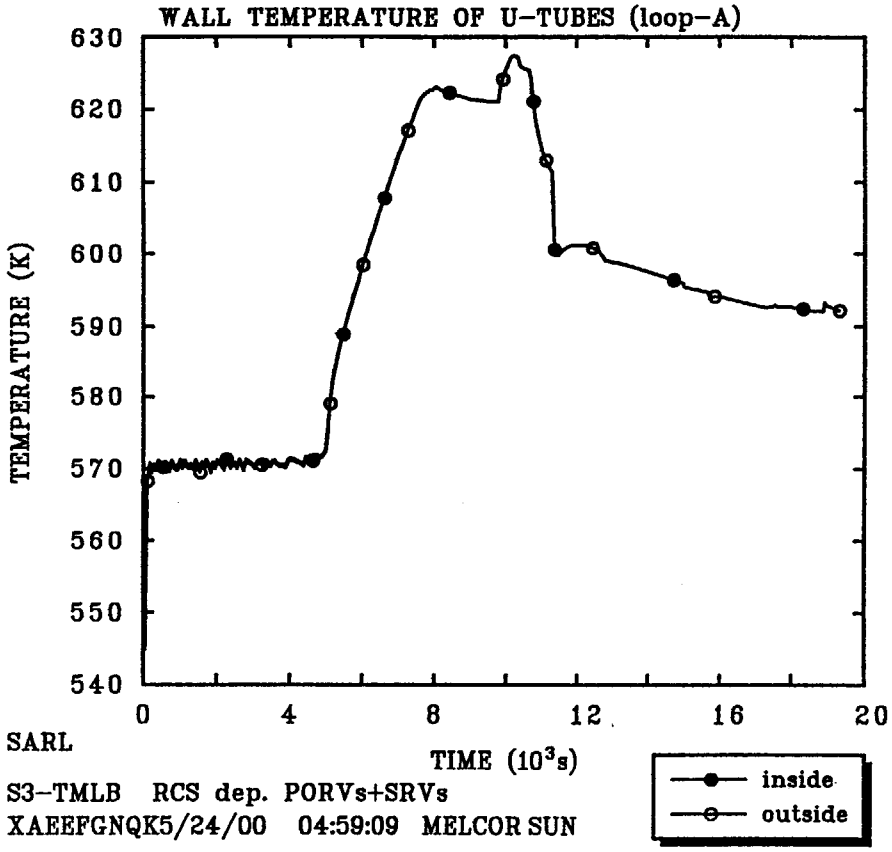

Figure 127. Run 4: Wall temperature of SG-A U-tubes.

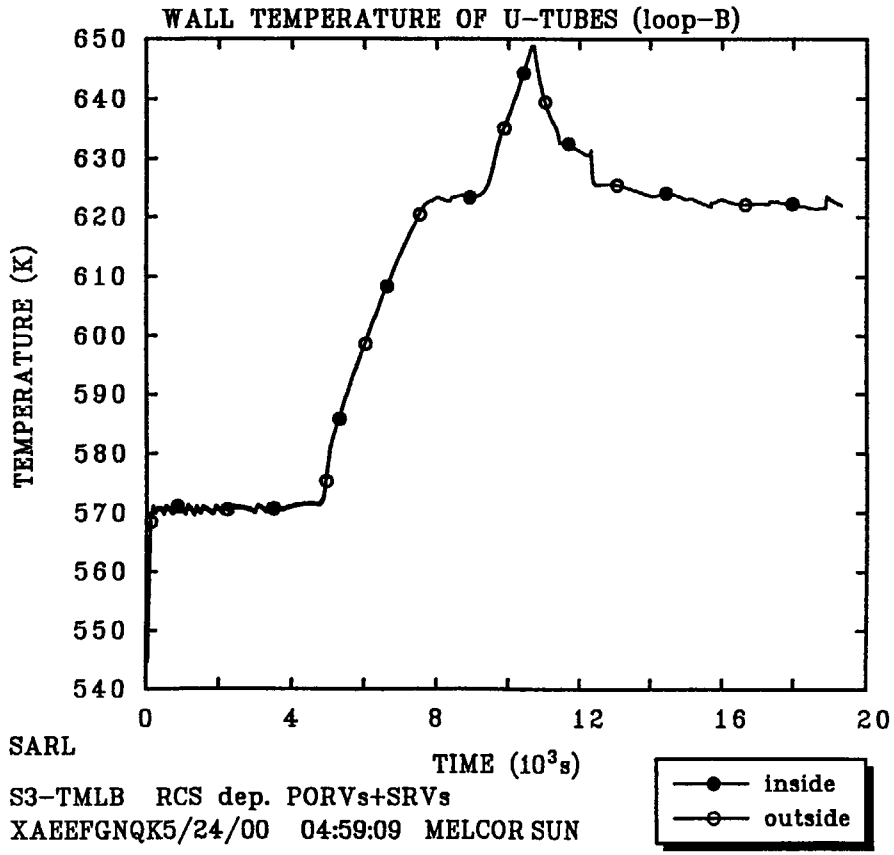

Figure 128. Run 4: Wall temperature of SG-B U-tubes.

7. CONCLUSIONS

The analytical calculations of Indian Point 3 PWR station blackout accident and its variation have been performed using the MELCOR 1.8.4 code. The following conclusions were obtained from the present study:

(1) The total station blackout initiating accident could lead to the severe core damage and, subsequently HPME phenomena. The current calculation predicted about 3.8 hr interval time from initiation of total station blackout to the reactor vessel melt-through.

(2) The reactor coolant pump seals LOCAs which might happen during a station blackout sequence resulted in different effects on accident progression depending on the timing of seal failure. The early failure caused an early core damage. Contrarily, the late failure of about 2.5 hr from initiation of station blackout tended to delay the accident progression. In this calculation the delay was more than 1.5 hr compared to the station blackout without pump seal LOCA.

(3) The intentional RCS depressurization by PORVs latched open during a TMLB′ accident was unable to delay the accident progression. Use of PORVs design capacity could not depressurize RCS fast enough to arrive at accumulator set point prior to the vessel failure. The lower head failure occurred as in the TMLB′ sequence without RCS depressurization.

(4) The calculation performed by assuming that pressurizer SRVs could also be latched open for increasing discharging flow area showed that the depressurization occurred faster, and accumulators set point was rapidly achieved. The initiation of cold borated water injection could provide sufficient cooling for the hot core materials. As consequence, the core damage progression was delayed. The lower head failure occurred at 6000 s later than the TMLB′ base case. But, in the case of S3-TMLB′ sequence, the assumed intentional RCS depressurization by PORVs and SRVs latched open could only delay the lower head failure for about 3000 s. The depressurization is less effective due to fast core uncovery.

ACKNOWLEDGEMENT

The first author wishes to thank to Science and Technology Agency (STA) of Japan for the financial support through STA Fellowships from March 1 to May 30, 2000. For all members of Severe Accident Research Laboratory (SARL) of JAERI, the first author would like to express a sincere appreciation for their kind collaborations.

REFERENCES

1) J.A. Giesike et al., "Source Term Code Package: A User's Guide (Mod 0)," NUREG/CR-4587, 1987.

2) R.M. Summers et al., "MELCOR Computer Code Manuals," NUREG/CR-6119, SAND93-2185, 1995.

3) U.S. Nuclear Regulatory Commission (USNRC), "MELCOR Homepage: MELCOR 1.8.4 Executive Summary," http://melcor.sandia.gov/excecsum.htm, (NUREG/CR-6119, SAND97-2398), 1999.

4) U.S. Nuclear Regulatory Commission (USNRC), "Severe Accident Risks: An Assessment for Five U.S. Nuclear Power Plants", NUREG-1150, 1990.

5) L.N. Kmetyk et al.,"MELCOR 1.8.2 Assessment: Surry PWR TMLB' (with a DCH Study)," Sandia Report, SAND93-1899.UC-610, 1994.

6) T.J. Heames and R.C. Smith, "Integrated MELPROG/TRAC analyses of a PWR Station Blackout," Nuclear Engineering and Design, 125, pp. 175-188, 1991.

7) A. Hidaka et al., "SCDAP/RELAP5 Analysis of Station Blackout with Pump Seal LOCA in Surry Plant," Journal of Nuclear Science and Technology, 325(6), pp. 527-538, 1995.

8) A. Hidaka et al., "Evaluation of Steam Generator U-Tube Integrity During PWR Station Blackout With Secondary System Depressurization, JAERI-Research 99-067, 1999.

9) R. Chambers et al., "Depressurization to Mitigate Direct Containment Heating," Nuclear Technology, 88, pp. 239-250, 1989.

10) D.A. Brownson et al., "Intentional Depressurization Accident Management Strategy for Pressurized Water Reactors, NUREG/CR-5937, EGG-2688, 1993.

11) Power Authority of the State of New York, "Indian Point 3 NPP Final Safety Analysis Report," Rev.0, DOCKET #05000286, July, 1982.

12) U.S. Nuclear Regulatory Commission (U.S. NRC), "Risk Assessment of Severe Accident Induced Steam Generator Tube Rupture," NUREG-1570, 1998.

13) G. Duijvestijn and J. Birchley, "Core Meltdown and Vessel Failure: a Coupled Problem," Nuclear Engineering and Design, 191, pp. 17 -30, 1999.

14) H. Kumamaru and Y. Kukita, "PWR Cold-leg Small-Break LOCA with Total HPI Failure. Effect of Break Area on

Core Dryout and Intentional Depressurization for Prevention of Excess Core Dryout," Journal of Nuclear Science and Technology, 29(12), pp. 1162-1172, 1992.

15) A. Hidaka, J. Sugimoto, Y. Yabushita and K. Soda, "Severe Accident Management of PWR by an Intentional Primary System Depressurization," JAERI-M 91-175, 1991. (in Japanese).

16) K. Soda, T. Ishigami, A. Hidaka and K. Abe, "Intentional Depressurization of the Primary and Secondary Circuits as an Accident Mitigation Measure," CSNI Report 158, 1989.

17) P.D. Baylese, "Analyses of Natural Circulation During Surry Station Blackout Using SCDAP/RELAP5," NUREG/CR-5214, 1988.

国際単位系 (SI) と換算表

表 1　SI 基本単位および補助単位

量	名称	記号
長さ	メートル	m
質量	キログラム	kg
時間	秒	s
電流	アンペア	A
熱力学温度	ケルビン	K
物質量	モル	mol
光度	カンデラ	cd
平面角	ラジアン	rad
立体角	ステラジアン	sr

表 2　SI と併用される単位

名称	記号
分，時，日	min，h，d
度，分，秒	°，′，″
リットル	l，L
トン	t
電子ボルト	eV
原子質量単位	u

$1\ \mathrm{eV} = 1.60218 \times 10^{-19}\ \mathrm{J}$

$1\ \mathrm{u} = 1.66054 \times 10^{-27}\ \mathrm{kg}$

表 5　SI 接頭語

倍数	接頭語	記号
10^{18}	エクサ	E
10^{15}	ペタ	P
10^{12}	テラ	T
10^{9}	ギガ	G
10^{6}	メガ	M
10^{3}	キロ	k
10^{2}	ヘクト	h
10^{1}	デカ	da
10^{-1}	デシ	d
10^{-2}	センチ	c
10^{-3}	ミリ	m
10^{-6}	マイクロ	μ
10^{-9}	ナノ	n
10^{-12}	ピコ	p
10^{-15}	フェムト	f
10^{-18}	アト	a

表 3　固有の名称をもつ SI 組立単位

量	名称	記号	他の SI 単位による表現
周波数	ヘルツ	Hz	s^{-1}
力	ニュートン	N	$m \cdot kg/s^2$
圧力，応力	パスカル	Pa	N/m^2
エネルギー，仕事，熱量	ジュール	J	N·m
工率，放射束	ワット	W	J/s
電気量，電荷	クーロン	C	A·s
電位，電圧，起電力	ボルト	V	W/A
静電容量	ファラド	F	C/V
電気抵抗	オーム	Ω	V/A
コンダクタンス	ジーメンス	S	A/V
磁束	ウェーバ	Wb	V·s
磁束密度	テスラ	T	Wb/m^2
インダクタンス	ヘンリー	H	Wb/A
セルシウス温度	セルシウス度	℃	
光束	ルーメン	lm	cd·sr
照度	ルクス	lx	lm/m^2
放射能	ベクレル	Bq	s^{-1}
吸収線量	グレイ	Gy	J/kg
線量当量	シーベルト	Sv	J/kg

表 4　SI と共に暫定的に維持される単位

名称	記号
オングストローム	Å
バーン	b
バール	bar
ガル	Gal
キュリー	Ci
レントゲン	R
ラド	rad
レム	rem

$1\ \mathrm{Å} = 0.1\ \mathrm{nm} = 10^{-10}\ \mathrm{m}$

$1\ \mathrm{b} = 100\ \mathrm{fm}^2 = 10^{-28}\ \mathrm{m}^2$

$1\ \mathrm{bar} = 0.1\ \mathrm{MPa} = 10^5\ \mathrm{Pa}$

$1\ \mathrm{Gal} = 1\ \mathrm{cm/s}^2 = 10^{-2}\ \mathrm{m/s}^2$

$1\ \mathrm{Ci} = 3.7 \times 10^{10}\ \mathrm{Bq}$

$1\ \mathrm{R} = 2.58 \times 10^{-4}\ \mathrm{C/kg}$

$1\ \mathrm{rad} = 1\ \mathrm{cGy} = 10^{-2}\ \mathrm{Gy}$

$1\ \mathrm{rem} = 1\ \mathrm{cSv} = 10^{-2}\ \mathrm{Sv}$

(注)

1. 表 1 ― 5 は「国際単位系」第 5 版，国際度量衡局 1985 年刊行による。ただし，1 eV および 1 u の値は CODATA の 1986 年推奨値によった。
2. 表 4 には海里，ノット，アール，ヘクタールも含まれているが日常の単位なのでここでは省略した。
3. bar は，JIS では流体の圧力を表わす場合に限り表 2 のカテゴリーに分類されている。
4. EC 閣僚理事会指令では bar，barn および「血圧の単位」mmHg を表 2 のカテゴリーに入れている。

換　算　表

力	N(=10^5dyn)	kgf	lbf
	1	0.101972	0.224809
	9.80665	1	2.20462
	4.44822	0.453592	1

粘　度　$1\ \mathrm{Pa \cdot s (N \cdot s/m^2)} = 10\ \mathrm{P}$(ポアズ)$(\mathrm{g/(cm \cdot s)})$

動粘度　$1\ \mathrm{m^2/s} = 10^4\ \mathrm{St}$(ストークス)$(\mathrm{cm^2/s})$

圧力	MPa(=10 bar)	kgf/cm²	atm	mmHg(Torr)	lbf/in²(psi)
	1	10.1972	9.86923	7.50062×10^3	145.038
	0.0980665	1	0.967841	735.559	14.2233
	0.101325	1.03323	1	760	14.6959
	1.33322×10^{-4}	1.35951×10^{-3}	1.31579×10^{-3}	1	1.93368×10^{-2}
	6.89476×10^{-3}	7.03070×10^{-2}	6.80460×10^{-2}	51.7149	1

エネルギー・仕事・熱量	J(=10^7erg)	kgf·m	kW·h	cal(計量法)	Btu	ft·lbf	eV
	1	0.101972	2.77778×10^{-7}	0.238889	9.47813×10^{-4}	0.737562	6.24150×10^{18}
	9.80665	1	2.72407×10^{-6}	2.34270	9.29487×10^{-3}	7.23301	6.12082×10^{19}
	3.6×10^6	3.67098×10^5	1	8.59999×10^5	3412.13	2.65522×10^6	2.24694×10^{25}
	4.18605	0.426858	1.16279×10^{-6}	1	3.96759×10^{-3}	3.08747	2.61272×10^{19}
	1055.06	107.586	2.93072×10^{-4}	252.042	1	778.172	6.58515×10^{21}
	1.35582	0.138255	3.76616×10^{-7}	0.323890	1.28506×10^{-3}	1	8.46233×10^{18}
	1.60218×10^{-19}	1.63377×10^{-20}	4.45050×10^{-26}	3.82743×10^{-20}	1.51857×10^{-22}	1.18171×10^{-19}	1

1 cal = 4.18605 J (計量法)
= 4.184 J (熱化学)
= 4.1855 J (15 °C)
= 4.1868 J (国際蒸気表)

仕事率　1 PS (仏馬力)
= 75 kgf·m/s
= 735.499 W

放射能	Bq	Ci
	1	2.70270×10^{-11}
	3.7×10^{10}	1

吸収線量	Gy	rad
	1	100
	0.01	1

照射線量	C/kg	R
	1	3876
	2.58×10^{-4}	1

線量当量	Sv	rem
	1	100
	0.01	1

(86 年 12 月 26 日現在)

Depressurization Analyses of PWR Station Blackout with MELCOR 1.8.4